Re-examining the Amazonian Dark Earth Phenomenon: Biochar

A THESIS
SUBMITTED TO THE FACULTY OF
UNIVERSITY OF MINNESOTA
BY

Edward Charles Colosky V

IN PARTIAL FULFILLMENT OF THE REQUIREMENTS
FOR THE DEGREE OF
MASTER OF SCIENCE

Kurt A. Spokas

August 2017

Acknowledgements

This thesis is the culmination of 4 ½ years of work. I would not have completed this thesis without many people's support. To everyone who knew of my project, ever asked how it's going, and/or wished me luck, I wish to say thank you for the moral and emotional support. Beyond that, however, there are a special few who gave time and effort worthy of select acknowledgment.

I would first like to say thank you to Martin Du Saire, Lee Yang, and the entire Spokas Lab Group. There were innumerable instances where Martin, Lee, and the Spokas Lab Group helped with projects and provided useful advice. Furthermore, I created friendships within the entire Spokas Lab Group that I will cherish for life. To Martin Du Saire, Lee Yang and the rest of the Spokas Lab Group I say thank you, this would not have been possible without you.

I would also like to acknowledge and thank Dr. Gordon Brown, an ecology professor with the College of Saint Benedict and Saint John's University that started me on the track to working with Kurt in the field of soil science 5 years ago. He helped me get my first project off the ground with Kurt. Without Gordy's initial encouragement in biochar research, I wouldn't be at this point.

I would also like to acknowledge the aid and help of two University of Minnesota Earth Sciences department researchers, Dr. Joshua Feinberg a professor with the University of Minnesota Earth Sciences Department, and Daniel Maxbauer, a fellow 2011 CSB/SJU graduate and a Ph. D candidate. Both of them helped Kurt and I focus our research efforts on ADE soils iron mineralogy. Although the specific project they were involved with is

not a direct part of this thesis, their insights and laboratory data were invaluable for the direction of what is presented in Chapter 4 of this thesis.

Finally, I would like to acknowledge two professors from Brazil, Drs. Newton La Scala and Jose Marques Junior. These two professors were very supportive of my experimental ideas. They were also the linkage by which we were able to acquire Brazilian soils (under the USDA-APHIS permit of my supervisor) that I investigated. Without them and their associated researchers I would not have completed the fourth chapter of this thesis.

Finally and most importantly, I equally thank Kurt Spokas, my mentor, and Xin Piao, my loving wife. I started this work believing that biochar was a novel soil amendment that could environmentally, sustainably, and efficiently increase soil fertility. Two and a half years into this project however, I realized for myself that biochar was not all that I had made it out to be. At that moment, I became disillusioned with biochar. It was through the encouragement of both Kurt and Xin that I could see beyond my perceived notions and find the energy to complete this thesis. If Kurt and Xin had not encouraged me to hang-on and pull through, I do not think I would have completed this thesis. To them I owe more than half of the energy I put into completing this thesis.

Dedication

This thesis is dedicated to *Kurt Spokas*, my mentor, and *Xin Piao*, my loving wife.

Abstract

This thesis presents three linked research projects. The first and second research chapters (Ch. 2 & 3) exhibit results from studies examining biochar material properties. The third and final research chapter (Ch. 4) provide two unique findings; 1) that there are mineralogical differences between Amazonian Dark Earth and Brazilian Oxisol soil profiles, and 2) that iron mineralogy does affect soil microbial respiration rates. These chapters are associated with each other through hypotheses surrounding Amazonian Dark Earth (ADE) pedogenesis. Biochar (a subset of black carbon materials) is often cited as the key factor for explaining the observed enhanced fertility of ADE soils when compared to natural occurring surrounding Brazilian Oxisol soils. Biochar is often researched to understand how the effects observed in ADE soils may be applied elsewhere. Data presented in chapters 2 & 3 of this thesis, however, raise questions regarding its soil enhancing properties. Data presented in chapter 4 provide evidence for how a previously overlooked factor in Amazonian Dark Earth soils, iron mineralogy, could potentially affect additional soil properties including soil microbial respiration rates. Differing soil microbial rates with time will alter carbon sequestration rates and soil fertility. The fundamental conclusion of this thesis is that the data collected here supports the suggestion that ADE soils should be reexamined, with a focus on the iron mineralogical differences found between ADE and Brazilian Oxisol soils.

Table of Contents

Contents

Chapter 1. Introduction

Amazonian Dark Earth (ADE) soils are unique soil epipedons within the vast expanse of the Amazon River Basin (German 2003; Neves et al. 2003; Woods 2003; Glaser et al. 2000). The ubiquitous soils of the Amazon River Basin are Brazilian Oxisols that are light-colored, clayey soils possessing a high concentration of iron and aluminum (Glaser et al. 2000). They show a strong degree of weathering and are notable for their lack of fertility, which subsequently leads to the common use of slash-and-burn agricultural practices throughout the region (Neves et al. 2003). Far from being ubiquitous, ADEs exist in small pockets ranging from 1 to 100s of hectares in size (Kern et al. 2003). They exhibit a profoundly contrasting characteristic to the surrounding Oxisols, namely dark and organic-rich surface soil horizons (Neves et al. 2003). Hence, to this date ADE soils are highly sought after by local farmers since they are highly productive (Madari, Sombroek, and Woods 2004).

Amazonian Dark Earth's have posed a conundrum for soil scientists ever since their discovery in the late 1800's. Many of the most fertile ADE sites underlie prehistoric human habitation sites, leading scholars to postulate that native human populations played a significant role in their formation (e.g., Neves et al. 2003; Glaser et al. 2000). However, not until over a 100 years later, has a plausible hypothesis been proposed as to how humans could have formed ADE sites. Specifically, in the early 2000's Glaser et al. (2001) presented a hypothesis where humans discarded refuse along with charcoal to the surrounding soils, and over centuries to millennia charcoal modified the soil properties to ultimately lead to greater soil fertility. Key to this hypothesis was the observation of increased concentrations of black carbon in ADE soils when compared to the surrounding

Oxisols. Thereby, correlating the beneficial soil fertility improvements to the black carbon constituents, since this was the initial linkage observed at these sites.

Since the work of Glaser et al. (2001) many in agricultural circles, especially those interested in sustainable practices, sought to mimic ADE soils in other parts of the world as a course of "sustainable" soil husbandry (i.e., Madari, Sombroek, and Woods 2004) by creating a "*synthetic Terra Preta soil*" (Chia et al. 2010). These research efforts soon focused on the application of black carbon to soils, or biochar soil amendments. Biochar is pyrolyzed organic material used with the intent to sequester atmospheric carbon (Spokas 2010; Atkinson, Fitzgerald, and Hipps 2010; Laird et al. 2010; Goldberg 1985). When used as a soil amendment, biochar has been shown to sometimes correlate with increased soil fertility and crop yields (Jeffery et al. 2011).

Four and a half years ago, my project began in earnest to elucidate the mechanisms behind how biochar was enhancing soil fertility and increasing crop production. Sometime midway during the research effort, a very important globally held assumption about biochar was questioned when our team discovered that biochar was not a physically recalcitrant material (Chap. 2). This observation contradicted the currently held hypothesis that the charcoal remained relatively unmodified and persistent over millennia during the formation of ADEs, which had been proposed by Glaser et al. (2001).

In addition, published research in the last 15 years has typically shown mixed results on whether biochar truly enhances soil fertility, indicating that charcoal interactions with soil properties may not be as straightforward as previously thought (Biederman and Harpole 2013). The above findings caused me to question whether charcoal was the dominating factor in increasing soil fertility in ADEs. Therefore, I chose to expand my

focus to include reinvestigation of Amazonian Dark Earths to examine other mechanisms of increased soil fertility.

What follows in this thesis is a chronological account of my research effort. Chapter 2 details the physical dissociation of biochar within aqueous solutions (i.e., biochar's non-recalcitrant physical nature). Chapter 3 investigates the mechanisms for increasing soil fertility by assessing biochars' capacity to adsorb nitrogen from aqueous and soil solutions. This work allowed me to explore computer programming by developing specialized software to assist in the calculation of the sorption constants through customized *Python* modules (available on GitHub). Chapter 4 summarizes the preliminary investigations of Amazonian Dark Earths, in which I started the research in observing the impact of iron mineralogy and its potential roll in ADE soils. This was noteworthy, since the typical difference has been the presence of black carbon, but the differing iron mineralogy also shed light on other potential soil formation hypotheses. I also assessed the effect of different iron mineral soil amendments on soil respiration, an often-used surrogate for soil fertility.

Chapter 2. Physical Disintegration of Biochar: An Overlooked Process

Appears in:

Spokas, K.A., Novak, J.M., Masiello, C.A., Johnson, M.G., Colosky, E.C., Ippolito, J.A. & Trigo, C. (2014) Physical Disintegration of Biochar: An Overlooked Process. Environmental Science & Technology Letters, 1, 326-332.

2.1. Overview

Data collected from both artificially and field (naturally) weathered biochar suggest that a potentially significant pathway of biochar disappearance is through physical breakdown of the biochar structure. Through scanning electron microscopy (SEM) we characterized this physical weathering which increased structural fractures and possessed higher numbers of liberated biochar fragments. This was hypothesized to be due to the graphitic sheet expansion accompanying water sorption coupled with comminution. These fragments can be on the micro and nano-scale, but are still carbon-rich particles with no detectable alteration in the oxygen to carbon ratio of the original biochar. However, these particles are now easily dissolved and could be moved by infiltration. There is a need to understand how to produce biochars that are resistant to physical degradation in order to maximize long-term biochar C-sequestration potential within soil systems.

2.2. Introduction

Black carbon (BC) is the continuum of solid residuals resulting from the chemical-thermal conversion of carbon-containing materials, and includes soot, char, and charcoal (Czimczik and Masiello 2007; Spokas 2010). Due to its economic, soil fertility, and archeological importance, BC have been examined over the last century for susceptibility to microbial and chemical oxidation (Nichols et al. 2000)·(Lehmann 2007). Biochar is intentionally created BC for soil carbon sequestration and soil fertility improvement (Lehmann 2007). Therefore, biochar is chemically a BC, but not all BC is biochar.

The degradability of BC in soils is a function of its chemical composition, physical incorporation, and host soil microbial community structure (Kuzyakov, Bogomolova, and Glaser 2014; Ameloot et al. 2013; Lattao et al. 2014), but with an overall consensus that BC does represent a carbon pool with increased resistance to microbial degradation (Zimmerman, Gao, and Ahn 2011; Fontaine et al. 2007). Since BC has extrapolated mean residence times from centuries to thousands of years in soils (Zimmerman, Gao, and Ahn 2011; Ameloot et al. 2013), it should be a major constituent in soils. Nevertheless, comparisons of the estimated BC generation rates with the measured soil BC pool require losses of BC to maintain mass balance: this is referred to as the "black carbon paradox" (Czimczik and Masiello 2007). Some potential solutions to this paradox include transportation of BC with surface run-off (Wang, Walter, and Parlange 2013; Major et al. 2010; Hockaday et al. 2007), explaining surface and hill slope losses (Rumpel et al. 2006). In addition, vertical movement in the soil profile also occurs and will be a function of BC particle size or its protective incorporation into the soil matrix (Foereid, Lehmann, and Major 2011; Novak et al. 2012). However, BC does not maintain its original physical size

following soil incorporation (Spokas 2013). Physical deterioration has been hypothesized to impact the longevity of BC in soils as well as its potential input into fluvial systems (Jaffé et al. 2013; Hockaday et al. 2007). It is our contention that the physical disintegration of BC is an important yet overlooked process in current biochar research, dramatically reducing BC longevity in soils.

Physical degradation of biochar occurs via several mechanisms. High oxygen:carbon (O:C) ratio BC materials (e.g., brown coals) are known to dissolve rapidly when exposed to desiccation and rewetting/saturation cycles (i.e. slacking) (Parr and Mitchell 1930). Sorption of water and water vapor can stress the physical structure of BC due to exothermic graphitic sheet swelling (Bangham and Razouk 1938). These mechanisms result in swelling and expanding the physical biochar structure which increases opportunities for further physical weathering (Théry-Parisot, Chabal, and Chrzavzez 2010). Furthermore, fresh exposures of new biochar surfaces and fissures could accelerate microbial mineralization (Sigua et al. 2014), abiotic reactions(Huisman et al. 2012), or surface sorption phenomenon (Zhao et al. 2013). BC typically is thought to be mechanically stronger than the original biomass, but is subject to structural fracturing at lower strains than the original biomass (Byrne and Nagle 1997). Furthermore, with aging (weathering) this mechanical strength is reduced (Théry-Parisot, Chabal, and Chrzavzez 2010). These structural defects will eventually lead to the formation of fragments, when BC is exposed to additional mechanical stresses (Gao and Wu 2014). Ultimately, the comminution of BC particles leads to the creation of small liberated fragments, termed dissolved black carbon (DBC) (Hockaday et al. 2006).

The fate of DBC is an especially uncertain aspect of global BC cycles. The mobilization of DBC from biochar-amended soils to wetlands and riparian areas could provide a source of DBC to ground and surface waters (Jaffé et al. 2013). It is also possible that DBC production is a major loss process for biochar-amended soils, reducing biochar's climate mitigation potential. However, the converse scenario is at least as plausible: it may be essential to break BC into smaller, more easily extractable fragments to increase the opportunity for these molecular pieces to react with soil minerals, creating stable organo-mineral complexes (Riedel et al. 2013; Naisse et al. 2014). These complexes are known to increase native soil organic carbon residence times (Masiello et al. 2004).

Here we present data confirming the physical disintegration of biochar over short time periods (24 hr), a result that has implications for this material as a soil carbon sink. Despite its documented recalcitrant nature to microbial reactions, biochar may be very susceptible to physical deterioration, abrasion, and subsequent transport by fluvial or alluvial processes. We suggest that physical comminution is a previously overlooked loss mechanism of biochar degradation and needs to be understood for accurate extrapolation of biochar's soil C sequestration potential and the interpretation of charcoal's presence in the archeological/geologic record (Cohen-Ofri et al. 2006).

2.3. Materials and Methods

In order to determine whether biochar physical stability is a control on its carbon residence time, we added various biochars (5 g oven dried weight) to distilled water (1:20 w/w) in triplicate 125 mL polyethylene bottles and placed in a reciprocating shaker (60 cycle min^{-1}) for 24 hr. Even though this artificial weathering does not fully mimic field weathering conditions (White and Brantley 2003), this methodology is also used for estimating water dispersible clays (Shaw, Truman, and Reeves 2002), batch sorption experiments(Yuan and Lavkulich 1997), and water extractable nutrients from biochar (Wu et al. 2011). Following this agitation period, the solution was filtered (20-25 µm; Whatman No. 40). The bottle was triple rinsed (20 mL DI water) to remove BC particles, which was also filtered. The solid residue collected on the filter paper was oven-dried (105 ^{o}C) for 24 hr and weighed to assess the overall biochar mass loss (Table 2.1). Due to the errors of manually rinsing and difficulty removing adsorbed biochar particles from the polyethylene bottle, this method may not be 100% accurate, but is used to assess the order of magnitude mass loss through physical fragmentation of the various biochars(Braadbaart, Poole, and van Brussel 2009). We also conducted inductively coupled plasma–optical emission spectrometry (ICP–OES) and dissolved carbon analysis (DOC) analyses of the filtrate to evaluate the dissolved content.

We analyzed pre- and post-rinsed biochars using scanning electron microscopy-electron dispersion spectroscopy (SEM-EDS). These biochars were mounted with a carbon conductive adhesive pad (PELCO Tabs™, Ted Pella, Inc; Redding, CA). In addition to the solid biochars, we also analyzed the dissolved residuals in the rinse water by direct evaporation of 100 µL directly on the aluminum SEM mount. In addition to these

artificially laboratory weathered biochars, two biochars were included that had been aged for 5 years in agricultural field plots in Rosemount, MN (Spokas 2013) and compared to the laboratory stored counterparts (Table 1). These biochars were applied to an agricultural soil (Waukegan silt loam; 1% w/w) under continuous corn production, with annual rototilling. Biochar particles located at the soil surface were collected, rinsed with DI water attempting to dislodge the entrapped soil, and then dried at 105 ^{o}C for analysis. These biochars were also attached to the SEM mounts by carbon conductive adhesive pads (PELCO Tabs™, Ted Pella, Inc; Redding, CA). Due to the conductivity of the charcoal, there was no surface coatings (i.e. gold, or carbon) used during this SEM imaging. The elemental composition was acquired using the point EDS analysis method, averaging a total of 10 different representative particles and locations (Chia et al. 2012). Unfortunately, EDS data is semi-quantitative measure of elemental concentration, and relative amounts can be inferred from differences in peak heights (Shepherd et al. 1998).

2.4. Results and Discussion

Fresh biochar had various salts and organic oils coating their surfaces (Figure 2.1). After 24 hr water rinsing, these coatings were reduced revealing further structural details not immediately visible on the "fresh" biochar (Figure 2.1). A majority of these surface deposits disappeared with water rinsing. In many cases, the EDS data indicates higher carbon content in the post-rinsed biochar (Table 2.1). Some of the deposits were inorganic salts due to the presence of inorganic elements (e.g., K, Cl, Ca, Mg, P, Ca, N, and O) visualized with EDS point data analyses, which was also confirmed in the ICP-OES analysis of the rinse waters (Figure 2.2). From these analyses, it was concluded that a majority of these deposits were precipitated surface salts, which upon water shaking were removed from the surface. The inorganic elements evaluated contained from 0.1 to 90% of the total mass loss observed from the biochar rinsing, which suggests that some of the mass lost from the biochar was DBC (see Figure 2.3). It is clear that these surface precipitates conceal the actual biochar surfaces and some of these salts are actually precipitated in pores limiting their immediate availability (Figure 2.2). Thereby, the removal of these surface coatings through dissolution opens additional porosity. However, under field conditions the release of these surface inorganic salts and organics would vary with climatic conditions and soil hydrology.

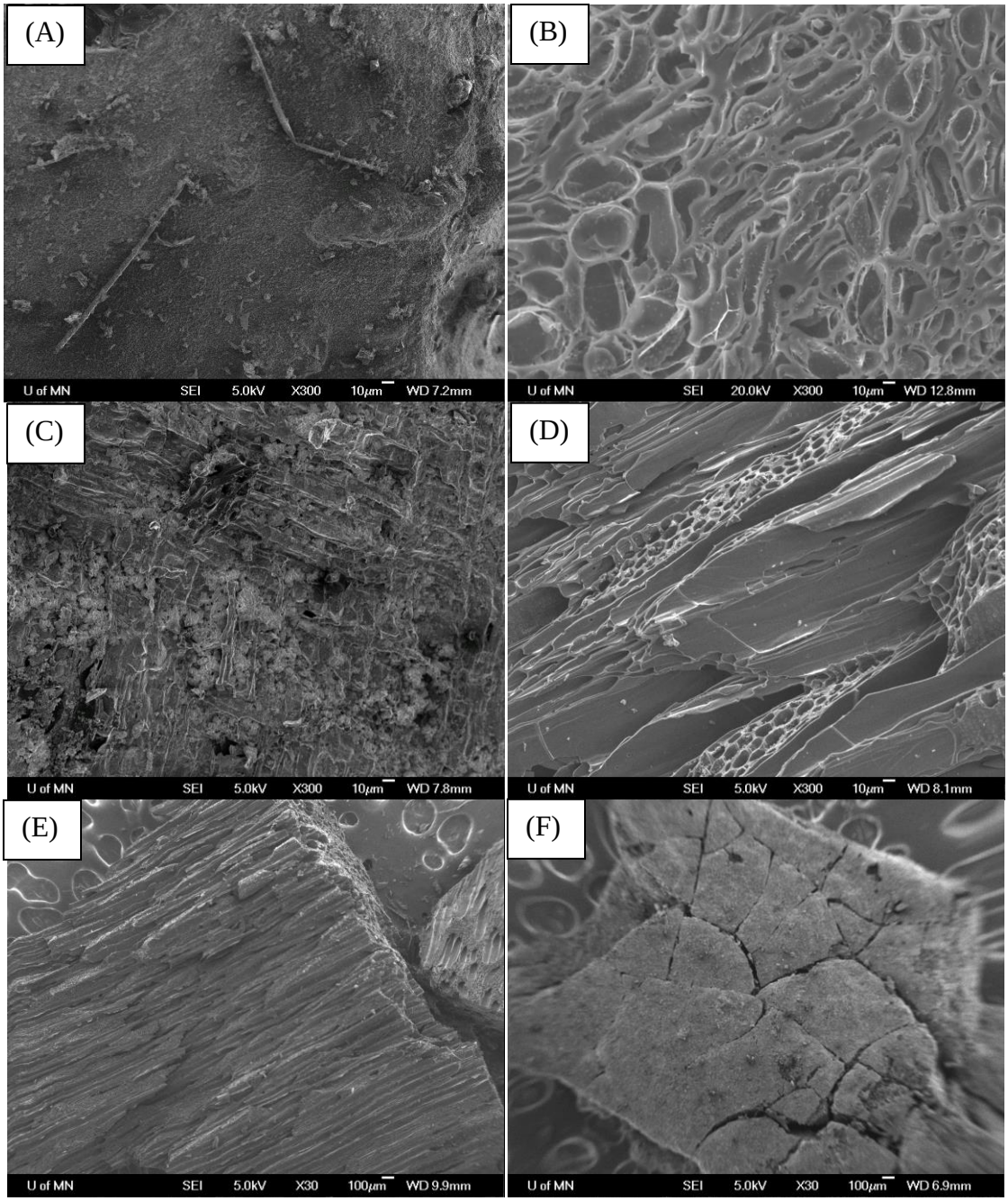

Figure 2.1. Representative SEM images of the (A) fresh fast pyrolysis macadamia nut biochar (BC# 8), (B) rinsed fast pyrolysis macadamia nut biochar (BC# 8), (C) fresh slow pyrolysis hardwood biochar (BC# 7), (D) rinsed slow pyrolysis hardwood biochar (BC# 7), (E) fresh slow pyrolysis hardwood biochar (BC# F2), and (F) a 5-yr field exposed biochar (BC# F2). All images were collected at 5.0 kV probe current, with each pair at identical magnification and the scale bar is shown in each panel.

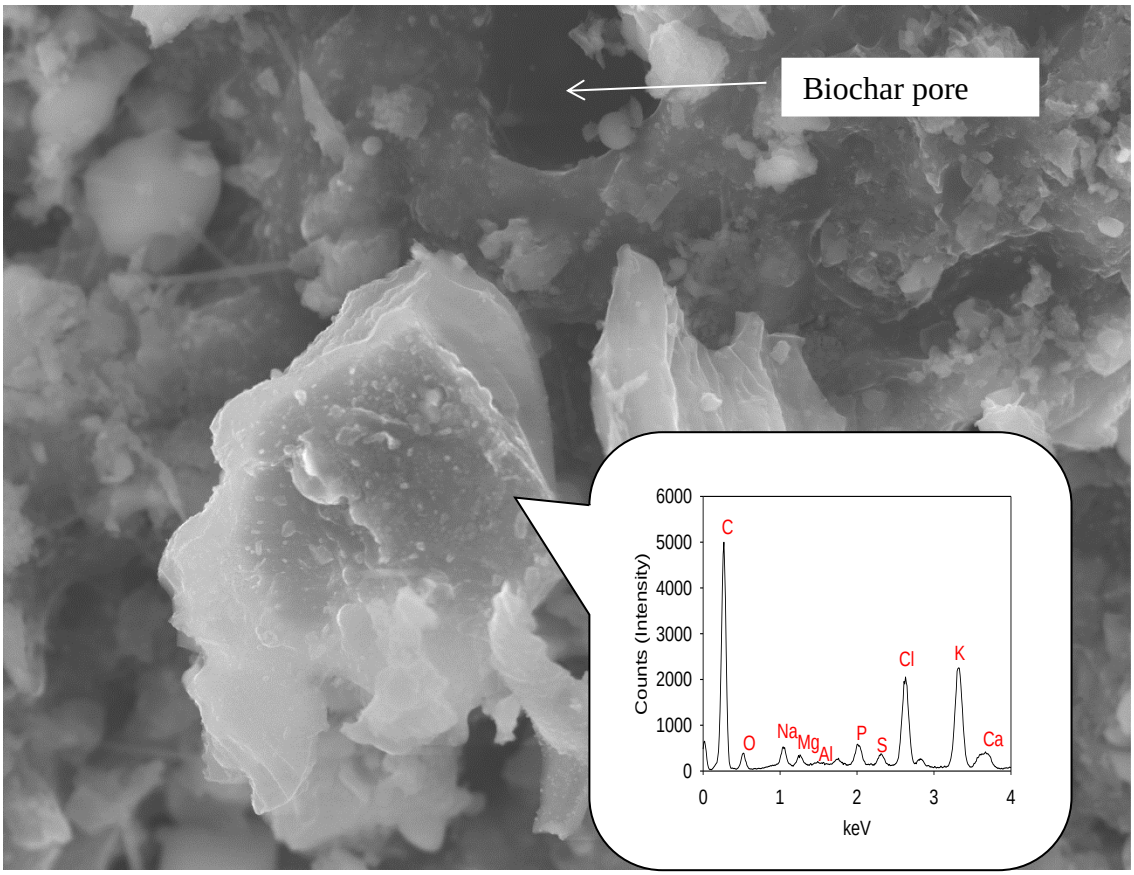

EDS Quantitative Results

Element	*Weight %*	*Weight % Error*	*Atom %*	*Atom % Error*
C	39.17	+/- 0.45	57.80	+/- 0.66
O	17.59	+/- 0.61	19.49	+/- 0.68
Na	3.41	+/- 0.09	2.63	+/- 0.07
Al	4.92	+/- 0.08	3.23	+/- 0.06
Si	0.04	+/- 0.02	0.03	+/- 0.02
P	0.80	+/- 0.06	0.46	+/- 0.03
S	2.10	+/- 0.09	1.16	+/- 0.05
Cl	15.53	+/- 0.13	7.77	+/- 0.07
K	16.36	+/- 0.10	7.41	+/- 0.04
As	0.08	+/- 0.21	0.02	+/- 0.05
Total	100.00		100.00	

Figure 2.2. SEM image of likely potassium chloride salt crystals (see inset EDS results) blocking pores on a poultry litter biochar particle.

Table 2.1. Summary of biochar characteristics and mass loss from physical dissolution for various biochars.

BC#	Feedstock	Pyrolysis Temperature (ºC)	From EDS Point Analysis C (%)	O (%)	% Mass Loss
1	Switch grass	500			5.7 (1.4)
	Original		85.6 (0.9)	12.3 (0.9)	
	24 hr Rinsed		81.8 (0.1)	12.5 (0.1)	
	Fragments		83.1 (0.1)	12.6 (0.2)	
2	Poultry Litter	350			47.0 (2.1)
	Original		47.9 (0.2)	20.6 (0.4)	
	24 hr Rinsed		80.1 (0.3)	14.8 (0.5)	
	Fragments		83.4 (0.5)	10.2 (0.1)	
3	Coconut Shell (2 pyrolysis steps)	500 then 900			1.0 (0.3)
	Original		94.7 (0.2)	5.0 (0.2)	
	24 hr Rinsed		95.8 (0.4)	3.9 (0.2)	
	Fragments		96.4 (0.2)	3.2 (0.1)	
4	Pine Chip	350			16.9 (0.9)
	Original		76.4 (0.2)	15.7 (0.1)	
	24 hr Rinsed		86.7 (0.2)	10.7 (0.3)	
	Fragments		85.4 (0.5)	9.8 (0.7)	
5	Pine Chip:Poultry litter (50:50)	350			27.9 (0.9)
	Original		53.3 (0.4)	15.9 (0.5)	
	24 hr Rinsed		78.4 (0.6)	11.0 (0.2)	
	Fragments		82.4 (0.5)	12.0 (0.9)	
6	Pine Chip	700			9.7 (0.3)
	Original		84.7 (1.2)	13.5 (0.5)	
	24 hr Rinsed		90.5 (0.2)	8.4 (0.2)	
	Fragments		91.7 (1.0)	7.9 (0.6)	
7	Hardwood	500			12.9 (1.6)
	Original		86.4 (0.2)	20.4 (0.8)	
	24 hr Rinsed		92.4 (0.3)	6.3 (0.3)	
	Fragments		93.0 (0.5)	5.4 (0.2)	
8	Macadamia nut shell	500			18.7 (2.0)
	Original		68.4 (1.2)	26.4 (1.8)	
	24 hr Rinsed		87.4 (3.1)	14.9 (1.2)	
	Fragments		89.7 (3.2)	11.4 (4.1)	
	FIELD EXPOSED BIOCHARS				
F1	Macadamia nut shell	500			24.9 (2.3)
	Original		55.4 (2.1)	36.4 (2.8)	
	24 hr Rinsed		65.7 (1.1)	11.0 (2.1)	
	Fragments		75.3 (2.1)	10.2 (1.9)	
F2	Hardwood Charcoal	550			34.9 (4.5)
	Original		92.4 (1.1)	19.4 (1.8)	
	24 hr Rinsed		95.1 (1.8)	9.6 (1.2)	
	Fragments		95.8 (3.1)	10.2 (1.4)	

Note: Processing and characterization of biochars are outlined elsewhere (Novak et al. 2014; Spokas 2013).

In addition, water rinsed biochars showed some interesting physical surface features, including occasional microscopic erosion features (Figure 2.3). These features suggest that the water shaking did remove material from the biochar surface leaving these relic erosion structures. In addition, the biochar surfaces had smaller micron and sub-micron size pieces of biochar that were structurally freed from the biochar particle (Figure 2.4). The results show water rinsing not only removed the fine biochar particles which are loosely attached to the biochar particle surface (via physical forces, see Figure 2.1A), but also modifies the surface morphology of the biochar particle itself removing material by physical forces. This exfoliation and structural friability of BC has been noted in other studies with exposure to water, particularly in an alkaline environment(Huisman et al. 2012). Biochar physical breakdown is more pronounced in lower temperature biochars (<500 ^{o}C), where >50% of mass loss could be attributed to this physical fragmentation process (Braadbaart, Poole, and van Brussel 2009). This increased friability could be responsible for its quicker transport through laboratory columns (Wang et al. 2013). Therefore, biochar particle size should not be regarded as a static property.

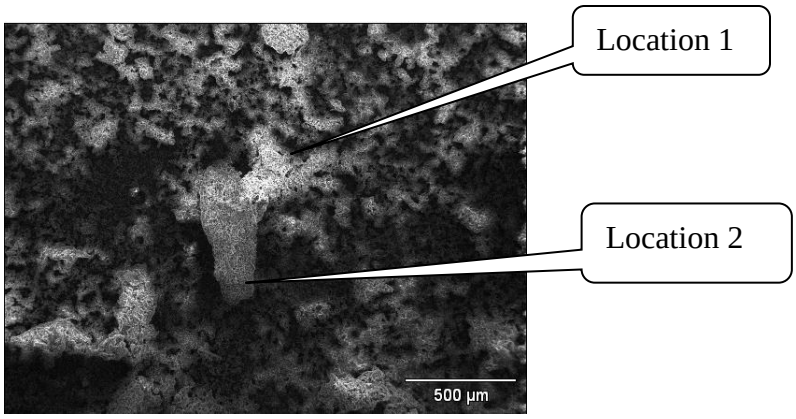

EDS Atom % Estimates

Location	*C*	*O*	*Na*	*Mg*	*Al*	*Si*	*P*	*S*	*Cl*	*K*	*Ca*	*As*	*Pd*
1	45.44	10.39	0.64	-	0.31	-	3.72	1.48	12.67	14.72	10.62	-	
2	--	19.08	2.26	0.69	11.79	0.88	0.43	-	36.62	28.04	-	-	0.22

Figure 2.3. A SEM image of a microscopic erosion feature seen on the surface of a poultry litter biochar. The KCl/clay particle (30 micrometers in width and 450 micrometers in length determined by the ruler tool in the SEM software) was suspended on a spire of some type of mixture of inorganic salts and BC fragments. Notice the difference in the EDS spectra for the two materials. The exact formation mechanisms are unknown, but do mimic erosion features seen in geologic areas (e.g. Goblin Valley, UT USA. See pictures at http://photosandsuch.wordpress.com/category/goblin-valley/).

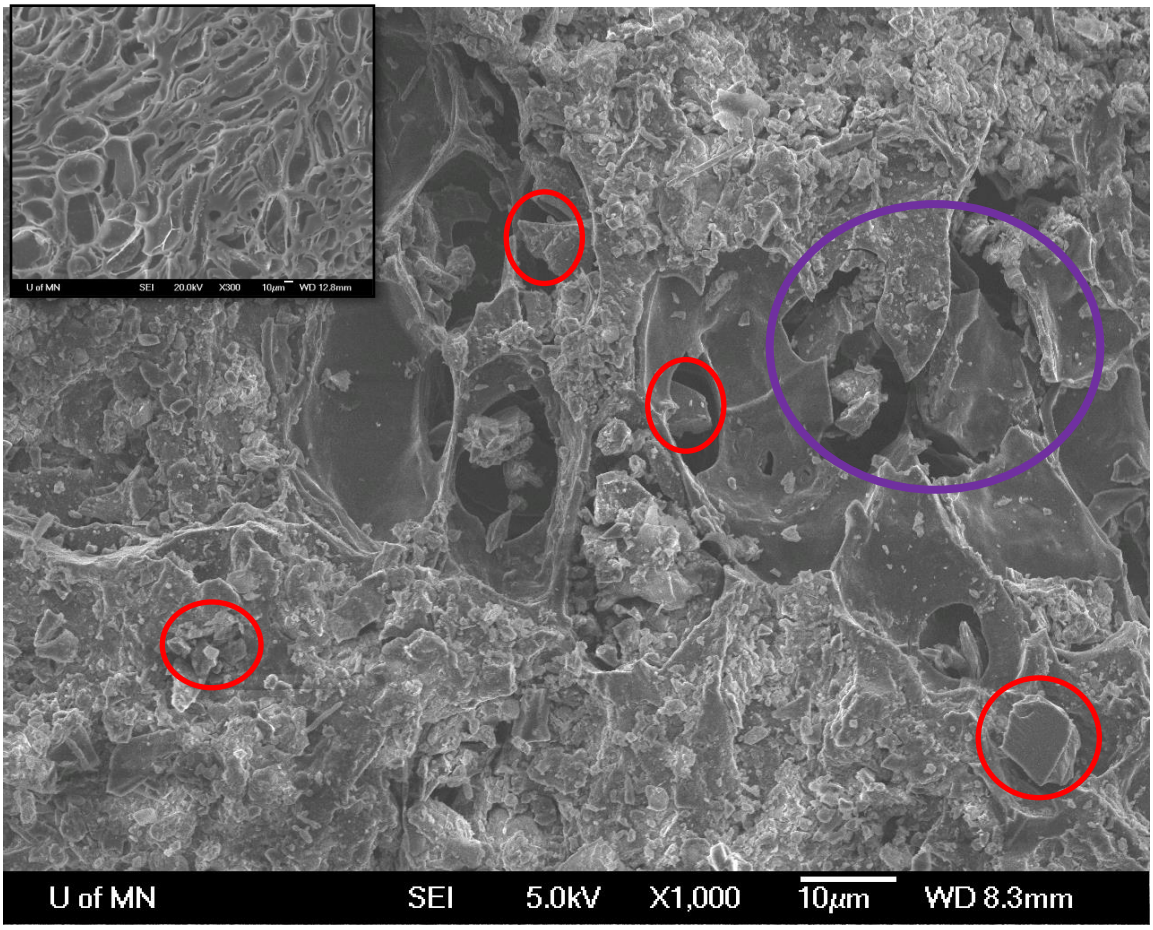

Figure 2.4. Illustration of the 5-year field exposed macadamia nut biochar. Note the collection of soil particles that are now on the surface (compared to Figure 2.1). The other feature is the large number of small pieces of biochar that have fragmented from the original biochar structure; a few of these pieces are highlighted with red circles. The purple circled area illustrates a section of the graphite sheet that has failed (or collapsed). This physical degradation was assumed due to the field exposure, since these biochar fragments and collapsed features were not observed on the original biochar (see inset in upper left corner and Figure 2.1).

In addition to these comminution processes, there was also evidence of cracking and fracturing of the biochar surface both with water and soil exposure (Figure 2.5 & 2.6). The SEM images present a suggestion of weaker layers of BC in the biochar matrix that are preferentially broken-down during water extraction (Figure 2.5), analogous to geologic sediment layer and geologic outcrop weathering (Dahlen and Suppe 1988). The original biochar prior to water rinsing is in Figure 2.7. More importantly, there are visible fragments from the biochar that have broken off from the parent BC physical structure (Figure 2.5). These disassociated BC fragments are estimated to range in size from nanoscale to over 100 µm as estimated through measurement with SEM software tools (e.g., ImageJ). This fragmentation occurs more readily in sandy textured soils (Figure 2.6). From our observations, wood and high lignin feedstocks appear to disintegrate into smaller particles more readily than the corresponding feedstocks with higher cellulose contents (e.g., manures, grasses, corn stalks). Higher pyrolysis temperature leads to smaller fragment formation, consequentially lower physical mass loss rates. This temperature dependency has already been noted for archeological reconstructions (Braadbaart, Poole, and van Brussel 2009) and the biochar particle size dependency agrees with observations of biochar particle movement in laboratory column (Wang et al. 2013) and field studies (Major et al. 2010).

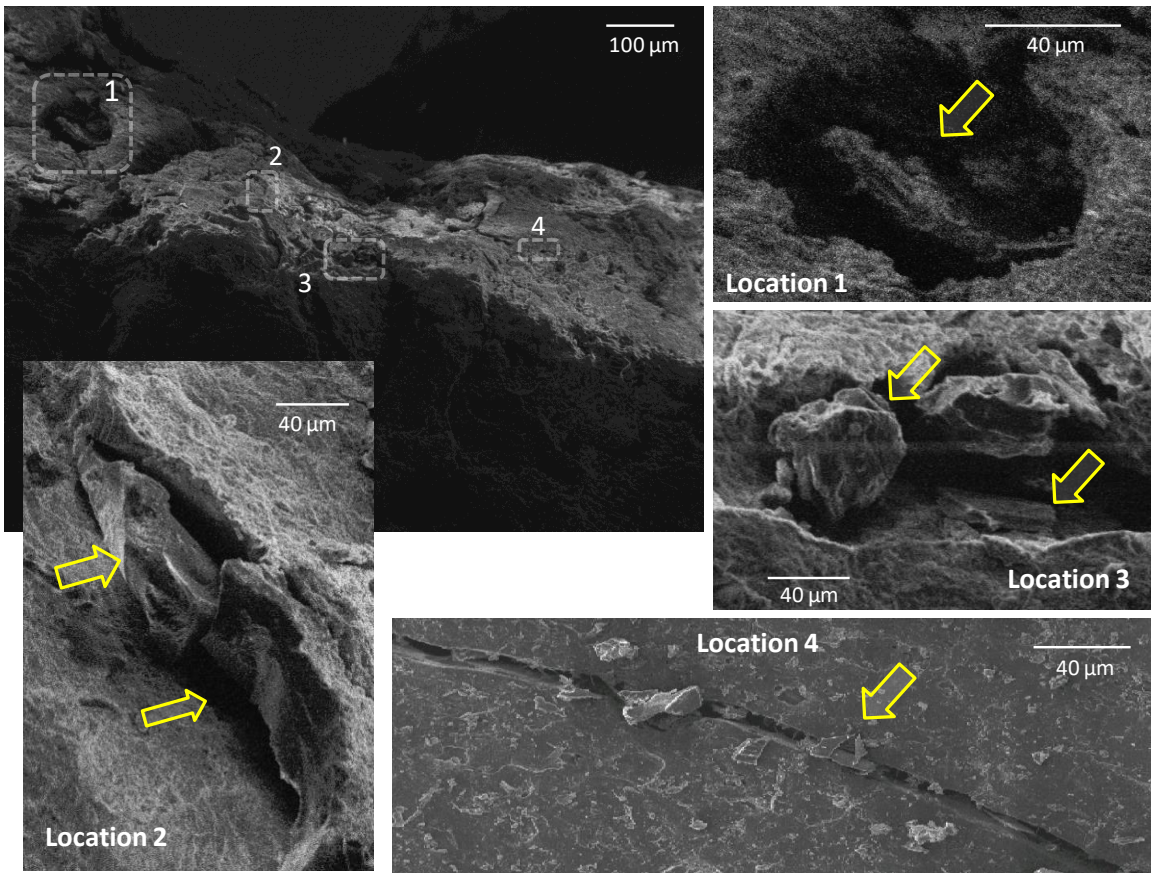

Figure 2.5. SEM images after 24 hr rinsing of a pine chip:poultry litter biochar (BC# 5). Location 1 illustrates a local collapse in the BC structure (i.e. sink hole) with a liberated BC particle approximately 100 microns being formed. Location 2 illustrates the expansion of the intrasheet spacing between the graphitic layers resulting in the structural failure (fragment designated by arrow). Location 3 illustrates the preferential erosion by water of the weaker BC layers, leading to the fragmentation of the top layer as support is removed. Location 4 illustrates a developing fracture in the biochar particle. Original biochar is shown in Figure 2.7. Arrows highlight described features.

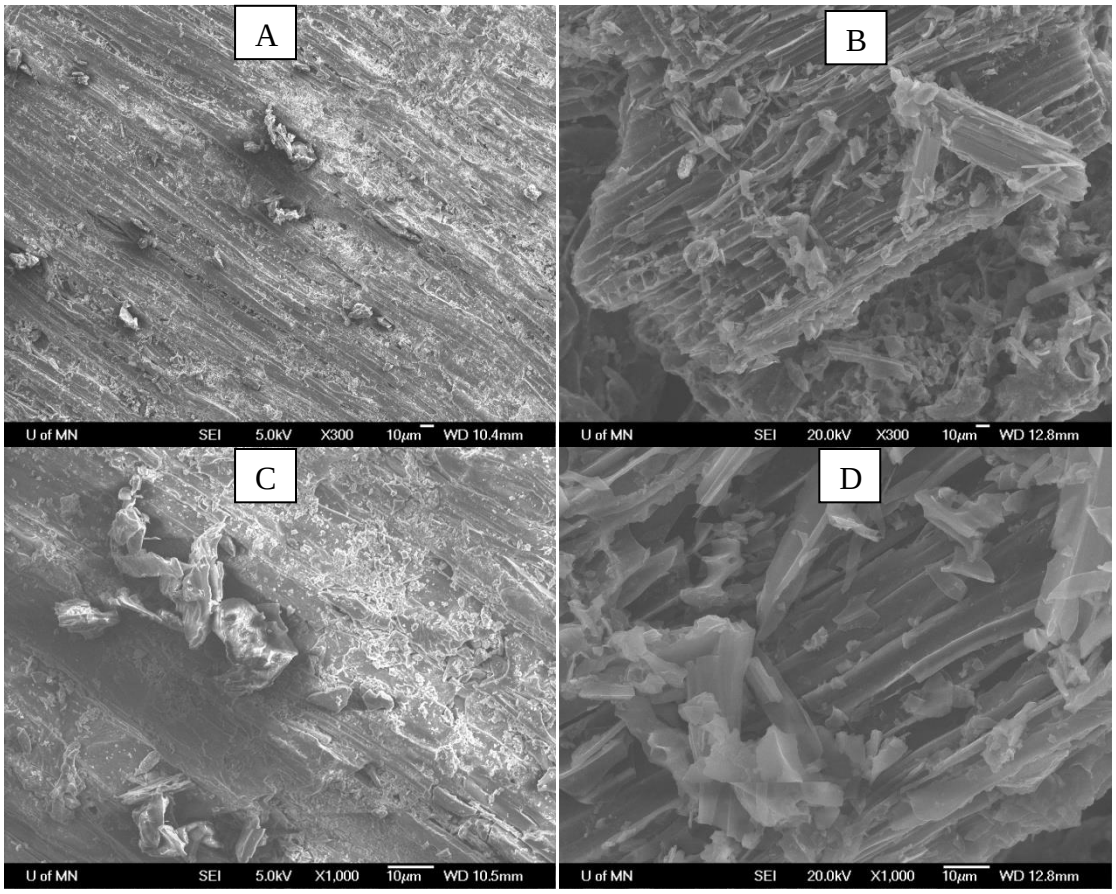

Figure 2.6. SEM images of the same biochar (wheat mids, slow pyrolysis) with a clay rich soil (A & C) and a fine sand soil (B & D) at 5% by weight at 30x and 1000x magnification. The biochar piece was manually removed from the mixture and analyzed by SEM imagery. The clay rich soil caused the biochar to become coated with a clay mineral veneer and the fine sand soil resulted in significant fragmentation. This could be a major mechanism for the dependency on soil texture (more favorable plant responses in sandy soils). This breakdown would be exposing the inner layers of the biochar to the soil environment, whereas the clay mixed biochar is protected from physical disintegration mechanisms.

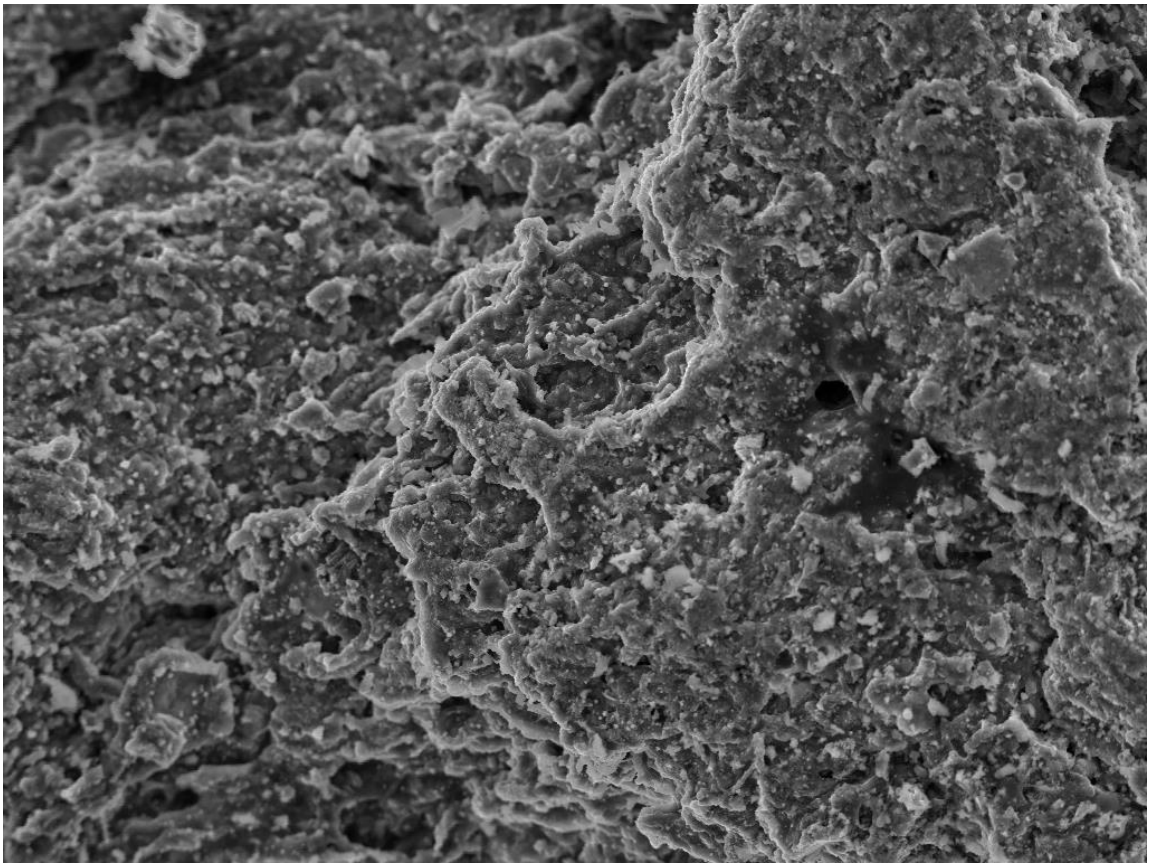

Figure 2.7. Illustration of the original poultry litter biochar – without rinsing. Compare with Figure 2.5 for post-water rinsing.

Despite being dislodged from the original biochar particle, these biochar pieces are chemically equivalent to the original biochar as confirmed by SEM-EDS data (Table 2.1). In other words, these fragments do not show signs of oxidative or other chemical weathering, just physical comminution. In the evaporated portion of the water extraction, we observed <20 μm and nanoscale particles of BC that were not removed by filtration (Figure 2.8). The presence of nanoscale particles have been previously demonstrated for pyrolyzed BC materials (Joseph et al. 2013) and could alter the mobility of sorbed organic compounds on these fragments (Ngueleu, Grathwohl, and Cirpka 2013). The presence of this DBC is important, since the typical dissolved organic carbon (DOC) analysis via persulfate-UV might not adequately detect these fragments of DBC without more intense chemical oxidation conditions (Glaser et al. 1998). This lack of quantification might further account for the "black carbon paradox" and confirms the suggestion by Jaffe et al. (Jaffé et al. 2013). To put this rapid mass loss in perspective, a recent study observed less than 5% of the carbon in biochar was mineralized over a 8.5 yr laboratory incubation (Kuzyakov, Bogomolova, and Glaser 2014).

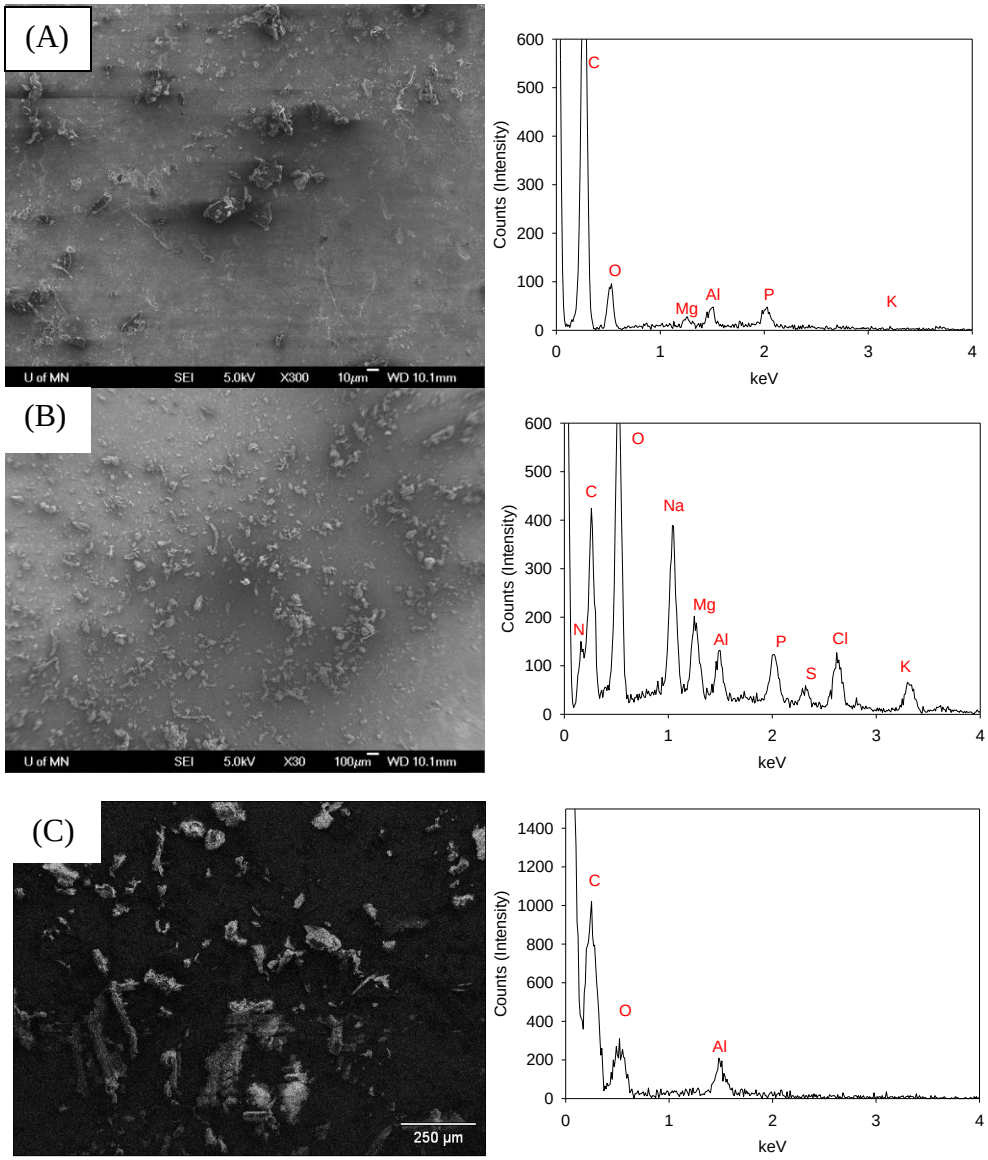

Figure 2.8. Illustration of observed particles in 100 uL of rinse water evaporated on a SEM mount for A) hardwood biochar (BC # 7), B) poultry litter biochar (BC# 9), and C) switchgrass biochar (BC# 1). The corresponding spectral scan of the view areas with EDS is shown immediately to the right of each panel. The presence of an Al peak could be due to the SEM mount itself and not conclusive evidence for its presence in the biochar rinse water (Table S1). There is evidence of a peak for carbon, but its exact amount cannot accurately be determined from this analysis.

Others have observed that once biochar is exposed to soils, soil particles can fill exposed cavities and fissures (Spokas 2013). These sealing processes could be accelerated by exothermic water sorption onto BC surfaces (Bangham and Razouk 1938) and accelerate desiccation drying. It is conceivable that the physical accumulation of colloidal, dissolved and particulate material, including soluble inorganic salts and/or alumino-silicates would rapidly infill fractures and pores (Brodowski et al. 2005). This infilling could potentially stabilize the BC particle from further physical degradation, analogous to the soil mineral protection of native soil organic material (Schmidt et al. 2011). Soil particle stabilization of biochar does require further scrutiny, but could be an essential mechanism for extending biochar's longevity, particularly in clay-rich soils.

It is well known that natural physical processes cause abrasion on geologic materials and shape their external morphology. We hypothesize that once charcoal is placed in the soil environment, it is subject to similar weathering and aging processes that act upon all geologic materials. While a majority of the current research has focused on surface chemical and microbial reactions, our observations stress the overwhelming importance of the physical friability of biochar and the need to account for the corresponding protection mechanisms when predicting long-term soil behavior.

2.5. Acknowledgements:

The information in this chapter was funded in part by the U.S. Environmental Protection Agency and the United States Department of Agriculture-Agricultural Research Service. It has been subjected to review by the National Health and Environmental Effects Research Laboratory's Western Ecology Division and approved for publication. Approval does not signify that the contents reflect the views of the Agencies, nor does mention of trade names or commercial products constitute endorsement or recommendation for use.

The author would like to acknowledge the exceptional laboratory work conducted by Martin DuSaire, Eric Nooker, Laura Colosky, Lee Yang, and Rena Weis. Parts of this work were carried out in the Characterization Facility-University of Minnesota, which receives partial support from National Science Foundation (NSF) through the Materials Research Science and Engineering Centers (MRSEC) program. In addition, the authors would also like to acknowledge the partial funding from the Minnesota Corn Growers Association/Minnesota Corn Research Production Council and the Minnesota Agricultural Utilization Research Institute (AURI). This research is part of the USDA-ARS Biochar and Pyrolysis Initiative and USDA-ARS GRACEnet (Greenhouse Gas Reduction through Agricultural Carbon Enhancement Network) programs. The authors also greatly appreciate the comments from two anonymous reviewers that improved the clarity and impact of this manuscript.

Chapter 3. A Survey of Biochars: Interactions with Dissolved Nitrogen

3.1. Overview

Biochars, also known as black carbon or charcoal, were assessed in their capacities to remove and adsorb nitrogen from aqueous solutions. Laboratory batch-equilibrium studies were used to assess the liquid phase adsorption capacity of various biochars. The forms of nitrogen used in this experiment were dissolved ammonium (NH_4^+) and nitrate (NO_3^-). The materials investigated include 21 biochars, four Minnesota top soils, 12 biochar and soil (1:10, w/w) mixtures, and 3 reference materials. Approximately 86% of biochars statistically removed NH_4^+ and 77% statistically removed NO_3^- from aqueous solution. However, only 52% and 33% of biochars exhibited statistically significant adsorption through better fits to adsorption isotherms for NH_4^+ and NO_3^- respectively. Once mixed with soils (1:10, bc:soil, wt:wt), only 18% of biochars exhibited increased NH_4^+ adsorption over unamended soil. It is noteworthy that no biochar addition increased soil NO_3^- removal or adsorption capacities. From this study, we hypothesize that biochar alone is likely to remove NH_4^+ from aqueous solution, while possessing a reduced impact on NO_3^- removal. Furthermore, biochars have a limited ability to alter N removal and adsorption upon soil additions at 10% soil amendments (wt/wt).

3.2. Introduction

Biochar is often associated and justified by the Amazonian Dark Earths (ADEs), also known as *Terra Preta de Indio* (TPI; Portuguese for Dark Earth of the Indians), located in the Amazonian River Basin, which today is a more fertile soil as compared to the surrounding weathered Oxisols (German 2003). Supported by the confirmation that ADEs contain a higher black carbon content, it has been hypothesized that the indigenous populations intentionally added biochar in soil to improve crop productivity (Glaser et al. 2001). Due to the stark difference between the ADE soil and the Oxisols, researchers further hypothesized that the elevated black carbon (biochar) concentrations are responsible for the improved agronomic ADE performance (Liang et al. 2006). However, research on soil enhancement with black carbon amendments have been inconsistent (Jeffery et al. 2011; Atkinson, Fitzgerald, and Hipps 2010). Even though a higher black carbon concentration occasionally correlates with increased soil productivity, the exact mechanisms have remained elusive. This has led to an increased effort to understand the mechanisms behind how black carbons may influence soil fertility.

Coal, charcoal, gunpowder, and activated charcoal are some examples of black carbons that previously have been extensively researched for various purposes from energy production to water filtration (Highwood and Kinnersley 2006; Malanima 2006). However, since the dawn of agricultural research, charcoal amendments to soil have been attempted and researched (Durden 1849). Within agriculture, previous research demonstrates that black carbons insignificantly add direct plant available nutrients, implying that if biochars affect soil fertility, they must do so indirectly by affecting the interaction between soil and plant growth factors (Biederman and Harpole 2013). Reasons suggested for the observed

crop yield variations in black carbon amended soil experiments include affecting cation exchange capacities, changing microbial populations/diversities, and interacting with soil nutrients (Glaser et al. 2001; DeLuca et al. 2006; Laird et al. 2010; Bailey et al. 2011). Notably, black carbon soil amendments do appear to reduce nitrogen leaching (Glaser, Lehmann, and Zech 2002; Spokas, Novak, and Venterea 2012; Barnes et al. 2014) and increase N-retention times (Asada et al. 2006; Laird et al. 2010; Yao et al. 2012), which have lead the same researchers to hypothesize that biochar may affect nitrogen leaching rates through nitrogen adsorption.

Nitrogen adsorption is a particularly compelling explanation for enhanced soil N-retention. Biochar and black carbons have been long-known to adsorb various substances (Hunter 1863). Individual chemical components in smoke (i.e., karrikins, cyanohydrins, strigolactones) are known to impact seed germination and plant growth (Nelson et al. 2012). These and other compounds have been observed adsorbing to black carbons (Spokas et al. 2011). Furthermore, studies have reported direct evidence of biochar removing ammonia and nitrate from both gas and aqueous solutions (Mizuta et al. 2004; Tsukagoshi et al. 2010; Taghizadeh-Toosi et al. 2011). Nitrate ions are removed from aqueous solution by a variety of processes. Some of these include: 1) chemical reduction with iron (Hansen et al. 1996; Huang and Zhang 2004), 2) microbial denitrification with carbon sources (Robertson, Ford, and Lombardo 2005), 3) autotrophic denitrification utilizing iron as the electron donor in the microbial reactions (Su and Puls 2007), 4) autotrophic denitrification with sulfur as the electron donor source (Furumai, Tagui, and Fujita 1996), 5) physical adsorption (Chatterjee et al. 2009), and 6) precipitation reactions (Otto, Blank, and Dahl 1988). The dilemma that remains, then, is to determine whether

biochar as a class of materials exhibit nitrogen retention properties, and to determine the primary adsorption mechanisms.

Laboratory adsorption kinetic studies provide a means of determining the nitrogen adsorption capacities of materials in a timely and efficient manner. Typically, in biochar adsorption studies there are a limited number of biochars examined, whereas other factors are examined to elucidate the material's adsorption behavior under different conditions (e.g. pH; temperature). However, because biochar is a diverse class of materials, there has not been a wide-reaching assessment of its ability to adsorb nitrogen. The present study aims to survey biochars in their capacity to adsorb nitrogen under standard laboratory conditions. Furthermore, since a primary objective in biochar research is to increase soil fertility, this study also includes adsorption tests of soil-biochar mixtures to improve our understanding into the effect of biochar additions on soil N-retention.

3.3. Materials and Methods

3.3.1 Biochar

The production and acquisition of biochars used in this study was previously described by Spokas et al. (2011). As a brief overview, biochars were obtained from a variety of commercial and research sources and were manufactured under an array of production processes, including homemade, laboratory, and pilot scale pyrolysis equipment. Because some biochars were created in pyrolysis units lacking industrial process monitoring equipment, not all production parameters are known. Nonetheless, biochars without fully known production parameters were included among the employed suite to capture variability in biochars currently available. There were 21 different biochars evaluated in this study (Table 3.1). All biochars were evaluated as received from the various suppliers. Three general conversion technologies were used to produce black carbons, which include fast pyrolysis (1), slow pyrolysis (16), and microwave-assisted pyrolysis (2). Pyrolysis unit definitions are further discussed by Spokas et al. (2011). The parent materials used to produce temperature sequence sets were soybean residue, coconut coir, urban yard waste (mixed leaves and grass), and pine pellets. One steam activated charcoal from a parent material of bituminous coal was included in this study.

Table 3.1. Biochar Source Information

Black Carbon	Parent Material	Supplier	Production Scale	Style	Temperature (°C)
Mix Wood 1	Mixed Hardwoods	eBay Lister 1	Homemade	Slow	n.a.
Mix Wood 2	Mixed Woodchips	Univ. of MN	Homemade	Slow	n.a.
Mix Wood 3	Mixed Hardwoods	Univ. of MN	Homemade	Slow	n.a.
Mix Wood 4	Hardwood Pellets	Chip Energy	Mass Prod.	Slow	n.a.
Mac. Nut	Mac. Nut Shell	Eterna Green	Mass Prod.	Fast	n.a.
Wheat Midds	Wheat Middlings	ICM	Mass Prod.	Slow	550
DDGs	Dried Distiller Grains	Univ. of MN	Laboratory	MAP	n.a.
Corn:DDGs	50:50, Stover:DDGs	Univ. of MN	Laboratory	MAP	n.a.
Mix Pine 550	Pine Woodchips	ICM	Mass Prod.	Slow	550
Mix Pine 650	Pine Woodchips	Sylva Corp.	Mass Prod.	Slow	650
Soy Res. 350	Soybean Stover	USDA-ARS	Laboratory	Slow	350
Soy Res. 500	Soybean Stover	USDA-ARS	Laboratory	Slow	500
Soy Res. 700	Soybean Stover	USDA-ARS	Laboratory	Slow	700
Coconut 350	Coconut Coir	USDA-ARS	Laboratory	Slow	350
Coconut 700	Coconut Coir	USDA-ARS	Laboratory	Slow	700
Urban 350	Yard Waste	USDA-ARS	Laboratory	Slow	350
Urban 500	Yard Waste	USDA-ARS	Laboratory	Slow	500
Pine Pell. 400	Pine Pellets	USDA-ARS	Laboratory	Slow	400
Pine Pell. 550	Pine Pellets	USDA-ARS	Laboratory	Slow	550
Unk. Biochar	n.a.	eBay Lister 2	Homemade	n.a.	n.a.
Activated Coal	Bituminous Coal	ACUREL	Mass Prod.	Act.	n.a.

3.3.2. Soil and Reference Materials.

Four Minnesota soils and three reference materials were included in this study. The physical and chemical properties of each soil are given in Table 3.2. Surface soil (0-5 cm) was collected from all sites (Fig. 3.1), sieved to <2 mm and homogenized for the incubation study. The Forest Nursery Soil was collected from the Hayward Wisconsin State Nursery (Hayward, WI) and was previously described by Spokas and Reicosky (2009). The agricultural soil (Rosemount) was collected from the University of Minnesota's Research and Outreach Station in Rosemount, MN. The Waukegan silt loam soil was collected near Morris, MN and the Becker sand was collected near Becker, MN (Fig. 3.1). Soil texture and TOC were determined with the hydrometer method (Gee and Bauder 1986) and the loss on ignition method (Nelson and Sommers 1996), respectively. The concrete was purchased from a local hardware store. Commercially available nitrate and phosphate removers (Rolf C. Hagen Corp, MA) were utilized as positive controls.

Table 3.2. Soil Physical Properties

Soil	Location	Soil Type	Sand (%)	Silt (%)	Clay (%)	TOC (%)	Moisture Capacity -33kPa (%w/w)
Becker, MN	45.50 ° N; 93.80° W;	Sandy, fridgid, entic hapludol (Hubbard loamy sand)	92	3	5	1.2	6
Hayward, WI	46.00 ° N; 91.30° W;	Vials loamy sand (sandy, Mixed, frigid, Entic Haplorthod)	84	9	7	1.1	12
Morris, MN	46.00 ° N; 91.30° W;	Barnes-Aastad, clay loam	40	40	20	2.5	24
Rosemount, MN	44.75 ° N; 93.07 ° W;	Wauken silt loam (fine-silty, over skeletal mixed super active, mesic typic Hapludoll)	22	55	23	2.6	15

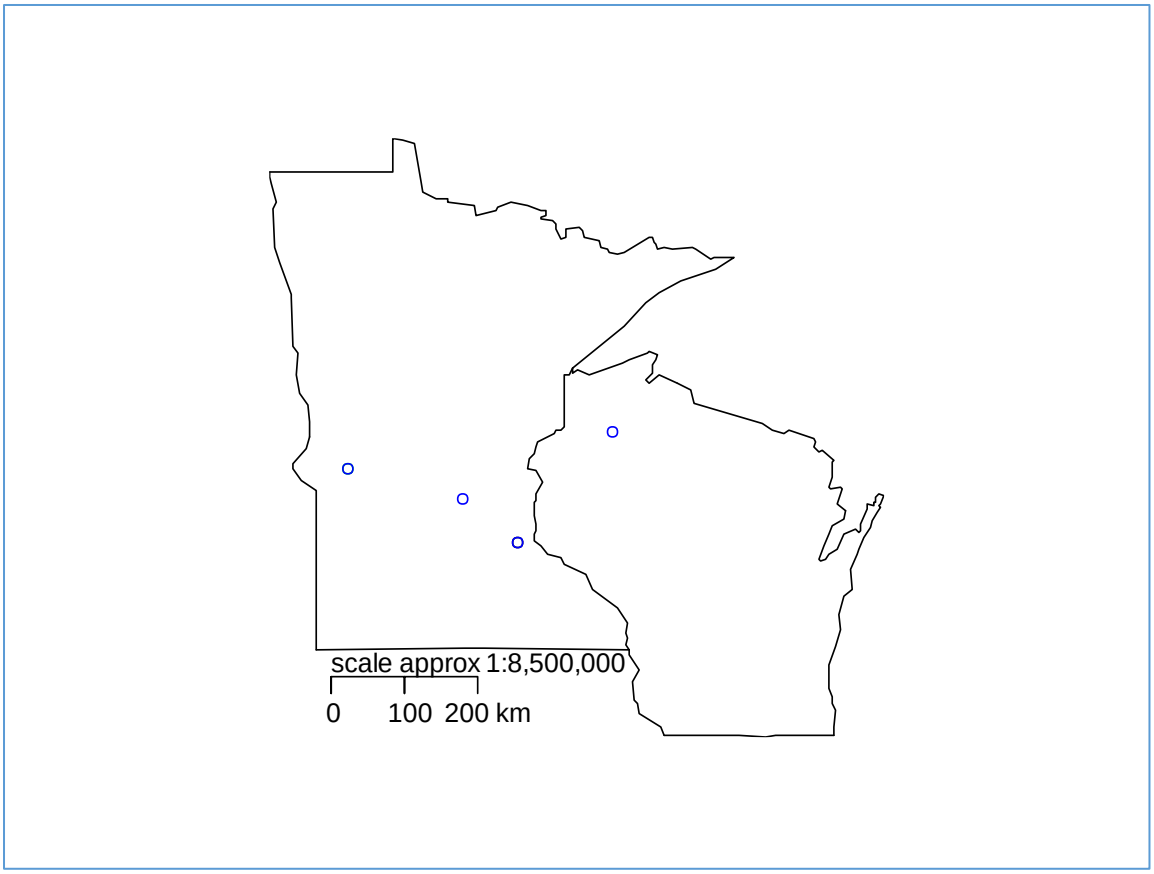

Figure 3.1. Locations where soil was sampled for this study (4 blue circles).

3.3.3. Ultimate, Proximate and pH Analysis

All materials used in the experiment were characterized by ultimate (ASTM D5373/D3176) and proximate analysis (ASTM D121/D5142/D7582), performed by Hazen Research (Golden, CO). The pH values were determined in a 1:5 (1g sample to 5 mL distilled water) slurry.

3.3.4. Batch Equilibrium Incubation and Analysis

Precisely 0.7634 g of ammonium chloride and 1.444g of potassium nitrate were dissolved in 1 L of 0.2 M phosphate buffer at pH 6.5 to produce a standard analyte solution of both 200 $mg \cdot L^{-1}$ $N(NH_4^+)$ and 200 mg $N(NO_3^-)$ per liter. Approximately 1 g of sample was placed into a 50 mL polypropylene centrifuge tube. The standard nitrogen solution and 0.2 M phosphate buffer were added at ratios of 0:30, 0.5:29.5, 1:29, 2:28, 4:26, and 6:24 to produce 0, 3.3, 6.6, 13.3, 26.6, and 40 mg $N \cdot L^{-1}$, respectively. The samples were shaken for 24 (±2) hours then were centrifuged for 5 min at 5000 rpm (Sorval RC-90). The samples were filtered (Whatman #2 filter paper) into polyethylene bottles and immediately frozen (-5 C°). The remaining solid sample was discarded. At the time of analysis, the frozen samples were thawed, shaken and analyzed for nitrogen (N) in the forms of ammonium (NH_4^+) and nitrate (NO_3^-) concentrations using a colorimetric injection-flow analyzer (Latchat QuickChem 8000 FIA Analyzer). Latchat QuickChem methods 12-107-06-2-A and 12-107-04-1-B were used for N-(NH_4^+) and N-(NO_3^-) analyses, respectively. Standards were run intermittently throughout the run and were used to correct for any observed instrument base line drift. The amount of N adsorbed was calculated using the following equation:

$$q_{ed} = \frac{C_i - C_e}{M_s} * V,$$

where q_{ed} is the amount of nitrogen adsorbed per unit mass of adsorbent at equilibrium ($mg \cdot g^{-1}$), C_i is the initial nitrogen concentration ($mg \cdot L^{-1}$), C_e is the equilibrium concentration ($mg \cdot L^{-1}$), V is the volume of the solution (L) and M_s is the mass of the sorbent (g).

In this experiment, the analyte is nitrogen either in the form of NH_4^+ or NO_3^-. The material substrate is one of either a biochar, soil, or a soil – biochar mixture. A primary assumption of the batch-equilibrium incubations was that the analyte existed within only one of two phases, either mobile aqueous phase or an immobile sorbed phase. In order to verify this assumption, first the experimental results must show that nitrogen was statistically removed from solution. In the customized adsorption-analysis Python modules, this is accomplished by fitting the data to a linear isotherm, represented as:

$$q_{ed} = K_d * C_e,$$

where K_d is the Linear isotherm constant, C_e is the liquid equilibrium concentration, and q_{ed} is the equilibrium sorbed concentration. For these incubations, it is assumed that the sorbed material was estimated by the difference between the initial material present and the observed liquid concentration.

The best fit linear isotherm is statistically ($\alpha = 0.05$) examined by the following hypothesis set:

$$H_0: K_d \leq 0,$$

$$H_a: K_d > 0,$$

where H_0 and H_a are the null and alternative hypotheses. In the case that a material's K_d

value is not greater than zero, then the material does not statistically remove N from solution, and theoretically cannot sorb N either. If the material's K_d value is statistically greater than zero, then other isotherms were fit against the data set and a best fit isotherm was selected by minimization of the sum of squared residuals [Akaike Index Criterion (AIC) or Bayesian Index Criterion (BIC)] to describe the adsorption behavior.

In this study, AIC was used to select the best fitting adsorption isotherm. A best fit linear isotherm indicates nitrogen removal occurs but not that the mechanism of removal is adsorption. If adsorption has occurred, the linear isotherm describes a constant behavior, where for any given concentration of an analyte in the mobile phase there will always be a constant offset amount in the immobile phase. However, other processes such as microbial N-uptake, atmospheric equilibration can conceivably remove N from solution through a linear relationship. Therefore, two other adsorption isotherms are used to determine adsorption occurrence beyond N removal.

One of the isotherms used to express adsorption behavior is the Freundlich isotherm, represented as:

$$q_{ed} = K_f * {C_e}^{1/n},$$

where K_f is the Freundlich isotherm constant related to the adsorption capacity and n is the adsorption intensity (Foo and Hameed 2010). The Freundlich adsorption model is one of the earliest model used to explain non-ideal and reversible adsorption of an analyte onto a material (Freundlich 1906). This model is often applied to multi-layered adsorption process over a heterogeneous surface, and describes an adsorption process where binding sites on the material substrate's surface are occupied in order from strong to weak sorption energy in a pattern of exponential decay. Nonetheless, where the Freundlich isotherm describes a

material's adsorption behavior well within the stated conditions of an experiment, it should not be used to extrapolate adsorption behavior beyond the range of concentrations used in this study. The Freundlich model is empirical by nature and does not approach Henry's law for vanishing concentrations, which means it lacks a fundamental thermodynamic basis (Foo and Hameed 2010). Therefore, in this study a best-fit Freundlich isotherm suggests that adsorption is a prominent nitrogen removal mechanism within the constraints of the experimental design, but it does not indicate that adsorption is the only removal mechanism or quantifies the limit (or capacity) of adsorption.

The other isotherm used to determine whether a material adsorbs nitrogen is the Langmuir isotherm, represented as:

$$q_{ed} = \frac{Q_o * K_l * C_e}{1 + K_l},$$

where K_l is the Langmuir isotherm constant and Q_o is the material's maximum mono-layer coverage capacity ($mg \cdot g^{-1}$). Data that fits a Langmuir isotherm suggests that adsorption is the primary removal mechanism of nitrogen, where Q_o is the equilibrium saturation point between C_e and q_{ed}. Often the Langmuir isotherm is used to characterize a homogeneous mono-layer adsorption process, where all adsorption sites express an equal affinity for adsorption (Foo and Hameed 2010). Although complex chemical systems do not meet the stringent requirements of all adsorption sites expressing equal affinities for adsorption, if a complex material (such as a biochar or soil) expresses an equilibrium saturation point, then the equilibrium mono-layer may be described as the layer of all available adsorption sites within the material. Therefore, in this study a best fit Langmuir isotherm model is not only used to state that adsorption occurs, but also determines the maximum adsorption capacity (Q_o).

3.3.5. Statistics

Adsorption results were analyzed using the *Python* programming language (Version 3.4). I designed statistical analysis and curve-fitting functions following commonly used statistical methods within the *numpy, scipy*, and *lmfit* packages for Python (Python Software Foundation. Python Language Reference, version 3.4. Available at http://www.python.org). This customized code is available on a GitHub repository (https://github.com/firebaker/adsorption-analysis). All graphs were produced using *matplotlib* and all statistical analyses used an alpha of 0.05 ($p < 0.05$).

3.4. Results and Discussion

3.4.1. Biochar Properties

Biochar pH values were predominantly alkaline (8.8 ±1.1) ranging from slightly acidic (6.2) to strongly alkaline (10.7). Ash contents (16.6 ±13.1%) and air-dried moisture content (8.0 ± 11.5% w/w) had considerable variation ranging from 1.9% to 55.5% and 2.4% to 56.6%, respectively. The carbon content was generally high (68.7±14.8%w/w) with less variation than other properties. In comparison, oxygen (10.9±8.0 %) and hydrogen (2.12±1.49 %) contents were lower. Biochar's nitrogen and sulfur fractions were lower than either carbon, oxygen, or hydrogen (Table 3.3). Overall, the pH and elemental composition match previously published ranges for other biochars (Yargicoglu et al. 2015; Atkinson, Fitzgerald, and Hipps 2010; Chan and Xu 2009; Singh, Singh, and Cowie 2010).

Table 3.3. Ultimate and Proximate Analysis of Biochars

Biochars	pH	H_2O	Ash	C	O	N	H	S
Mix Wood 1	9.08	6.49	13.26	71.87	12.16	0.60	2.08	0.03
Mix Wood 2	7.04	15.54	14.29	51.70	29.95	0.25	3.77	0.04
Mix Wood 3	9.42	3.67	1.86	91.88	5.30	0.40	0.54	0.02
Mix Wood 4	10.18	6.79	10.78	82.94	4.13	0.42	1.70	0.03
Mac. Nut	6.20	9.54	1.92	93.15	1.68	0.67	2.56	0.02
Wheat Midds	8.86	3.62	12.53	81.83	4.75	0.52	0.32	0.05
DDGs	9.00	4.92	17.35	73.08	1.20	6.69	1.05	0.63
Corn:DDGs	9.50	3.27	24.56	70.00	1.54	2.81	0.68	0.41
Mix Pine 550	9.54	11.27	25.20	64.33	6.16	3.11	1.16	0.04
Mix Pine 650	6.60	6.08	5.19	73.94	17.31	0.24	3.30	0.02
Soy Res. 350	8.28	4.11	17.80	57.40	18.95	1.43	4.40	0.02
Soy Res. 500	8.89	3.87	37.51	48.00	11.07	1.26	2.12	0.03
Soy Res. 700	10.74	4.59	33.42	56.24	8.10	1.17	1.01	0.06
Coconut 350	8.41	4.68	11.12	64.13	20.51	0.47	3.74	0.02
Coconut 700	9.47	4.35	13.95	71.75	12.72	0.52	0.98	0.07
Urban 350	8.08	4.20	13.89	59.07	20.23	2.00	4.81	0.00
Urban 500	9.16	5.56	17.50	63.07	14.53	2.12	2.74	0.03
Pine Pell. 400	8.84	4.19	2.72	75.60	17.27	0.10	4.33	0.00
Pine Pell. 550	8.49	2.42	3.59	77.15	16.22	0.18	2.86	0.00
Unk. Biochar	9.60	56.55	55.47	32.75	0.00	0.16	0.00	0.00
Activated Coal	9.40	3.21	10.24	83.00	5.47	0.43	0.52	0.35

Notes: All values reported are percent by dry weight (w/w_{DB} x 100), with the exception of moisture content (H_2O), which is percentage by wet weight.

3.4.2. Temperature Effect on Biochar Properties

Pyrolysis temperature do correlate positively with sulfur ($r^2 = 0.50$) and negatively with oxygen ($r^2 = 0.36$) and hydrogen ($r^2 = 0.58$). All other elemental correlations with temperature were trivial ($r^2 < 0.11$). The H:C ($r^2 = 0.65$), O:C ($r^2 = 0.47$), and (O+N):C ($r^2 = 0.49$) ratios correlated negatively with pyrolysis temperature. Others have observed similar trends with the exception that generally with increasing pyrolysis temperatures there is an increase in dry ash content (Yao et al. 2012; Gai et al. 2014). However, across several feedstock and pyrolysis units, these relationships do not appear to be as strong or universal as often stated. Typically, existing laboratory studies examine biochars immediately after production. However, in the case of this experiment, biochars possessed variable storage times and conditions. Remembering that storage conditions affect biochar properties such as oxygen content, surface moieties, ash content and moisture values, these alterations could affect the overall response of the soil system to biochar additions (LeCroy et al. 2013; Iida et al. 2013; Delaplace et al. 2015; Spokas 2013; Puri et al. 1958; Puri, Murari, and Singh 1961).

3.4.3. Soil Properties

Soil pH values ranged from slightly acidic (4.8) to neutral (6.8) with a mean of 5.7 (± 0.9), which is common for the Upper Midwest US. The soil ash content (93.7 ±3.4) was expected for mineral soils (Table 3.4). The percent soil moisture (0.64 ± 1.0) for the air-dried soils was rather consistent given the range in textures. The total carbon (3.0 ± 1.1%) and oxygen (2.9 ± 2.1%) fraction of the evaluated soils was low.

Table 3.4. Ultimate and proximate analysis for soils and reference materials.

Soils	pH	H_2O	Ash	C	O	N	H	S
Rosemount	5.23	2.19	92.50	3.72	3.35	0.26	0.13	0.03
Morris	6.84	0.12	89.45	4.10	5.64	0.27	0.32	0.00
Hayward	4.78	0.14	96.50	2.08	1.26	0.11	0.00	0.00
Becker	6.02	0.11	96.49	2.01	1.38	0.00	0.00	0.00

Reference Material	pH	H_2O	Ash	C	O	N	H	S
Concrete	10.16	1.70	95.03	3.60	0.98	0.10	0.39	0.00
Phosphate Remover	7.31	3.87	88.01	1.71	8.79	0.10	1.48	0.00
Nitrate Remover	2.84	54.55	0.00	70.54	15.79	4.00	9.59	0.08

Notes: All values reported are percent by dry weight (w/w_{DB} x 100), with the exception of moisture content (H_2O), which is percentage by wet weight.

3.4.4. Nitrogen incubations

3.4.4.1. Biochar N Sorption Incubations.

Among the 21 biochars investigated for NH_4^+ adsorption, 18 (86%) showed statistically significant NH_4^+ removal and 11 (52%) expressed NH_4^+ adsorption behavior by a best fit Freundlich or Langmuir isotherm (Figure 3.2). The 3 biochars that removed the most NH_4^+ at the initial concentration of 40 mg N-(NH_4^+) · L^{-1} were coconut coir 350 ºC, macademia nut shell, and soybean residue 350 ºC. These biochars also expressed adsorption behavior by best fits to either Freundlich or Langmuir isotherms and were selected for further experimentation as soil amendments.

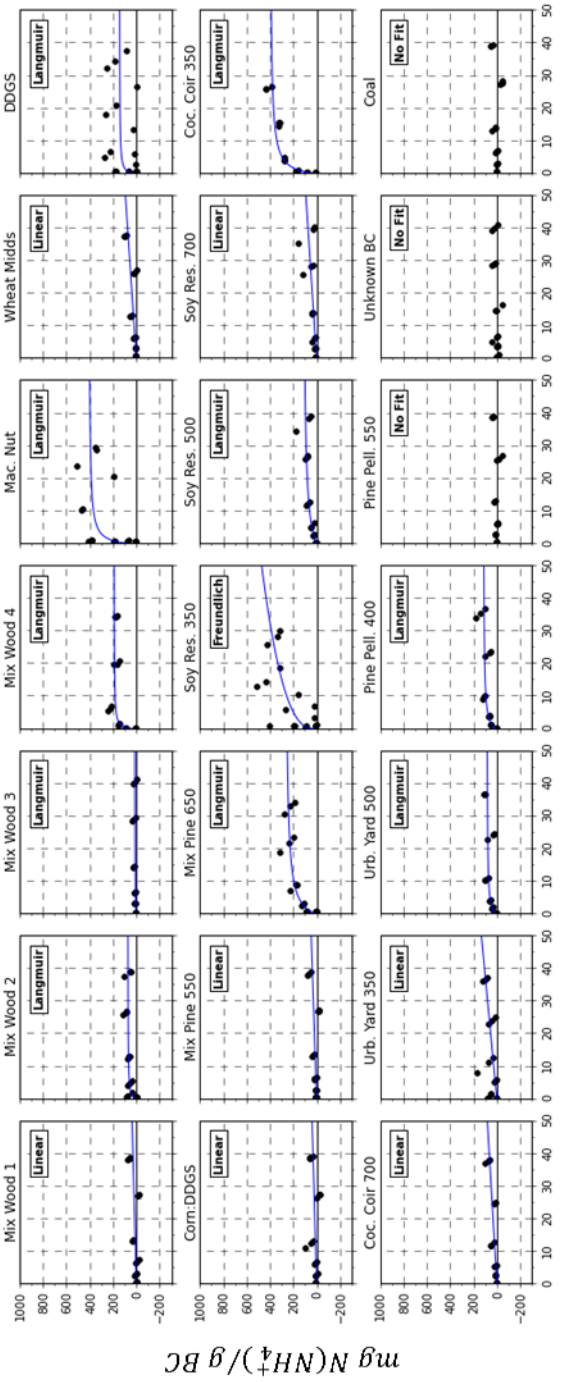

Figure 3.2. Black carbon best fit NH_4^+ adsorption isotherms.

In contrast to the NH_4^+ results, 15 (71%) of the black carbons showed statistically significant NO_3^- removal and 7 (33%) expressed NO_3^- adsorption described by a Langmuir isotherm (Figure 3.3). The 4 biochars that removed the most NO_3^- at the initial concentration of 40 mg $N(NO_3^-)$ L^{-1} were mixed hardwood #3, activated bituminous coal, coconut coir 700C, and soybean residue 700C. Mixed hardwood #3, coconut coir 700C, and soybean residue 700C were selected for further experimentation as soil amendments. Activated bituminous coal was not selected for further examination, since it isn't considered a biochar as it is not created with the intent to sequester carbon or for soil application.

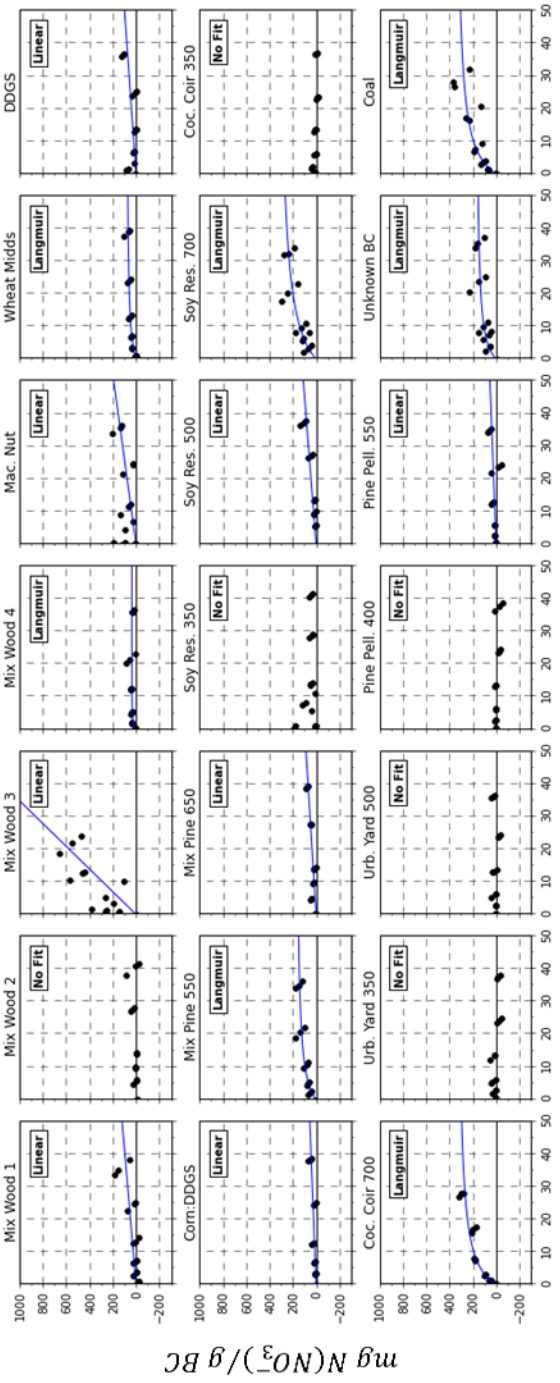

Figure 3.3. Black carbon best fit NO_3^- adsorption isotherms.

Biochars exhibited a greater affinity for removing NH_4^+ from aqueous solution than NO_3^-, which is consistent with results from other studies (Yao et al. 2012; Gai et al. 2014). Upon examining the best fit isotherms, where NH_4^+ is more likely to be removed from solution and adsorbed, NO_3^- is only likely to be removed. For both forms of N, fewer biochars fit adsorption isotherms than those that removed nitrogen, suggesting the possibility that separate processes compete with adsorption during nitrogen removal (Haider et al. 2016). Importantly, for both types of nitrogen, neither the removal nor adsorption pass the 95% confidence limit needed to state that biochars as a class of materials, remove or adsorb N from aqueous solution.

Interestingly, no physical nor chemical biochar property correlated with the maximum removal of NH_4^+ ($r^2 < 0.15$). Similarly, no biochar property was strongly associated with the maximum removal rate of NO_3^-; however, ash content ($r^2 = 0.22$), % air-dried moisture content ($r^2 = 0.36$), C content ($r^2 = 0.22$), and H content ($r^2 = 0.24$) do seem to be weakly correlated. This suggests that these physical and chemical biochar properties are not strongly associated with NO_3^- removal.

Among the pyrolysis-temperature-gradient sets of biochars, temperature negatively correlated with NH_4^+ removal ($r^2 = 0.29$). In contrast, temperature positively correlated with NO_3^- removal ($r^2 = 0.70$). These results indicate that within sets of biochars produced from the same starting material, pyrolysis temperatures play a trivial and significant role for NH_4^+ and NO_3^- removal, respectively. Both Yao et al. (2012) and Mizuta et al. (2004), observed similar results for NO_3^- removal among pyrolysis-temperature-gradient biochars produced from the same starting materials.

Previous studies suggest that acid functional groups (Asada et al. 2002; Kastner, Miller, and Das 2009) specifically carboxylic oxygen groups (Spokas, Novak, and Venterea 2012) are responsible for gaseous NH_3 removal. However, within this study and others pertaining to aqueous solutions (Yao et al. 2012), biochar pH values do not correlate with NH_4^+ removal/adsorption. This potentially suggests that in aqueous solutions different mechanisms are responsible for NH_4^+ removal than for NO_3^- removal. Proposed mechanisms for NH_4^+ removal in aqueous solution by biochars include electrostatic attraction with other cationic species on the biochar surface (Mukherjee, Zimmerman, and Harris 2011), NH_4^+ capture within biochar pores (Jansen and van Bekkum 1994; Vinke et al. 1994; Haider et al. 2016), and the intercalation of NH_4^+ between graphitic sheets (Seredych, Tamashausky, and Bandosz 2010).

The removal of NO_3^- from aqueous solution is a well-studied phenomenon, especially since the USEPA dictates that NO_3^- levels must meet drinking water standards [<10 ppm] (Reilly, Horne, and Miller 1999). Activated black carbons and activated biochars have been shown to adsorb nitrate from aqueous solution (Mizuta et al. 2004; Namasivayam and Sangeetha 2005; Iida et al. 2013). Two primary mechanisms have been proposed for nitrate adsorption by black carbon species, chemisorption and anion exchange (Namasivayam and Sangeetha 2005). In both mechanisms, nitrate is captured by the black carbon surface functional groups, however, only the anion exchange mechanisms allow for subsequent desorption of nitrate. Black carbon surface area, porosity, and pore volume positively correlate with nitrate adsorption tendencies (Namasivayam and Sangeetha 2005; Zanella, Tessaro, and Féris 2015), and when observed provides further mechanistic evidence for adsorption's occurrence. Furthermore, previous studies have shown that increasing

pyrolysis temperatures activate the black carbon, i.e. increase the surface area and pore volume. In the present study, among biochars produced from the same parent material along a temperature sequence, temperature correlated with increased nitrate removal. However, nitrate adsorption was not significant in all cases across all biochars.

Although not all biochars are chemically activated, some may exhibit similar properties to activated carbons. Clearly, in regards to the present study, nitrate adsorption by biochars are not dictated by elemental and chemical properties alone. An objective of this study was to determine whether biochars as a class of materials adsorb nitrate. With only 33% of biochars in this study exhibiting nitrate adsorption behavior, clearly, biochars as a class of materials do not adsorb nitrate. However, some biochars do possess nitrate sorbing properties, although have a very limited sorption capacity. Future research would benefit from focusing on the physicals and chemical mechanisms of favorable nitrate adsorbing biochars.

Multiple studies have investigated whether biochars can be used in biological denitrification systems (Christianson et al. 2011; Bock et al. 2015). Denitrification is generally understood to follow the microbial driven chemical reactions. (Firestone et al. 1979) However, the quality of the added residue controls microbial mineralization rates (Broder and Wagner 1988; Qin et al. 2015). Nonetheless, studies show that non-aromatic carbon provides the least complicated (lowest activation energy) form of carbon utilization in biological processes (Qin et al. 2015). Questions remain on whether the graphitic carbon framework structure of biochars is utilizable by microbes or not (Zimmerman, Gao, and Ahn 2011). The present study is not broad enough in scope to determine whether biologically driven denitrification occurred during the experiments. Kinetic investigations

can provide insight into the mechanisms and fundamental pathways of reactions in a system and thereby are useful for determining the potential mechanisms involved in the observed sorption processes. Future nitrate-biochar adsorption experiments would benefit from measurements of either microbiological activity and/or N_2 outgassing (the byproduct of denitrification), which could direct conclusions on whether biological denitrification occurs during biochar NO_3^- removal.

3.4.4.2. Soil N Incubations

Among the 4 soils, only 2 showed significant but slight amounts of NH_4^+ removal (Figure, 3.4), while none of the soils alone expressed NH_4^+ adsorption (Figure 3.5). Additionally, none of the soils expressed NO_3^- removal or adsorption.

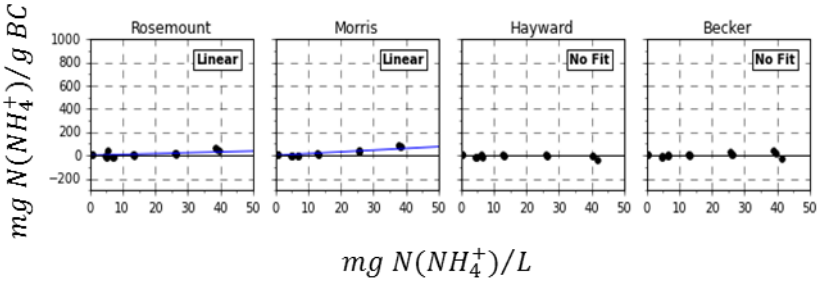

Figure 3.4. Soil best fit NH_4^+ isotherms. adsorption

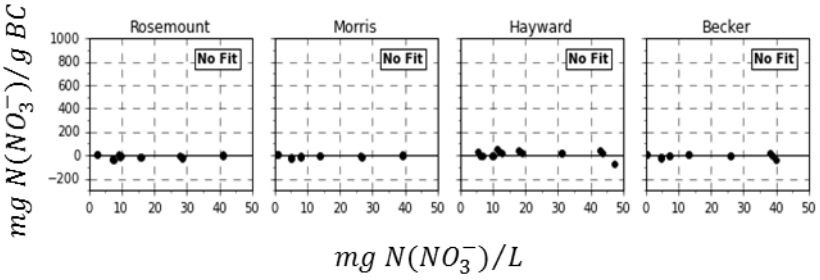

Figure 3.5. Soil best fit NO_3^- adsorption isotherms.

3.4.4.3. Reference Materials N Incubations.

Among the commercial sorbents, the phosphate remover and concrete showed statistically significant NH_4^+ removal, but did not express adsorption (Figure 3.6). The nitrate remover did not show NH_4^+ removal behavior, see Figure 3.6. In contrast to the NH_4^+ results, the nitrate remover removed most NO_3^- from solution (> 1000 mg/g), as expected (Figure 3.7). Neither the phosphate remover nor concrete showed statistically significant NO_3^- removal, see Figure 3.7.

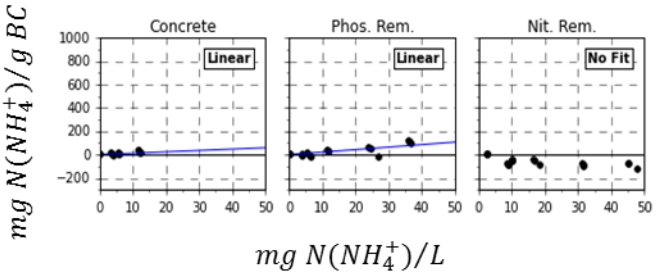

Figure 3.6. Reference material best fit NH_4^+ adsorption isotherms.

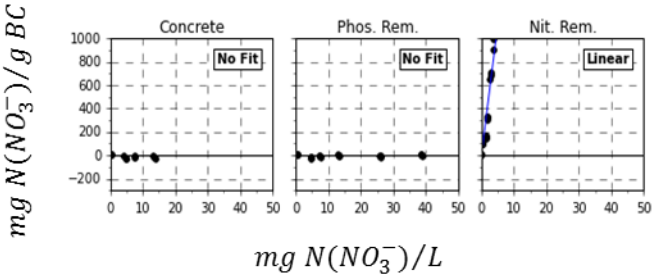

Figure 3.7. Reference material best fit NO_3^- adsorption isotherms.

3.4.4.4. Biochar Amended Soil N Incubations.

Of the 12 soil and black carbon mixtures, all (12/12) showed significant NH_4^+ removal (Figure 3.8). However, only 3 (25%) expressing NH_4^+ adsorption by a best fit Langmuir isotherm. In contrast, none of the soil – biochar mixtures showed statistically significant NO_3^- removal (Figure 3.9). Recalling that the selection criteria for biochars to be amended to soils was the 3 best at removing NH_4^+ and NO_3^-, there was a suppression in the observed sorption from the biochar alone (Biochar 100%). For the NH_4^+ results, only 2 (Rosemount with Coconut Coir 350, and Morris with Soybean Combine Residue 350) out of 12 soil and biochar combinations showed an increase in nitrogen removal over the soil results without biochar amendments. No biochar amended soil was observed to alter removal of NO_3^-.

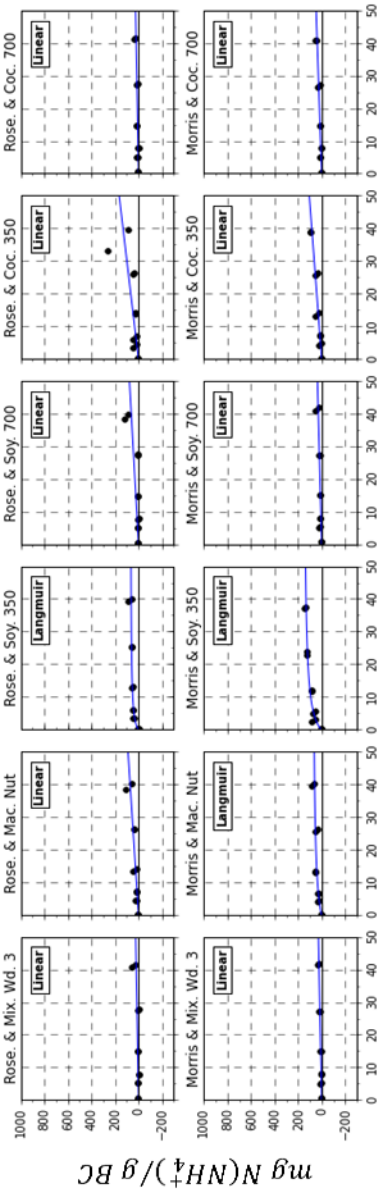

Figure 3.8. Soil + 10% black carbon amendment best fit NH_4^+ adsorption isotherms.

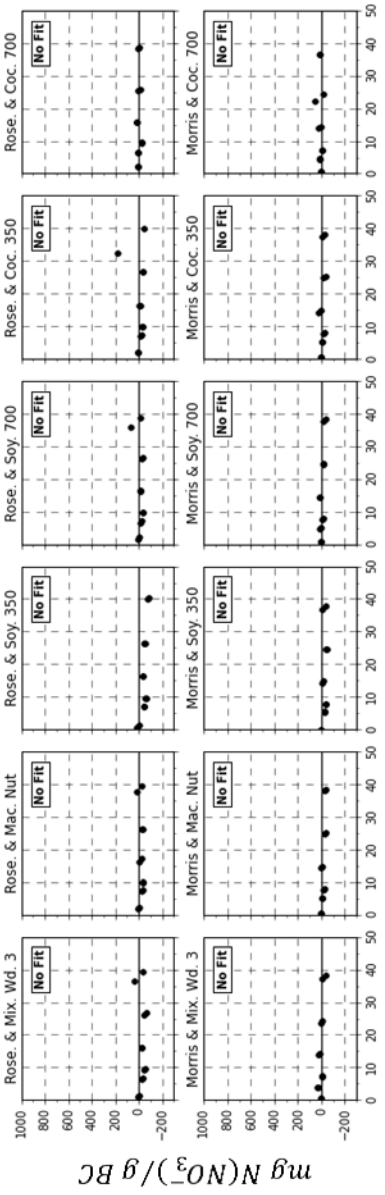

Figure 3.9. Soil + 10% black carbon amendment best fit NO_3^- adsorption isotherms.

Many studies have investigated how biochar soil amendments affect nitrogen leaching. Studies on the Amazonian Dark Earth soils (a.k.a. *Terra Preta* soils), showed that these sites had reduced N leaching when compared to the surrounding Oxisols (Glaser et al. 2001; Glaser, Lehmann, and Zech 2002). Later studies suggested that the reduced leaching was a result of the increased black carbon concentrations. For example, Midwestern USA soils Laird et al. (2010) showed that biochar amended soil columns decreased N leaching by 11% over control columns after fertilization with equal swine manure applications. Additionally, biochar amendments totally eliminated N and other nutrient leaching spikes, which at the time insinuated that biochar amendments increase soil N retention. Laird et al.'s (2010) study provides the best comparison to the present study, since biochar N adsorption studies have not previously investigated biochar amended soils, and Laird et al.'s (2010) study was conducted on geographically similar soils as the current study. Nonetheless, from the present study it seems that biochar amendments exhibit a capacity to reduce NH_4^+ leaching, while unable to modify NO_3^- leaching values.

3.5. Conclusions

The results seem to point towards biochars having a much greater affinity to remove NH_4^+ than NO_3^- from aqueous solution. Few biochar physical and chemical values correlate with NH_4^+ removal rates, albeit slightly. In comparison, for the biochars that do remove NO_3^-, pyrolysis temperature correlates strongly with NO_3^- removal. In examining biochar effects on biochar-amended soils, biochars have a reduced effect to remove NH_4^+ from soil solutions, but approximately ¼ of the biochar additions show statistically significant increases in NH_4^+ removal. The same cannot be said for NO_3^- removal, whatever effect biochars had on removing NO_3^- from aqueous solution, it completely disappeared in biochar soil amendments in this study.

Chapter 4. Preliminary Investigations for the Effect of Iron Mineralogy on Soil Gas Respiration

4.1. Overview

Biochar (a subset of black carbon materials) is often cited as the key factor for explaining the observed enhanced fertility of Amazonian Dark Earth soils when compared to natural occurring surrounding Brazilian Oxisols. This chapter proposes a new hypothsis surrounding Amazonian Dark Earth pedogenesis, which is the impact of contrasting iron mineralogy on soil microbial rates, which could then lead to differences in observed rates of soil carbon sequestration rates.

By examining the impact of iron mineralogy and black carbon amendments on soil microbial respiration rates, two unique observations were supported: 1) there are mineralogical differences between Amazonian Dark Earth and Brazilian Oxisol soil profiles and 2) these iron minerals affect soil microbial respiration rates differently when added to soil incubations. Differing soil microbial rates with time will indirectly alter carbon sequestration rates and soil fertility. The fundamental conclusion based on this data suggests that Amazonian Dark Earth research should consider iron mineralogical differences found between Amazonian Dark Earth ADE and Brazilian Oxisol soils.

4.2. Introduction

Most soils underlying the Amazonian Rain Forest (61% area) are classified as *Oxisols* by the USDA-NRCS soil classification system (Schaefer, Fabris, and Ker 2008). Of note, Brazilian Oxisol soils are classified as *Latosols* by the Brazilian soil classification system (Lima et al. 2002; Eswaran et al. 2002) and *Ferralsols* by the Food and Agricultural Organization of the United Nations (Eswaran et al. 2002). Brazilian Oxisol soils are often characterized as having greater concentrations of oxidized iron forms, and are notorious for their lack of nutrients and low concentrations of soil carbon (Macedo and Bryant 1989; Kämpf and Schwertmann 1983; Fontes and Weed 1991), which results in poor agronomic crop performance. Nonetheless, within small pockets of the Amazonian Rain Forest, generally 0.5 – 20 ha in areal extent, there exist a unique soil type known as *Amazonian Dark Earth* (ADE) (Kern et al. 2003; Neves et al. 2003), also referred to as *Terra Preta de Indio* (Portuguese for dark earth of the Indians). Amazonian Dark Earth soils are classified as *Anthrosols*, and owe their designation to the established hypothesis that they formed under human controlled conditions (Kämpf et al. 2003). Irrespective of the classification system, ADE soils share many properties with the agriculturally productive *Mollisol* soil types in other parts of the world (Campos et al. 2011). Amazonian Dark Earth soils exhibit dark colored epipedons (brown-to-blackish; 10YR3/1; 5YR2/2), strong fertility, high nutrient concentrations (i.e. nitrogen and phosphorus), and greater soil carbon accumulation than neighboring Brazilian Oxisol soils (Kämpf et al. 2003; Kern et al. 2003; Campos et al. 2011). Compared to Brazilian Oxisol soils, ADE soils are more fertile and are in high demand for agricultural use by the local population (Glaser et al. 2001; Neves et al. 2003), which is analogous to peat use in northern climates. The stark contrast between

these soil profiles is apparent from examining Figure 1 of Glaser et al. (2001).

While Brazilian Oxisol soils natively formed from local parent material over millions of years (Schaefer 2001), ADEs are believed to have formed after human influence on Brazilian Oxisol soils, where the primary influential component is the input of black carbon (i.e. charcoal or biochar) over the last 10 millennia (Glaser et al. 2000; Glaser et al. 2001). Many hypotheses have been proposed and investigated as to how black carbon soil amendments may increase soil fertility, which include affecting cation exchange capacity, changing microbial populations/diversities, and interacting with soil nutrients (Glaser et al. 2001; DeLuca et al. 2006; Laird et al. 2010; Bailey et al. 2011). However, research on biochar soil amendments, the proxy to black carbon soil amendments, has not elucidated a strong or consistent mechanistic understanding of how biochar (black carbon) converts a non-agriculturally productive soil into productive ADE soil (Biederman and Harpole 2013; Jeffery et al. 2011; Atkinson, Fitzgerald, and Hipps 2010).

While the greater scientific community hypothesized that enhanced concentrations of the black carbon within ADE sites account for their increased soil fertility and plant productivity, their conclusions relied upon the assumption that the mineralogical components between the Oxisols and ADEs were similar (Glaser et al. 2001). Recent studies, however, have shown that while elemental compositions are similar, there are significant differences in iron mineralogy between the two soil types: ADE soils display stronger magnetic susceptibility (Figure 4.1), thereby containing greater concentrations of magnetic iron forms, such as maghemite or magnetite (Silva et al. 2011). Given the fact that the presence of specific iron minerals have been linked to enhanced soil carbon stability (Kaiser and Guggenberger 2007; Adhikari and Yang 2015; Ketrot et al. 2013), and

iron minerals have been linked to soil microbial effects (Ding et al. 2013), there is a foundation for an alternative explanation on for how ADE soils retain carbon as a result of differing iron mineralogy, rather than solely through a function of the black carbon alone.

Iron is the fourth most abundant element within Earth, and comprises approximately 5% of the Earth's crust (Lutgens and Tarbuck 1999). Within agriculture, iron has been known to play a crucial role in soil fertility since the 1920's (Brewer and Carr 1926). Today, crop advisors are often taught that iron is a micronutrient that in scarcity or excess may reduce specific crop production (Hodges 1995). However, iron can affect crops indirectly by affecting soil ecosystem dynamics.

Within the soil column, iron may be analyzed through distinctly different methods. Soil iron may be differentiated into inorganic (mineral) and organic (organo-Fe) pools. Iron oxidation states, such as ferric (Fe^{3+}) and ferrous (Fe^{2+}) species, are often used to determine the mechanisms of various soil-iron chemical reactions. Additionally, different iron minerals, some even with the same atomic composition, display vastly different chemical, thermodynamic, and electro-magnetic properties (Chesworth 2008). Furthermore, research has shown that different iron minerals concentrate under separate pedogenic conditions (Schwertmann 1985). Brazilian Oxisols are highly weathered tropical soils that accumulate iron in the forms of hematite (Fe_2O_3) and goethite (α-FeOOH) (Schaefer, Fabris, and Ker 2008; Camargo et al. 2014). Hematite, goethite, and related aluminum-oxide weathering products, such as kaolinite and gibbsite, are known to aggregate strongly with organic matter (Chesworth 2008). Nonetheless, although various iron minerals such as hematite, goethite, and magnetite ($Fe^{2+}Fe^{3+}{}_2O_4$) have been shown in laboratory experiments to adsorb organic matter from aqueous solution (Adhikari and Yang

2015; Day et al. 1994; Safiur Rahman, Whalen, and Gagnon 2013), studies have noted positive relationships between non-hematitic iron and soil organic carbon accumulation in Brazilian Oxisol soils (Schwertmann 1971; Kämpf and Schwertmann 1983).

Established soil science theory dictates that soil carbon output is primarily controlled by microbial activity, where microbes consume soil organic matter and subsequently emit gases such as N_2, N_2O, CO_2, and CH_4 (Smith et al. 2003). Therefore, to understand how iron mineralogy affects soil carbon retention, we measured the impact of different soil iron mineralogical amendments on microbial respiration rates. Specifically, in this study we provide evidence for differences in iron mineralogy between one site's adjacent Brazilian Oxisol soil and ADE soil. We then evaluate the effect of five amendments to agricultural topsoil from Rosemount, MN, USA. Three iron mineral amendments (hematite, goethite, and magnetite) and two black carbon amendments were used in this study. Because previous research has shown that iron minerals adsorb and increase the stability of organic matter in soils, we hypothesize (H_{a1}) that all iron mineralogical amendments will increase carbon stability and subsequently decrease measurable soil respiration rates. Furthermore, because hematite has not been strongly correlated with organic matter in natural soils, we additionally hypothesize (H_{a2}) that goethite and magnetite amendments will decrease soil respiration rates to a higher degree than hematite.

4.3. Materials

4.3.1. Soil

Brazilian Soils. The study area is located to the south of the state of Amazonas, in

the vicinity of the Santo Antônio de Matupi, which is near the trans-Amazonian Highway (BR 319; 07º 59' 77.1" S and 61º 39' 51.2" W) (Figure 1a). The locations have an elevation of 60-150 m above sea level. Local inhabitants aided in the selection of the study areas. The climate is group A (Rainy Tropical) and Am (Monsoon Rains), per the Köppen classification system. Average annual temperatures range from 25 to 27 °C, and annual relative humidity is between 85 and 90 %. The area is a tropical rain forest, with dense trees between 20 and 50 m in height with dense tree cover. The Amazonian Dark Earth (ADE) area that was sampled had been cropped for 14 years. It is unknown when the tree cover was removed from this area. In the first six years, rice, corn, beans, and watermelon were grown, and later cacao was planted (as of the 2014, during sampling). The "natural" soil sample was taken from the edge of the neighboring rain forest. Soils were sampled in discrete intervals: 0-20, 20-40, 40-75, and 75-100 cm. Modifications did occur to these depth intervals when a discrete break in the soil horizons was noted close to the designated interval.

Minnesota, USA Agricultural Soil. The surface (0-5 cm) Minnesota agricultural soil was collected at the University of Minnesota's Research and Outreach Station in Rosemount, MN (Figure 1b). The soil was sieved to <2 mm and homogenized for the incubation study.

The physical properties of the soils used in this experiment are given in Table 4.1. Soil texture and total organic carbon (TOC) were determined with the hydrometer method (Gee and Bauder 1986) and the loss on ignition method (Nelson and Sommers 1996), respectively.

Soil analyses were performed for physical, chemical and mineralogical properties. The soils were classified per criteria established by the Brazilian Soil Classification System (Mattos 2006).

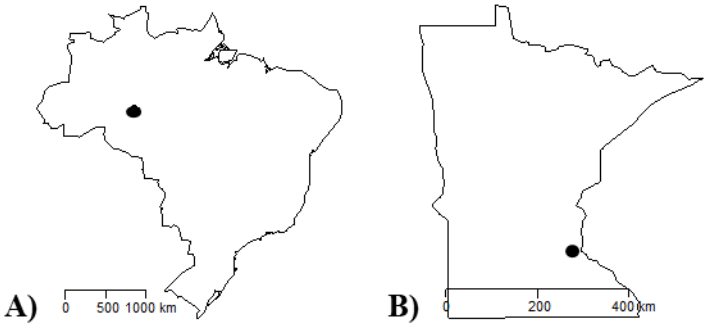

Figure 4.1. Location of (**A**) ADE and Forest sample sites within Brazil (the two locations were less than 1 km apart) and (**B**) location of Rosemount, MN in Minnesota for the agricultural soil sample.

Table 4.1. Soil Physical Properties

Horizon	Depth (cm)	Sand (coarse) $g.kg^{-1}$	Sand (fine) $g.kg^{-1}$	Silt $g.kg^{-1}$	Clay $g.kg^{-1}$	WDC $g.kg^{-1}$	GF %	Silt/Clay Ratio -	B_D $g.cm^{-3}$	P_D $g.cm^{-3}$	Φ_{TOT} -	Soil Color (Munsell)
Rosemount, MN												
A	0-15	220		550	230	n.a.	n.a.	2.39	n.a.	n.a.	n.a.	n.a.
Amazonian Dark Earth												
Ap1	0-19	246.19	145.64	412.17	196.00	94.74	38.55	2.10	1.49	2.60	43	7.5 YR 4/4
Ap2	19-35	367.32	143.79	289.13	199.76	114.88	42.49	1.45	1.73	2.87	40	7.5 YR 5/6
AB	35-64	282.24	131.87	258.85	327.04	226.64	30.70	0.79	1.74	2.88	39	7.5 YR 5/6
BA	64-89	253.67	122.98	155.75	467.60	319.42	31.69	0.33	1.86	2.90	36	7.5 YR 5/8
BT1	89-121	235.59	128.60	165.79	470.02	290.26	38.25	0.35	1.85	2.90	37	7.5 YR 5/8
BT2	121-150	267.08	119.93	153.17	459.82	266.98	41.94	0.33	1.84	2.88	36	7.5 YR 5/6
Forest (Brazilian Oxisol)												
A	0-20	n.a.	n.a.	n.a.	n.a.	n.a.	n.a.	n.a.	n.a.	n.a.	n.a.	n.a.
AB	20-35	n.a.	n.a.	n.a.	n.a.	n.a.	n.a.	n.a.	n.a.	n.a.	n.a.	n.a.
BA	35-58	n.a.	n.a.	n.a.	n.a.	n.a.	n.a.	n.a.	n.a.	n.a.	n.a.	n.a.
BW1	58-78	n.a.	n.a.	n.a.	n.a.	n.a.	n.a.	n.a.	n.a.	n.a.	n.a.	n.a.
BW2	78-102	n.a.	n.a.	n.a.	n.a.	n.a.	n.a.	n.a.	n.a.	n.a.	n.a.	n.a.
BW3	102-121	n.a.	n.a.	n.a.	n.a.	n.a.	n.a.	n.a.	n.a.	n.a.	n.a.	n.a.
BC	121-150	n.a.	n.a.	n.a.	n.a.	n.a.	n.a.	n.a.	n.a.	n.a.	n.a.	n.a.

4.2.2. Soil Amendments.

A total of 5 amendments were evaluated in the laboratory incubations, Table 4.2.

All the amendments were obtained and evaluated as received from the various suppliers.

Table 4.2. Soil Amendments

Amendment	Source	Source Label	Source ID No.
Goethite	Sigma-Aldrich	Goethite	71063
Hematite	Alpha Chemicals	Red Iron Oxide (Fe_2O_3)	n.a.
Magnetite	Sigma-Aldrich	Iron(II, III)	637106
Act. Charcoal	Sigma-Aldrich	Activated Charcoal	242233
Carbon (meso)	Sigma-Aldrich	Carbon, mesoporous	699632

4.3. Methods

4.3.1. Greenhouse Gas Incubations

For the Brazilian Oxisol and ADE comparison portion of this experiment, Brazilian Oxisol and ADE soils were used as received. For the iron and black carbon amendment portion of this experiment, soil and amendments were manually mixed in plastic bags prior to experimentation. A sequence of soil amendment additions, (0.20 %, 0.40 %, 1.96 %, 3.85 %, 7.41 %, 13.79 %; wt/wt) was used, which parallels previous laboratory soil incubation experiments with various black carbon species (Spokas et al. 2009; Yanai, Toyota, and Okazaki 2007). Control incubations with no amendment (0.00 % amendment) were examined with each soil amendment set to assess gas production/consumption rates of non-amended soils under the same experimental conditions. Incubations did not received microbial inoculum other than through possible contamination (from spores and re-colonization) during storage.

Experimental soils (5 g) and DI water (1 mL DI H_2O addition; soil moisture potential = -33 kPa) were added to incubation chambers and sealed, following the method from Spokas and Reicosky (2009). Briefly, independent triplicate incubations were conducted in sterilized 125 mL serum vials (Wheaton Glass, Millville, NJ) and sealed with red butyl rubber septa (Grace, Deerfield, IL). Periodic gas samples were withdrawn from the incubations for analysis on a gas chromatographic-mass (GC-FID; GC-ECD) system to quantify gas production over ~ 40 days of incubation. Production rates were calculated by taking the linear rate of change (slope) for gas production from day 4 - 21.

4.3.2. Gas Sampling and Analysis

To sample the incubations, initially 5 mL of air (known composition) was injected into the sealed vials. The syringe was flushed 5 times to allow for adequate mixing of the serum bottle headspace. Five milliliters of gas was then pulled back into the syringe and injected into a 10 mL sampling vial that was previously helium-flushed for analysis. Concentrations from the gas chromatograph (GC) were corrected for dilution from the 5 mL of air. The samples were analyzed on three GC columns, and three detectors, on two systems (GC-FID/TCD; GC-ECD) system described elsewhere (Spokas et al. 2009). Briefly, the GC system consisted of a headspace sampler (Agilent, Foster City, CA, model 7694) that was modified with the addition of a 10-port diaphragm sample valve (Valco, Houston, TX, model DV22-2116). In this fashion, the sampler injects two independent sample loops onto two different analytical columns that are contained in two gas chromatograph ovens (Agilent HP 5890).

The first column (60 µL loop) is a RT-Molesieve 5A (0.32mm x 30 m, Restek, Bellefonte, PA) with a 2.0 mL · min^{-1} He flow rate. The second column (120 µL loop) is a RT-QSPLOT (0.32mm x 30 m, Restek, Bellefonte, PA), also with a 2 ml · min^{-1} He flow rate. The third column (1.0 mL loop) is a CTR-1 (Grace; Deerfield, IL) with a 45 mL · min^{-1} He flow rate that is connected to a thermal conductivity detector (TCD) and flame ionization detector (FID) in series.

The GC quantifies CO_2 (3.5 min; column 2), N_2O (4.0 min; column 2), CH_4 (8.0 min; column 1). The TCD is used to quantify O_2 and N_2 and the FID is used as a supplemental quantification of CH_4. The column temperature program started at 35 °C for 5 minutes then to 120 °C at 20 °C · min^{-1} with a 0 min hold time for both columns. The

system is calibrated using multiple traceable gas standards (Scott Specialty Gases; Troy, MI and Minnesota Oxygen Supply; Minneapolis, MN).

4.3.3. Statistics

Results for the CO_2 and N_2O production and CH_4 oxidation activities were arithmetic means of triplicate samples calculated using Microsoft Excel. All greenhouse gas production rates were determined from the decrease or increase in concentration over time in the headspace of the incubation. Data were analyzed using an analysis of variance (ANOVA) procedure for independent samples to test for statistically significant differences using the Microsoft Excel Analysis ToolPak (Microsoft Corp. Redmond, WA, USA). If significant differences existed among the factors, as indicated by the F-ratio, a Tukey's Honest Significant Difference (HSD) test was performed to determine which pair-wise interactions were significantly different at $\alpha = 0.05$ (i.e. significant difference is indicated by $p \leq 0.05$).

4.4. Results

4.4.1. Organic Carbon Concentration, CO_2 Respiration Rates, and Magnetic Susceptibility Analysis of Adjacent Brazilian Oxisol and Amazonian Dark Earth Soils.

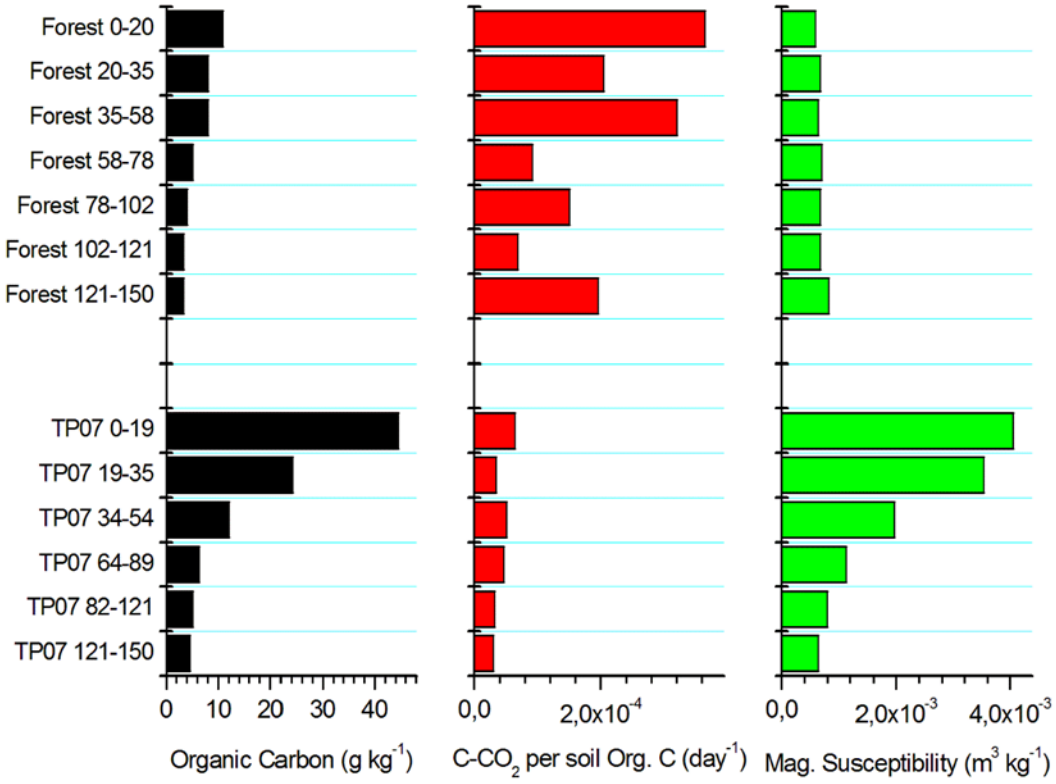

Figure 4.2. Comparison of an Amazonian Dark Earth (ADE) soil profile from the Amazon basin (see map inset above) and the companion forest soil profile near to this location. The graphs show the forest site (Forest) profile on the top section and the ADE soil (TP07) results on the bottom section of the figure. The main distinguishing differences are the normalized microbial respiration rates (C-CO_2 per organic carbon C day-1) and the magnetic susceptibility measurements. (Yang, 2012)

4.4.2. N_2O & CO_2 Production of Soil + Iron Minerals

4.4.2.1. Hematite Soil Amendments

N_2O The data shows no significant ($p = 0.242 > 0.05$) correlation ($R^2 = 0.08$) between soil N_2O respiration rates and concentration of hematite, Figure 4.3 (A). Notably, all the hematite amended soil incubations are not statistically different from the control soil incubations. Finally, hematite soil additions up to 13.79 % do not statistically ($\alpha = 0.05$) alter Rosemount, MN topsoil N_2O respiration rates under experimental conditions.

CO_2 Comparatively, there is no significant ($p = 0.467 > 0.05$) correlation ($R^2 = 0.03$) between soil CO_2 respiration rates and the concentration of hematite, Figure 4.3 (B). As with the N_2O respiration rates, all the hematite amended soil incubations did not show statistically different from the control soil incubation's rates. Therefore, hematite soil additions up to 13.79 % (wt/wt) concentration do not statistically ($\alpha = 0.05$) alter Rosemount, MN topsoil CO_2 respiration rates under experimental conditions.

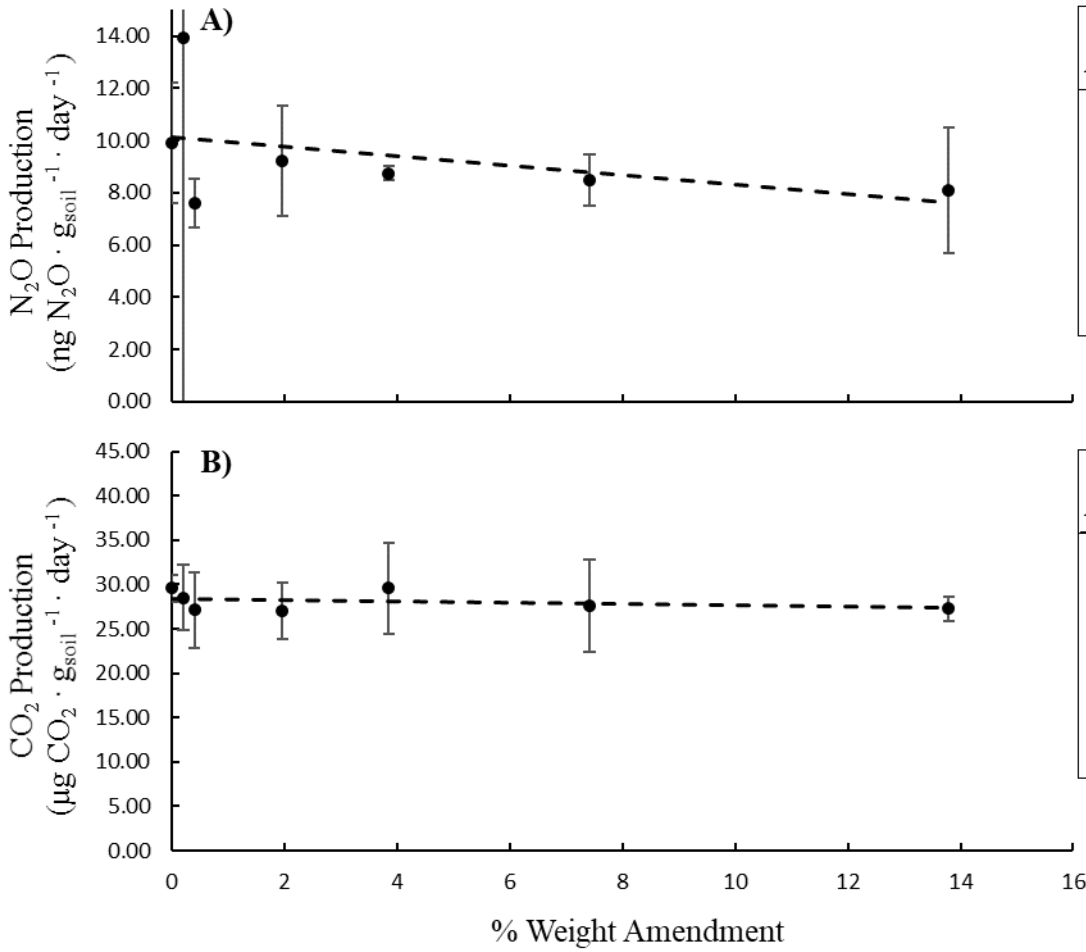

% Weight Amendment	(ng-N_2O g_{soil}^{-1} day^{-1})
0.00 %	9.90 (2.30)
0.20 %	13.94 (14.38)
0.40 %	7.59 (0.92)
1.96 %	9.22 (2.11)
3.85 %	8.74 (0.27)
7.41 %	8.49 (0.99)
13.79 %	8.09 (2.43)

Linear Regression	
m	-0.18 (0.15)
b	10.20 (0.97)
R^2	0.08
df_{n-2}	17
t_m	-1.21
p_m	2.42E-01

% Weight Amendment	(µg-CO_2 g_{soil}^{-1} day^{-1})
0.00 %	29.57 (1.49)
0.20 %	28.54 (3.73)
0.40 %	27.12 (4.22)
1.96 %	27.02 (3.15)
3.85 %	29.58 (5.17)
7.41 %	27.62 (5.15)
13.79 %	27.26 (1.40)

Linear Regression	
m	-0.07 (0.09)
b	28.22 (0.56)
R^2	0.03
df_{n-2}	17
t_m	-0.74
p_m	4.67E-01

Figure 4.3. N_2O (**A**) & CO_2 (**B**) production rates of Hematite soil amendments. XY-axis values are given in adjacent tables, 2σ (~ 95%) CI are shown in data plot whiskers and in table parenthesis. Fitted linear regression parameters are given in right most table.

4.4.2.2. Goethite Soil Amendments

N_2O Changes in soil N_2O respiration rates significantly ($p = 9.61E\text{-}4 < 0.05$) and positively ($m = 0.22$) correlate ($R^2 = 0.50$) with the concentration of goethite, Figure 4.4 (A). Additionally, the greatest concentration of goethite amended soil (13.79% goethite amendment) shows statistically ($p \leq 0.05$) significant difference of N_2O production from control soil incubations. Notably, although the 0.40%, 3.85%, and 7.41% goethite concentration incubation sets show statistically overlapping (i.e. not different) populations from the control incubation N_2O respiration rates, these goethite-amended-incubation sets display average N_2O respiration rates that are above and outside the 95% confidence interval of the control incubation's N_2O respiration rate. This indicates potentially positive effects on N_2O respiration rates for goethite concentrations as low as 0.40% (wt/wt). Nonetheless, only half of the variation in N_2O respiration rates is described by the linear regression ($R^2 = 0.50$). This moderate fitting R^2 value indicates that goethite has potential to drive N_2O respiration rates, but rates are affected equally by the cumulative effect of other environmental factors under the experimental conditions.

Therefore, increasing goethite soil additions increase N_2O production rates ($\alpha = 0.05$) for Rosemount, MN topsoil. Although, there is statistically significant increased N_2O respiration rates of 13.79% goethite amendments, further studies are needed to ascertain the true impact of lower concentrations of goethite additions.

CO_2 Changes in soil CO_2 respiration rates significantly ($p = 6.78E\text{-}8 < 0.05$), but negatively ($m = -1.09$), correlate with increasing concentrations of goethite ($R^2 = 0.85$), Figure 4.4 (B). Three of the concentrations of goethite amended soils (1.96%, 3.85%, and 13.79%) show statistically ($p \leq 0.05$) significant difference in CO_2 production rates from control soil incubations. Notably, although the 0.40% and 7.41% goethite concentration incubation sets' CO_2 respiration rates are not statistically different from control incubation's rate, these goethite-amended-incubation sets display averages CO_2 respiration rates that are below and outside the 95% confidence interval of the control incubation's CO_2 respiration rate, indicating potential for goethite soil amendments as low as 0.40% to reduce CO_2 respiration rates. Interestingly, most of the variation in CO_2 respiration rates is described by the linear regression ($R^2 = 0.85$). This strong fitting R^2 value with the negative slope of the fitted linear regression indicates that increasing goethite amendments negatively affect CO_2 respiration rates.

Therefore, increasing goethite soil additions decrease CO_2 production rates ($\alpha = 0.05$) in Rosemount, MN topsoil. Although, there is statistically significant decreased CO_2 respiration rates of 1.96% goethite amendments and greater, further studies are needed to ascertain the true impact of lower addition concentrations of goethite.

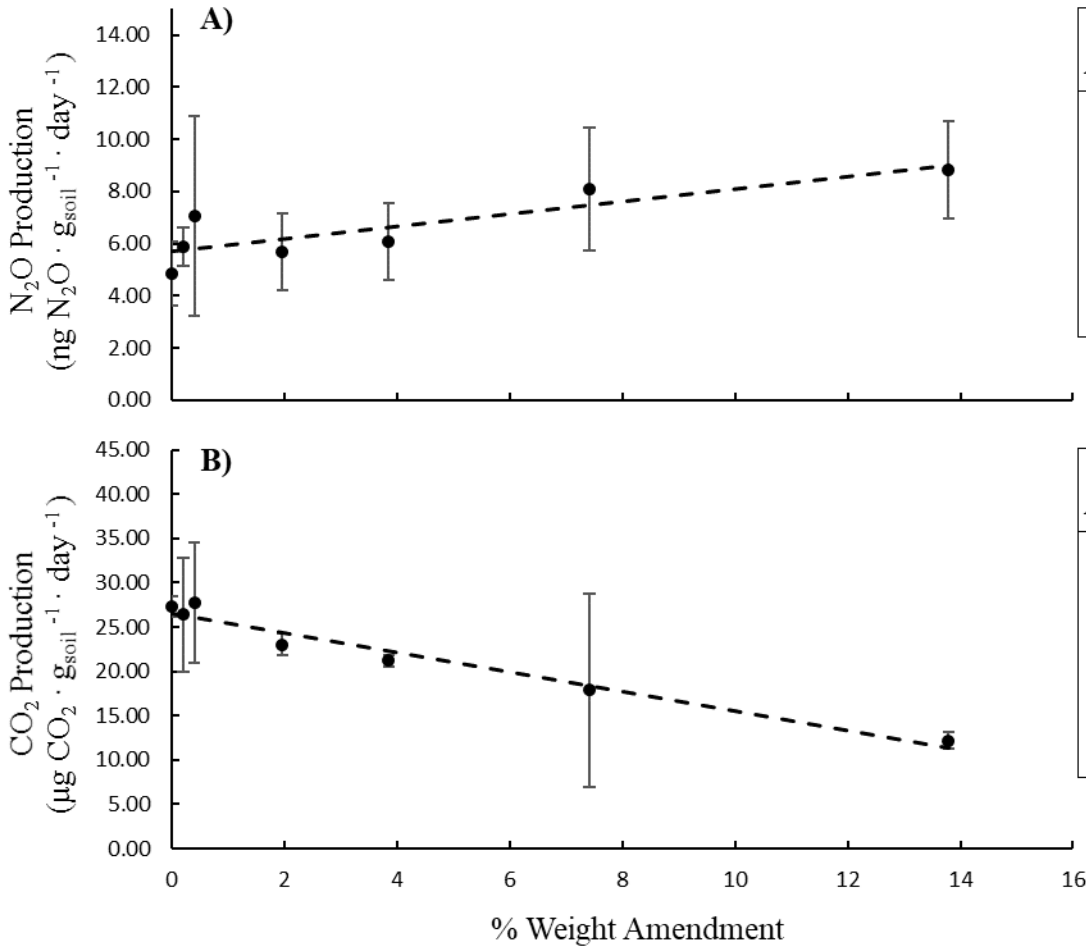

% Weight Amendment	(ng-N_2O g_{soil}^{-1} day^{-1})
0.00 %	4.86 (1.21)
0.20 %	5.89 (0.73)
0.40 %	7.07 (3.83)
1.96 %	5.69 (1.46)
3.85 %	6.07 (1.48)
7.41 %	8.08 (2.35)
13.79 %	*8.83 (1.85)

Linear Regression	
m	0.22 (0.06)
b	5.81 (0.35)
R^2	0.50
df_{n-2}	16
t_m	4.03
p_m	9.61E-04

% Weight Amendment	(µg-CO_2 g_{soil}^{-1} day^{-1})
0.00 %	27.27 (1.17)
0.20 %	26.38 (6.48)
0.40 %	27.77 (6.83)
1.96 %	*23.01 (1.23)
3.85 %	*21.18 (0.68)
7.41 %	17.87 (10.88)
13.79 %	*12.20 (0.96)

Linear Regression	
m	-1.09 (0.12)
b	26.63 (0.75)
R^2	0.85
df_{n-2}	16
t_m	-9.37
p_m	6.78E-08

Figure 4.4. N_2O (**A**) & CO_2 (**B**) production rates of Goethite soil amendments. Sample values are given in adjacent table, 2σ (~ 95%) CI are shown in data plot whiskers and in table parenthesis. Asterisk (*) indicates statistically significant (α = 0.05) difference of respiration rates from control soil incubations (0.00 % wt. amendment). Parameters of the fitted linear regression are provided in the right most table.

4.4.2.3. Magnetite Soil Amendments

N_2O Changes in soil N_2O respiration rates significantly ($p = 0.032 < 0.05$) and negatively ($m = -0.10$) correlate ($R^2 = 0.22$) with magnetite concentration, Figure 4.5 (A). However, none of the magnetite amended soils show statistically ($p \leq 0.05$) significant difference of N_2O production from control soil incubations. Although the fitted linear regression is statistically significant, most of the variation in CO_2 respiration rates is not described by the linear regression ($R^2 = 0.22$). This weak fitting R^2 value indicates that magnetite has slight potential to drive CO_2 respiration rates down, but rates are mostly controlled by the cumulative effect of other environmental factors under the experimental conditions. Therefore, while magnetite soil additions show a statistically negative effect on Rosemount, MN topsoil N_2O respiration rates, there is not a large practical effect, evinced by the weak fitting R^2 value.

CO_2 Changes in soil CO_2 respiration rates significantly ($p = 7.30E\text{-}7 < 0.05$) and negatively ($m = -0.72$) correlate ($R^2 = 0.73$) with magnetite concentration, Figure 4.5 (B). Curiously, the lowest (0.20 %) and highest (13.79 %) magnetite additions show statistically significant difference in CO_2 production rates. The 0.20% magnetite amended soil incubations show a statistically significant increase in CO_2 respiration rate, while the 13.79 % magnetite amended soil incubations shows a statistically significant decrease. Furthermore, while the lowest and highest concentrations of magnetite additions show opposite effects, the average CO_2 respiration rates for the intermediary concentrations fit remarkably well along the fitted linear regression ($m = -0.72$ and $R^2 = 0.73$). This indicates an inverse, trending negative effect on CO_2 production from low ($+ 4.76\ \mu g\ CO_2 \cdot g_{soil}^{-1} \cdot$

day^{-1}) to high (- 7.76 μg $CO_2 \cdot g_{soil}^{-1} \cdot day^{-1}$) concentrations of magnetite when compared to control incubations.

Ultimately, there is a strong ($R^2 = 0.73$) negative (m = -0.72) relationship between magnetite additions to Rosemount, MN topsoil and CO_2 production rates ($\alpha = 0.05$). Furthermore, low concentrations of magnetite affect soil CO_2 respiration rates inversely from higher concentrations ($\alpha = 0.05$).

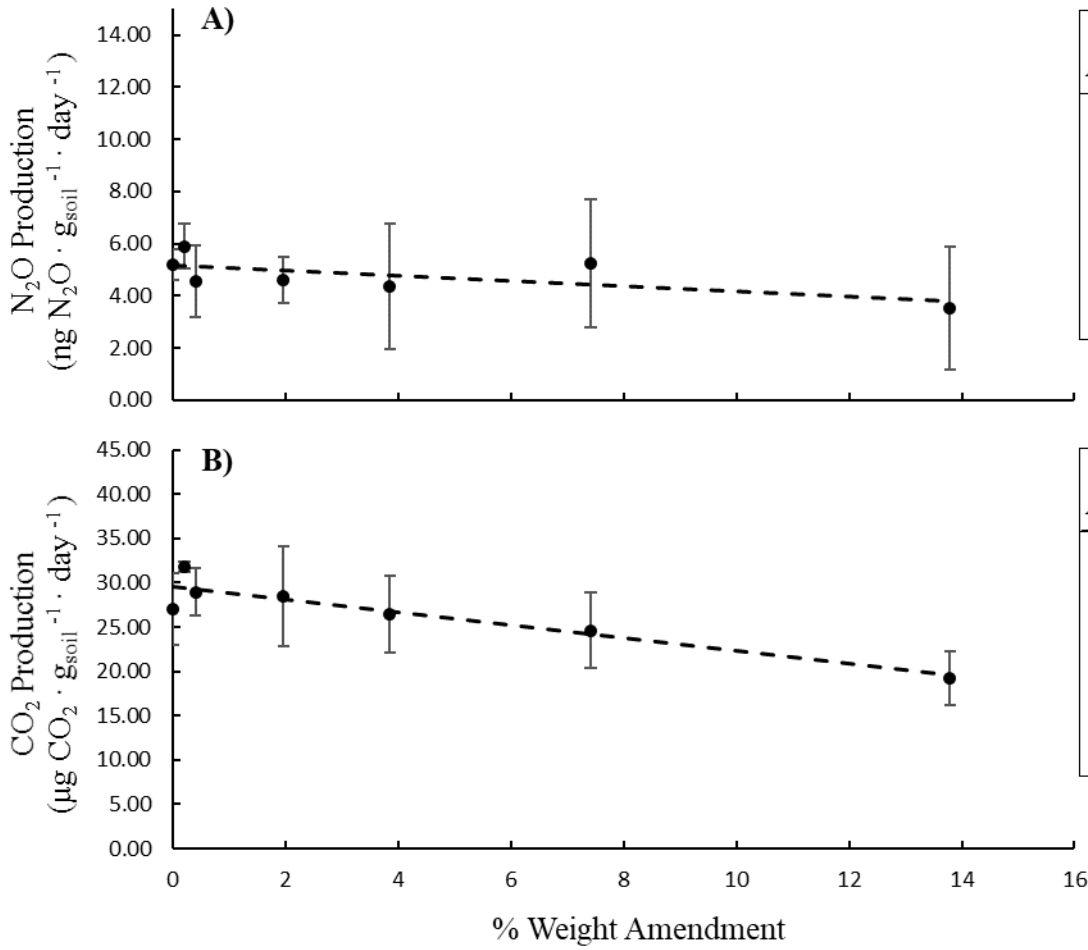

% Weight Amendment	(ng-N_2O g_{soil}^{-1} day^{-1})
0.00 %	5.19 (0.58)
0.20 %	5.90 (0.87)
0.40 %	4.56 (1.39)
1.96 %	4.60 (0.88)
3.85 %	4.34 (2.40)
7.41 %	5.24 (2.47)
13.79 %	3.52 (2.34)

Linear Regression	
m	-0.10 (0.04)
b	5.16 (0.27)
R^2	0.22
df_{n-2}	19
t_m	-2.31
p_m	3.25E-02

% Weight Amendment	(µg-CO_2 g_{soil}^{-1} day^{-1})
0.00 %	27.03 (4.03)
0.20 %	*31.79 (0.63)
0.40 %	28.95 (2.71)
1.96 %	28.51 (5.61)
3.85 %	26.47 (4.29)
7.41 %	24.61 (4.29)
13.79 %	*19.27 (3.02)

Linear Regression	
m	-0.72 (0.10)
b	29.52 (0.61)
R^2	0.73
df_{n-2}	19
t_m	-7.23
p_m	7.30E-07

Figure 4.5. N_2O (**A**) & CO_2 (**B**) production rates of Magnetite soil amendments. Sample values are given in adjacent table, 2σ (~ 95%) CI are shown in data plot whiskers and in table parenthesis. Asterisk (*) indicates statistically significant (α = 0.05) difference of respiration rates from control soil incubations (0.00 % wt. amendment). Parameters of the fitted linear regression are provided in the right most table.

4.4.3. N_2O & CO_2 Production of Soil + Black Carbon

4.4.3.1. Activated Charcoal Soil Amendments

N_2O Changes in soil N_2O respiration rates significantly ($p = 3.32E\text{-}5 < 0.05$) and negatively ($m = -0.26$) correlate ($R^2 = 0.63$) with activated charcoal concentrations, Figure 4.6 (A). Additionally, the greatest concentration of charcoal amended soil (13.79 %) shows statistically ($p \leq 0.05$) significant difference of N_2O production from control soil incubations. Nonetheless, just greater than half of the variation in N_2O respiration rates is described by the linear regression ($R^2 = 0.63$). This moderate fitting R^2 value indicates that charcoal has potential to reduce N_2O respiration rates, but variation in N_2O rates are affected strongly by other environmental factors under the experimental conditions.

CO_2 Reductions ($m = -0.84$) in soil CO_2 respiration rates significantly ($p = 1.03E\text{-}6 < 0.05$) correlate ($R^2 = 0.74$) with activated charcoal concentrations, Figure 4.6 (B). Nonetheless, while there is a strong correlation, none of the charcoal amended incubations show statistically different CO_2 respiration rates from the control incubation. Essentially, increasing additions of activated charcoal to Rosemount, MN topsoil reduces CO_2 respiration rates ($\alpha = 0.05$). However, there is great variability within experimental units, i.e. triplicate incubations, at the three largest charcoal amendment rates, i.e. 3.85% 7.41%, and 13.79%. This suggests potential imprecision of the calculated effect ($m = -0.84$) caused by charcoal amendments greater than 3.85%. Therefore, further studies are needed to ascertain the true impact of activated charcoal amendments on CO_2 respiration rates for Rosemount, MN topsoil.

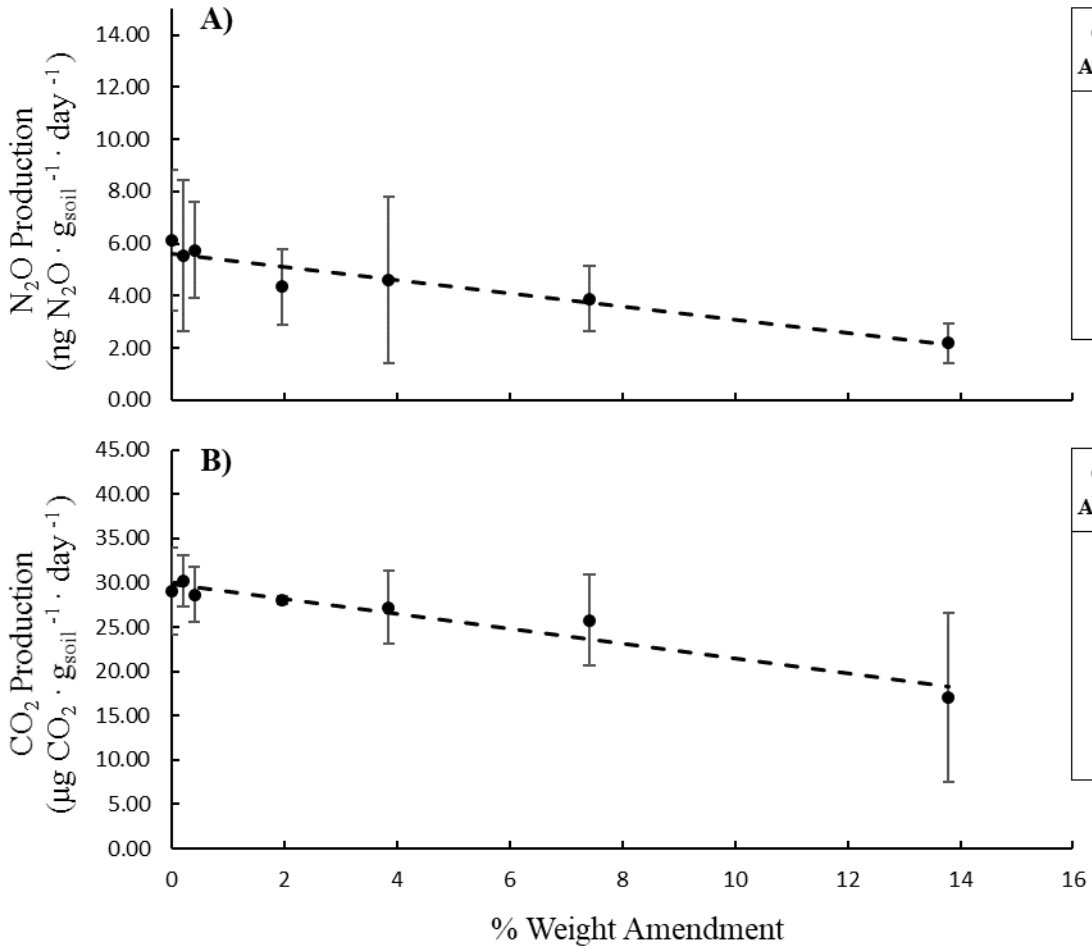

% Weight Amendment	(ng-N_2O g_{soil}^{-1} day^{-1})
0.00 %	6.12 (2.70)
0.20 %	5.55 (2.89)
0.40 %	5.75 (1.85)
1.96 %	4.34 (1.46)
3.85 %	4.60 (3.20)
7.41 %	3.88 (1.24)
13.79 %	*2.18 (0.78)

Linear Regression	
m	-0.26 (0.05)
b	5.69 (0.30)
R^2	0.63
df_{n-2}	18
t_m	-5.48
p_m	3.32E-05

% Weight Amendment	(µg-CO_2 g_{soil}^{-1} day^{-1})
0.00 %	29.05 (4.87)
0.20 %	30.20 (2.92)
0.40 %	28.69 (3.04)
1.96 %	28.08 (0.41)
3.85 %	27.19 (4.13)
7.41 %	25.80 (5.11)
13.79 %	17.09 (9.56)

Linear Regression	
m	-0.84 (0.12)
b	29.90 (0.73)
R^2	0.74
df_{n-2}	18
t_m	-7.22
p_m	1.03E-06

Figure 4.6. N_2O (**A**) & CO_2 (**B**) production rates of Activated Charcoal soil amendments. Sample values are given in adjacent table, 2σ (~ 95%) CI are shown in data plot whiskers and in table parenthesis. Asterisk (*) indicates statistically significant ($\alpha = 0.05$) difference of respiration rates from control soil incubations (0.00 % wt. amendment). Parameters of the fitted linear regression are provided in the right most table.

4.4.3.2. Carbon (Mesoporous) Soil Amendments

N_2O Changes in soil N_2O respiration rates significantly ($p = 2.43E\text{-}3 < 0.05$) and negatively ($m = -0.20$) correlate ($R^2 = 0.39$) with mesoporous carbon concentrations, Figure 4.7 (A). Additionally, the greatest concentration of carbon amended soil (13.79%) shows statistically ($p \leq 0.05$) significant difference of N_2O production from control soil incubations. Nonetheless, less than half of the variation in N_2O respiration rates is described by the linear regression ($R^2 = 0.39$). This low fitting R^2 value indicates that mesoporous carbon has potential to reduce N_2O respiration rates, but rates are affected more by the cumulative effect of other environmental factors under the experimental conditions.

Therefore, increasing mesoporous carbon soil additions decrease N_2O production rates ($\alpha = 0.05$) in Rosemount, MN topsoil. Although, there is statistically significant decreased N_2O respiration rates for the 13.79% carbon amendments, further studies are needed to ascertain the true impact of lower concentration carbon additions.

CO_2 Similar to N_2O respiration rate effects, reductions in soil CO_2 respiration rates significantly ($p = 7.97E\text{-}6 < 0.05$) and negatively ($m = -1.34$) correlate with increasing concentrations of mesoporous carbon ($R^2 = 0.66$), Figure 4.7 (B). Three of the concentrations of carbon amended soils (3.85%, 7.41%, and 13.79%) show statistically ($p \leq 0.05$) significant difference in CO_2 production rates from control soil incubations. Furthermore, although the 1.96% carbon incubation is not statistically different from control incubation, its average is, indicating potential for goethite soil amendments as low as 1.96% to affect CO_2 respiration rates. Importantly, most of the variation in CO_2 respiration rates is described by the linear regression ($R^2 = 0.66$) comparing respiration to carbon addition amounts. This moderate fitting R^2 value indicates that mesoporous carbon has potential to reduce CO_2 respiration rates, but rates are almost equally affected by the cumulative effect of other environmental factors under the experimental conditions.

Therefore, increasing mesoporous carbon soil additions decrease CO_2 production rates ($\alpha = 0.05$) in Rosemount, MN topsoil. Although, there is statistically significant decreased CO_2 respiration rates of 3.85% mesoporous carbon concentrations and greater, further studies are needed to ascertain the true impact of lower concentration of mesoporous carbon.

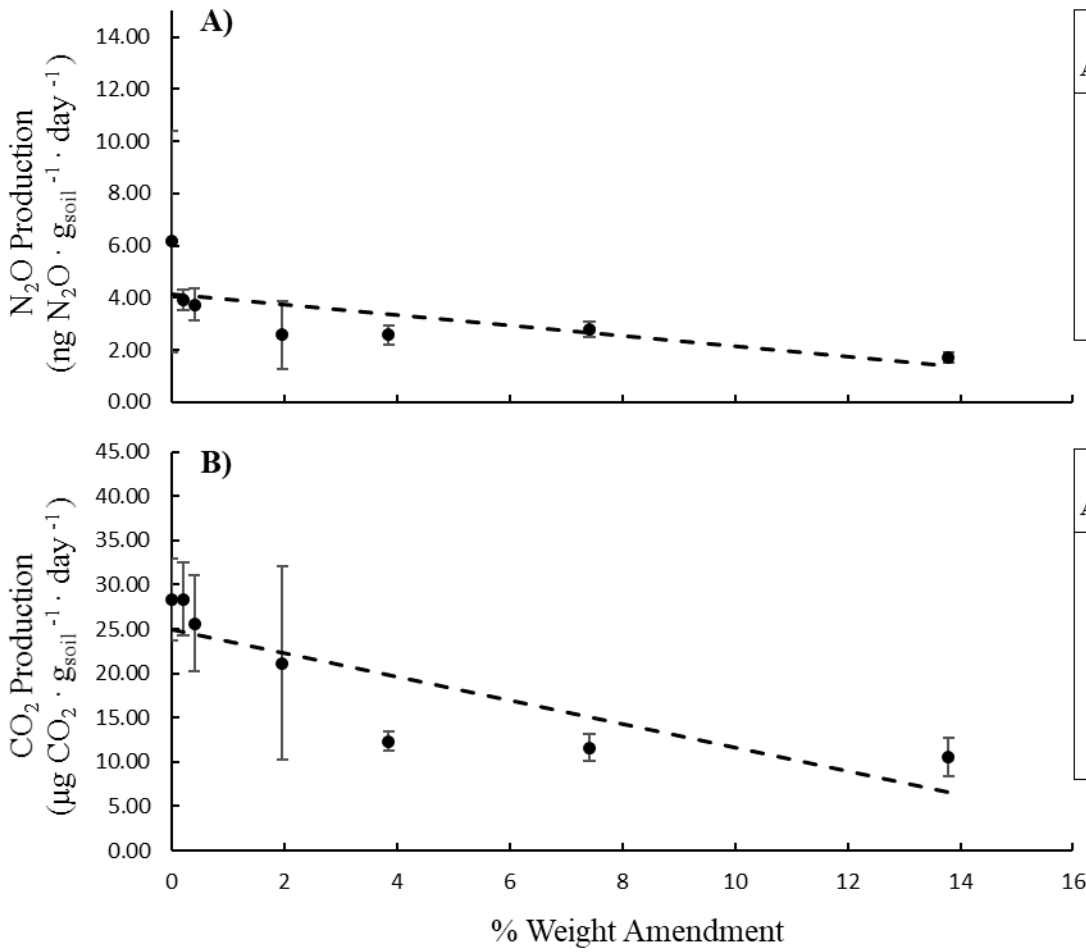

% Weight Amendment	(ng-N_2O g_{soil}^{-1} day^{-1})
0.00 %	6.16 (4.23)
0.20 %	3.92 (0.41)
0.40 %	3.74 (0.62)
1.96 %	2.58 (1.30)
3.85 %	2.57 (0.37)
7.41 %	2.80 (0.30)
13.79 %	*1.70 (0.18)

Linear Regression	
m	-0.20 (0.06)
b	4.14 (0.35)
R^2	0.39
df_{n-2}	19
t_m	-3.49
p_m	2.43E-03

% Weight Amendment	(µg-CO_2 g_{soil}^{-1} day^{-1})
0.00 %	28.30 (4.60)
0.20 %	28.39 (4.07)
0.40 %	25.61 (5.39)
1.96 %	21.14 (10.88)
3.85 %	*12.33 (1.05)
7.41 %	*11.63 (1.55)
13.79 %	*10.56 (2.22)

Linear Regression	
m	-1.34 (0.22)
b	24.99 (1.36)
R^2	0.66
df_{n-2}	19
t_m	-6.06
p_m	7.97E-06

Figure 4.7. N_2O (**A**) & CO_2 (**B**) production rates of Carbon (meso) soil amendments. Sample values are given in adjacent table, 2σ (~ 95%) CI are shown in data plot whiskers and in table parenthesis. Asterisk (*) indicates statistically significant ($\alpha = 0.05$) difference of respiration rates from control soil incubations (0.00 % wt. amendment). Parameters of the fitted linear regression are provided in the right most table.

4.5. Discussion

4.5.1. Comparison of Brazilian Oxisol with ADE soils Magnetic Susceptibility, Organic Carbon Concentration, and CO_2 respiration rates.

The magnetic susceptibility results demonstrate that the iron mineralogy between Brazilian Oxisol and ADE soils are indeed different (Figure 4.2). Although these results demonstrate differences in iron mineralogy, they do not elucidate more detail than the fact that ADE soils contain more ferromagnetic or ferrimagnetic minerals. Examples of naturally occurring iron minerals that display strong magnetic tendencies at ambient temperatures include magnetite, maghemite, and greigite. Because previous studies on ADE soils have shown conclusively, with X-Ray Diffraction (XRD) analysis, that some ADE soils contain greater concentrations of maghemite and magnetite compared with Brazilian Oxisols (Silva et al. 2011), we hypothesize that increased concentrations of maghemite and/or magnetite account for the observed increased magnetic susceptibility of ADE soils over Brazilian Oxisols. Nonetheless, future understanding of ADE mineralogy would benefit from more precise measurements of mineralogy as provided by XRD analysis (Khodadad et al. 2011; Yao et al. 2017).

4.5.2. Iron mineralogical effects on soil respiration

Previous studies have suggested that soil iron mineralogy plays a significant role in stabilizing soil organic matter (SOM) (Kaiser and Guggenberger 2000; Kaiser and Zech 2000; Lalonde et al. 2012). Upon further investigation, various iron minerals have been shown to adsorb SOM (Adhikari and Yang 2015; Chen, Kukkadapu, and Sparks 2015; Day et al. 1994; Illés and Tombácz 2003). Authors have hypothesized that iron minerals' effect on SOM stability and accumulation may occur from SOM occlusion from microbial processes (Keil et al. 1994; Jones and Edwards 1998; Kaiser and Guggenberger 2000). As previously mentioned, microbial processes are the predominant mechanism for SOM mineralization into gaseous forms, including N_2O and CO_2 (Smith et al. 2003).

Previous studies have documented microbial taxonomic differences following addition of iron and charcoal amendments to soils (Ding et al. 2013). However, our results elucidate microbial functionality differences as a result of the iron mineralogy, affecting both N_2O and CO_2 soil respiration rates. Although this study does not measure direct indicators of soil microbial populations such as soil microbial abundance or diversity (e.g., Ding et al. (2013)), the observation of changing soil respiration rates suggests that microbial communities are impacted by iron mineralogy. Nonetheless, we observed that iron minerals do not affect soil respiration rates uniformly.

4.5.2.1. Hematite Soil Amendments.

The results that showed hematite amendments having no impact ($\alpha = 0.05$) on either N_2O or CO_2 soil respiration rates were unexpected since previous studies had shown that hematite adsorbs SOM, and all iron minerals were hypothesized to occluded SOM from microbial accessibility. Two reasons may explain the discrepancy between our results and our hypothesis. First, SOM-hematite adsorption studies derive most of their conclusions from aqueous experiments (e.g., Gu et al. (1994), Hagare, Thiruvenkatachari, and Ngo (2001), and Adhikari and Yang (2015)). However, soil experiments incorporate complex inter-species processes that constrained aqueous experiments cannot fully capture (Jacobs et al. 2004; White and Brantley 2003). Second, although hematite has been correlated with adsorption of SOM in both soil and aqueous solutions, iron mineralogists have shown that soil hematite mottles are often surrounded by several molecular layers of goethite (Schwertmann 1971; Chesworth 2008), where goethite has been shown to increase organic matter stability through adsorption and physical protection (see section 4.5.2.3). The implications are that, while hematite is the predominant mineral in these hematite-rich soil mottles, the interacting surface of hematite mottles may in fact be due to goethite. This is supported by studies examining dissolved hematite (Jang, Dempsey, and Burgos 2007).

4.5.2.3. Goethite Soil Amendments.

In contrast to hematite additions, increasing goethite additions reduced soil CO_2 and increased soil N_2O respiration rates. Previous studies have shown that goethite adsorbs SOM in aqueous solutions (Day et al. 1994; Safiur Rahman, Whalen, and Gagnon 2013). Additionally, SOM adsorption by goethite and other metal-oxyhydroxides has been hypothesized to protect organic matter from microbe mineralization (Jones and Edwards 1998; Ransom et al. 1997). Although measures of in-situ microbial community diversity and abundance was not measured in this study, the CO_2 respiration results would support a hypothesis of goethite occluding organic matter decreasing microbial accessibility.

Surprisingly, however, increasing goethite additions correlated with increasing N_2O respiration rates. If N_2O production rates were solely affected by microbial respiration, this result would negate support for organic matter occlusion from microbial accessibility. However, previous studies have shown that some iron oxides, including goethite, facilitate abiotic N_2O production from nitrate (NO_3^-) and nitrite (NO_2^-) (Dhakal 2013). Specifically, goethite had the capacity to convert nearly all in-soil solution NO_3^- and NO_2^-. The present study did not measure NO_3^- and NO_2^- during the experiment; therefore it remains unclear as to whether the abiotic process described by Dhakal (2013) was responsible for the observed increases of N_2O production. Therefore, the observation of increasing N_2O production rates with increasing goethite concentrations does not necessarily negate the hypothesis of goethite facilitating organic matter accumulation and reduced microbial activity.

4.5.2.3. Magnetite Soil Amendments.

Since the seminal work of Le Borgne (1955) where the magnetic susceptibility of topsoil was found to be generally greater than that of the subsoil, researchers have increasingly used magnetic susceptibility measurements to confirm the existence of various physical, chemical, and anthropogenic processes (Mullins 1977). Magnetite and the structurally similar ferromagnetic mineral maghemite (Fe_2O_3, γ-Fe_2O_3), are known to concentrate in soils through the erosion of primary mafic minerals, airborne deposition from industrial pollution or loess deposits, and microbial and/or thermally driven transformation of antiferrimagnetic to ferrimagnetic forms (Dearing et al. 1996). Therefore, magnetite was selected for this experiment because of the potential indications in ADE soil profiles by magnetic susceptibility measurements and because of the ease by which the authors could procure standardized nano-magnetite forms from a reputable supplier (i.e. Sigma Aldrich). Nonetheless, the present study is unique in investigating the relationship between soil magnetite concentrations and soil organic matter and microbial respiration rates. There have been observations that the size of the iron minerals may control the rate of microbial iron reduction reactions (Bosch et al. 2010), but no study was located on the influence of GHG production from the iron-amended soil.

Magnetite additions showed statistically significant, but not practically significant decreases of N_2O respiration rates, see Figure 4.5A. Interestingly, magnetite additions showed increased and decreased CO_2 respiration rates at low and high concentrations, respectively, see Figure 4.5B. Previous studies on nano-sized magnetite particles in solution have shown that magnetite has the capacity to adsorb organic material (Illés and Tombácz 2003; Illes and Tombacz 2006; Safiur Rahman, Whalen, and Gagnon 2013).

Therefore, it is plausible to hypothesize that the adsorption of SOM may drive SOM's occlusion from microbial processes, resulting in decreased carbon mineralization. Of note, however, is the statistical and practically significant observation of increased CO_2 respiration rates at the magnetite addition of 0.05 %. This observation indicates that magnetite has a stimulating effect on carbon mineralization at low concentrations. Nonetheless, the authors are unsure of the underlying mechanisms by which magnetite may stimulate carbon mineralization at these low concentrations.

Furthermore, the contrasting observations where magnetite additions exhibit significant reduction of CO_2 respiration rates with non-practically different N_2O respiration rates may be a result of similar abiotic processes of iron conversions of nitrate and nitrite as hypothesized for goethite (Dhakal 2013; Dhakal et al. 2013). While Dhakal et al. (2013) determined that magnetite abiotically facilitates NO_3^- and NO_2^- mineralization to N_2O, magnetite was not as efficient in conversion as goethite was. Therefore, and like the discussion on goethite, the observation of non-practically different N_2O production rates with increasing magnetite concentrations does not necessarily negate the hypothesis that magnetite facilitates organic matter accumulation.

4.5.3. Black Carbon Effects on Soil Respiration Rates

Table 4.3. Comparing GHG production rates to physical properties of the carbon additions

	Activated Charcoal	Mesoporous Carbon
Surface Area (m^2/g)	1600	175
Total Porosity (cm^3/g)	2.0	0.2
CO_2 production ($\mu g\ C/g/day)/g_{carbon}$	-0.84	-1.34
N_2O production (ng N/g/day)/ g_{carbon}	-0.26	-0.20

As seen in Table 4.3, the two carbon additions had drastically different physical properties, especially for the total surface area and pore volume. Surprisingly, these physical properties were not predictors for the impact on CO_2. Other authors have postulated that the porosity of the biochar provides additional microbial habitat for microbes to thrive following black carbon additions (e.g. Lehmann et al. (2011); Warnock et al. (2007)). However, the data collected in this study does not show any positive impact resulting from the higher porosity black carbons, despite the order of magnitude difference in their pore volumes.

Also fascinating was the fact that the impact on N_2O was statistically equivalent for both carbon sources, again despite the differences in pore volume and surface areas. This does question the validity of hypotheses that have linked pore water entrapment (Haider et al. 2016) to effects on N_2O production due to affecting microbial processes (Lin et al. 2014). However, not enough experiments were conducted to fully support a conclusion on

this pathway.

4.6. Conclusion

In conclusion, the research presented here provides the larger scientific community a plausible alternative explanation for how Amazonian Dark Earth (ADE) soils may affect soil organic matter dynamics and carbon content. As seen in figure 4.2 with the magnetic susceptibility measurements, the ADE soil profile contains greater concentrations of ferrimagnetic/ferromagnetic iron minerals than its adjacent Brazilian Oxisol. Furthermore, based on the carbon content analysis and soil gas incubations, one can draw the conclusion that while gross carbon mineralization rates are greater for ADE than Brazilian Oxisol soils, the net carbon mineralization rates are less. Therefore, the observed differences in magnetic iron mineralogy necessitate further investigation on the effect of iron mineralogy for soil organic matter accumulation and soil carbon content.

The soil incubation studies on iron mineralogical amendments give credence to the hypothesis that differences in iron mineralogy affect long-term soil organic matter accumulation. Although the results do not support an encompassing hypothesis where all iron minerals decrease soil CO_2 respiration rates, evidence indicates that specific forms of iron do. Goethite and magnetite additions reduce CO_2 respiration rates, while hematite does not show a significant effect. Moreover, while N_2O respiration rates increase with goethite amendments, and are non-practically significantly different with magnetite additions, a literature review offers plausible explanations for how N_2O evolution could occur without soil microbial consumption of organic matter, i.e. abiotic transformation.

Future studies on ADE sites would benefit from exploring ADE and Brazilian

Oxisol soil iron mineralogy. The incubation study does not conclusively show that differences in iron mineralogy alone account for the observed differences in soil organic matter accumulation between ADE and Brazilian Oxisol soils since the original incubation soils came from elsewhere (agricultural topsoil, Rosemount, MN, USA). Consequently, it would also be beneficial for future studies to examine different iron mineralogical amendments to Brazilian Oxisol soils, to elucidate whether Brazilian Oxisols could be coerced to reduce carbon respiration and subsequently increase organic matter accumulation. Furthermore, although this study shows that iron mineralogy may play a significant role in indirect measurements of soil organic matter accumulation (soil respiration rates), there would be greater benefit in analyzing more direct measurements of soil microbial activity, such as soil microbial population and diversity analyses. Finally, this study did not examine the combined effect of iron mineralogy and black carbon additions. Amazonian Dark Earths formation factors may very well include combined effects of iron mineralogy transformation and black carbon accumulation.

Chapter 5. Conclusion

This thesis summarized two research projects on biochar soil amendments and one research project on iron mineralogy effects on soil carbon mineralization rates. The subject bridging these chapters together is a close examination of the aspects of the Amazonian Dark Earth (ADE) pedogenesis model. The first two research chapters (Chapters 2 & 3) present data that does not support the prevailing beliefs on biochar soil amendment effects. The third research chapter (Chapter 4) shows evidence justifying that the difference in iron mineralogy between ADE and Brazilian Oxisol soils could be an overlooked factor in the fabric of the soil system, since the differing, iron minerals correspondingly have a different impact on soil respiration rates. Ultimately, these research chapters shed light on how the prevailing ADE pedogenic model may be missing a primary factor altering microbial processes. Therefore, it is argued that ADE pedogenesis models should be expanded to include current findings on biochar soil amendment effects (or lack thereof) and iron mineralogical differences between ADE and Brazilian Oxisol soils. I believe that the differences and/or transformations in iron mineralogy can provide a mechanism that should be considered for affecting soil properties and soil carbon accumulation.

Currently, the most often cited and accepted model for Amazonian Dark Earth Soil Pedogenesis is that pre-Columbian Native South Americans amended black carbon (biochar) to Brazilian Oxisol soils, which over the course of millennia formed ADE soil profiles (Glaser et al. 2001). This hypothesis developed over multiple publications dating from the late 1990's to 2000's (Glaser et al. 2000; Glaser et al. 1998; Glaser et al. 2001; Glaser, Lehmann, and Zech 2002), and is best described by Glaser et al. (2001). In short, Glaser et al. (2001) states that assuming 1) black carbon is recalcitrant in nature, 2) black

carbon is a primary component of the humic matter of ADE soils, 3) soil mineralogy beyond organic material is the same between both Brazilian Oxisol Soils and ADE soils, that black carbon amendments are the sole reason for the greater fertility of ADE soils over surrounding Brazilian Oxisol soils.

Nonetheless, for the past 15 years since the publication by Glaser et al. (2001) there have been multiple attempts to observe, describe, and understand mechanistically how black carbon soil amendments (biochar) can enhance and affect soil properties. While some publications have shown positive results, research publications generally show non-statistically significant effects regarding soil fertility improvement or increased crop productivity. This research is best presented by the multiple meta-analytic studies on biochar research results (Jeffery et al. 2011; Biederman and Harpole 2013).

While the greater research community was conducting research on black carbon soil amendments (i.e. biochar) on crop yield and microbial degradation, the research in Chapters 2 and 3 of this thesis had already been started. The data collected and observations made in these chapters were some of the first scientific observations that did not support the growing hype of biochar use. The physical disintegration of biochars were postulated in prior studies to explain the disappearance of carbon from soil systems (Major et al. 2010), but there was not a true assessment of how significant this mass loss could be. In addition, the sorption of biochar by nitrate was another over hyped potential impact, when a survey of different biochars in nitrogen adsorption were completed, few (~33 %) demonstrated capacity to remove nitrate from aqueous solution, which has also been demonstrated in other recent studies, e.g. Yao et al. (2012). In addition, many of the supposed benefits and effects on soil properties from biochar have also been shown to be

statistically insignificant (Jeffery et al. 2011; Atkinson, Fitzgerald, and Hipps 2010; Biederman and Harpole 2013).

Chapter 2 of this Thesis details the physical dissociation of biochar within aqueous solutions. Previous studies on biochar and ADE soils cite black carbon's recalcitrant and persistent nature as decreasing carbon turnover rates and increasing carbon retention (Zimmerman, Gao, and Ahn 2011), with authors suggesting this effect ultimately enhances soil fertility (Biederman and Harpole 2013). Nonetheless, while studies show that black carbon is less susceptible to microbial and biochemical degradation than organic matter, chapter 2 of this thesis provides compelling evidence that black carbon is not stationary within the soil column. Furthermore, the second chapter's research indicate that that most (if not all) black carbon species have strong potential to dissolve and flow away from initial points of deposition. Essentially, the hypothesis that black carbon soil additions drive changes in soil properties over long durations (> 10 yrs) is not supported by the data presented in chapter 2.

Chapter 3 of this Thesis details how black carbon species were not found to statistically increase soil nitrogen retention rates. Essentially, while some black carbon species exhibited a capacity to adsorb nitrogen, the best nitrogen adsorbing samples were unable to significantly affect soil nitrogen retention when amended at the high concentration of 10% (wt/wt) to soils. Previous studies for both biochar and ADE soils cite correlations between black carbon soil amendments and increased nutrient retention (Novak et al. 2009; Laird et al. 2010). However, the results presented in the third chapter of this thesis suggest this is not the norm and biochars, as a class of materials, do not have a significant impact on nitrogen sorption.

Prompted by the results presented in chapters 2 and 3 of this thesis, it was chosen to reexamine biochar's fundamental analogy, i.e. ADE Soil Pedogenesis. After preliminary work examining magnetic susceptibility of ADE and Brazilian Oxisol soils, the iron mineralogy was discovered to be different between both soil profiles. This was an important finding because a key assumption in the hypothesis presented by Glaser et al. (2001) was that soil mineralogy did not differ between the two soil profiles. Therefore, Chapter 4 of this Thesis presented 1) the preliminary analysis evincing differences in iron mineralogy between ADE and Brazilian Oxisol soils, and 2) the effect different iron mineral amendments could have on soil organic matter mineralization rates, by impacting microbial CO_2 respiration rates. Simply stated, the results of the iron mineralogical amendments on soil carbon mineralization rates were unexpected. While the broader scientific community has generally known that iron, as a micronutrient, is important for plant growth, these results indicated that the three-examined iron mineralogical amendments (hematite, goethite, and magnetite) affect soil respiration rates differently. Where hematite had no discernable effect on soil mineralization rates, goethite, and magnetite had seemingly contrasting effects. Essentially, the results show that iron mineralogy affects soil functionality beyond solely elemental concentration.

Overall, the three research chapters present reasons to add another potential mechanism to the ADE pedogenesis hypothesis. First, biochar as the novel soil amendment has not produced reliable and reproducible effects. Second, a key assumption for biochar's role in ADE pedogenesis (direct influence of biochar on the soil system) has been shown to be lacking experimental evidence. Therefore, in a simple statement, ADE pedogenesis should be expanded to include iron mineralogy effects as well as black

carbon/anthropological impacts.

References

Adhikari, D., and Y. Yang. 2015. 'Selective stabilization of aliphatic organic carbon by iron oxide', *Sci Rep*, 5: 11214.

Ameloot, N., E. R. Graber, F. G. A. Verheijen, and S. De Neve. 2013. 'Interactions between biochar stability and soil organisms: review and research needs', *European Journal of Soil Science*, 64: 379-90.

Asada, Takashi, Shigehisa Ishihara, Takeshi Yamane, Akemi Toba, Akifumi Yamada, and Kikuo Oikawa. 2002. 'Science of Bamboo Charcoal: Study on Carbonizing Temperature of Bamboo Charcoal and Removal Capability of Harmful Gases', *J. Health Sci.*, 48: 473-79.

Asada, Takashi, Takashi Ohkubo, Kuniaki Kawata, and Kikuo Oikawa. 2006. 'Ammonia Adsorption on Bamboo Charcoal with Acid Treatment', *Journal of Health Science*, 52: 585-89.

Atkinson, Christopher J., Jean D. Fitzgerald, and Neil A. Hipps. 2010. 'Potential mechanisms for achieving agricultural benefits from biochar application to temperate soils: a review', *Plant and Soil*, 337: 1-18.

Bailey, Vanessa L., Sarah J. Fansler, Jeffrey L. Smith, and Harvey Bolton Jr. 2011. 'Reconciling apparent variability in effects of biochar amendment on soil enzyme activities by assay optimization', *Soil Biology and Biochemistry*, 43: 296-301.

Bangham, DH, and RI Razouk. 1938. 'The swelling of charcoal. Part V. The saturation and immersion expansions and the heat of wetting', *Proceedings of the Royal Society of London. Series A. Mathematical and Physical Sciences*, 166: 572-86.

Barnes, R. T., M. E. Gallagher, C. A. Masiello, Z. Liu, and B. Dugan. 2014. 'Biochar-induced changes in soil hydraulic conductivity and dissolved nutrient fluxes constrained by laboratory experiments', *PLoS One*, 9: e108340.

Biederman, Lori A., and W. Stanley Harpole. 2013. 'Biochar and its effects on plant productivity and nutrient cycling: a meta-analysis', *GCB Bioenergy*, 5: 202-14.

Bock, Emily, Nick Smith, Mark Rogers, Brady Coleman, Mark Reiter, Brian Benham, and Zachary M. Easton. 2015. 'Enhanced Nitrate and Phosphate Removal in a Denitrifying Bioreactor with Biochar', *Journal of Environment Quality*, 44: 605.

Bosch, Julian, Andreas Fritzsche, Kai U. Totsche, and Rainer U. Meckenstock. 2010. 'Nanosized ferrihydrite colloids facilitate microbial iron reduction under flow conditions', *Geomicrobiology Journal*, 27: 123-29.

Braadbaart, F., I. Poole, and A. A. van Brussel. 2009. 'Preservation potential of charcoal in alkaline environments: an experimental approach and implications for the archaeological record', *Journal of Archaeological Science*, 36: 1672-79.

Brewer, P. H., and R. H. Carr. 1926. 'Fertility of a soil as related to the forms of its iron and manganese', *Soil Science*, 23: 9.

Broder, M. W., and G. H. Wagner. 1988. 'Microbial colonization and decomposition of corn, wheat, and soybean residue', *Soil Science Society of America Journal*, 52.

Brodowski, Sonja, Wulf Amelung, Ludwig Haumaier, Clarissa Abetz, and Wolfgang Zech. 2005. 'Morphological and chemical properties of black carbon in physical soil fractions as revealed by scanning electron microscopy and energy-dispersive X-ray spectroscopy', *Geoderma*, 128: 116-29.

Byrne, C. E., and D. C. Nagle. 1997. 'Carbonization of wood for advanced materials applications', *Carbon*, 35: 259-66.
Camargo, Livia Arantes, JosÃ\copyright Marques JÃºnior, Gener Tadeu Pereira, AngÃ\copyrightlica Santos Rabelo de Souza Bahia, A. Ahlbom, N. Day, M. Feychting, E. Roman, J. Skinner, J. Dockerty, M. Linet, M. McBride, J. Michaelis, J. H. Olsen, and et al. 2014. 'Clay mineralogy and magnetic susceptibility of Oxisols in geomorphic surfaces
A pooled analysis of magnetic fields and childhood leukaemia', *Scientia Agricola*, 71: 244-56.
Campos, M. C. C., M. R. Ribeiro, V. S. Souza Júnior, M. R. Ribeiro Filho, R. V. C. C. Souza, and M. C. Almeida. 2011. 'Characterization and classification of archaeological dark earths from the Middle Madeira River Region', *Bragantia*, 70: 598.
Chan, K Yin, and Zhihong Xu. 2009. 'Biochar: nutrient properties and their enhancement', *Biochar for environmental management: science and technology*: 67-84.
Chatterjee, Sudipta, Dae S. Lee, Min W. Lee, and Seung H. Woo. 2009. 'Nitrate removal from aqueous solutions by cross-linked chitosan beads conditioned with sodium bisulfate', *Journal of Hazardous Materials*, 166: 508-13.
Chen, C., R. Kukkadapu, and D. L. Sparks. 2015. 'Influence of Coprecipitated Organic Matter on Fe2+(aq)-Catalyzed Transformation of Ferrihydrite: Implications for Carbon Dynamics', *Environ Sci Technol*, 49: 10927-36.
Chesworth, Ward. 2008. *Encyclopedia of soil science* (Springer: Dordrecht, Netherlands).
Chia, Chee H, Bin Gong, Stephen D Joseph, Christopher E Marjo, Paul Munroe, and Anne M Rich. 2012. 'Imaging of mineral-enriched biochar by FTIR, Raman and SEM–EDX', *Vibrational Spectroscopy*, 62: 248-57.
Chia, Chee Hung, Paul Munroe, Stephen Joseph, and Yun Lin. 2010. 'Microscopic characterisation of synthetic Terra Preta', *Soil Research*, 48: 593-605.
Christianson, Laura, Mike Hedley, Marta Camps, Helen Free, and Surinder Saggar. 2011. "Influence of Biochar Amendment on Dentitrification Bioreactor Performance." In.: Massey University.
Cohen-Ofri, Ilit, Lev Weiner, Elisabetta Boaretto, Genia Mintz, and Steve Weiner. 2006. 'Modern and fossil charcoal: aspects of structure and diagenesis', *Journal of Archaeological Science*, 33: 428-39.
Czimczik, Claudia I., and Caroline A. Masiello. 2007. 'Controls on black carbon storage in soils', *Global Biogeochemical Cycles*, 21: GB3005.
Dahlen, FA, and John Suppe. 1988. 'Mechanics, growth, and erosion of mountain belts', *Geological Society of America Special Papers*, 218: 161-78.
Day, Geoffrey McD, Barry T. Hart, Ian D. McKelvie, and Ronald Beckett. 1994. 'Adsorption of natural organic matter onto goethite', *Colloids and Surfaces A: Physicochemical and Engineering Aspects*, 89: 1-13.
Dearing, J. A., K. L. Hay, S. M. J. Baban, A. S. Huddleston, E. M. H. Wellington, and P. J. Loveland. 1996. 'Magnetic susceptibility of soil: an evaluation of conflicting theories using a national data set', *Geophysical Journal International*, 127: 728-34.

Delaplace, Pierre, BenjaminM Delory, Caroline Baudson, Magdalena Mendaluk-Saunier de Cazenave, Stijn Spaepen, Sébastien Varin, Yves Brostaux, and Patrick du Jardin. 2015. 'Influence of rhizobacterial volatiles on the root system architecture and the production and allocation of biomass in the model grass *Brachypodium distachyon* (L.) *P. Beauv*', *BMC Plant Biology*, 15: 1-15.

DeLuca, T. H., M. D. MacKenzie, M. J. Gundale, and W. E. Holben. 2006. 'Wildfire-Produced Charcoal Directly Influences Nitrogen Cycling in Ponderosa Pine Forests', *Soil Science Society of America Journal*, 70: 448-53.

Dhakal, P., C. J. Matocha, F. E. Huggins, and M. M. Vandiviere. 2013. 'Nitrite reactivity with magnetite', *Environ Sci Technol*, 47: 6206-13.

Dhakal, Prakash. 2013. 'Abiotic nitrate and nitrite reactivity with iron oxide minerals', University of Kentucky.

Ding, G. C., G. J. Pronk, D. Babin, H. Heuer, K. Heister, I. Kogel-Knabner, and K. Smalla. 2013. 'Mineral composition and charcoal determine the bacterial community structure in artificial soils', *FEMS Microbiol Ecol*, 86: 15-25.

Durden, EH. 1849. 'On the application of peat and its products, to manufacturing, agricultural, and sanitary purposes', *Proceedings of the Geological and Polytechnic Society of the West Riding of Yorkshire*, 3: 339-66.

Eswaran, Hari, Robert Ahrens, Thomas J Rice, and Bobby A Stewart. 2002. *Soil classification: a global desk reference* (CRC Press).

Firestone, M. K., M. S. Smith, R. B. Firestone, and J. M. Tiedje. 1979. 'The influence of nitrate, nitrite, and oxygen on the composition of the gaseous products of denitrification in soil', *Soil Science Society of America Journal*, 43: 1140-44.

Foereid, Bente, Johannes Lehmann, and Julie Major. 2011. 'Modeling black carbon degradation and movement in soil', *Plant and Soil*: 1-14.

Fontaine, Sebastien, Sebastien Barot, Pierre Barre, Nadia Bdioui, Bruno Mary, and Cornelia Rumpel. 2007. 'Stability of organic carbon in deep soil layers controlled by fresh carbon supply', *Nature*, 450: 277-80.

Fontes, MPF, and SB Weed. 1991. 'Iron oxides in selected Brazilian oxisols: I. Mineralogy', *Soil Science Society of America Journal*, 55: 1143-49.

Foo, K. Y., and B. H. Hameed. 2010. 'Insights into the modeling of adsorption isotherm systems', *Chemical Engineering Journal*, 156: 2-10.

Freundlich, H. M. F. 1906. 'Über die Adsorption in Lösungen', *Zeitschrift für Physikalische Chemie*, 57: 385-470.

Furumai, Hiroaki, Hideki Tagui, and Kenji Fujita. 1996. 'Effects of pH and alkalinity on sulfur-denitrification in a biological granular filter', *Water Science and Technology*, 34: 355-62.

Gai, Xiapu, Hongyuan Wang, Jian Liu, Limei Zhai, Shen Liu, Tianzhi Ren, and Hongbin Liu. 2014. 'Effects of Feedstock and Pyrolysis Temperature on Biochar Adsorption of Ammonium and Nitrate', *PLoS ONE*, 9: 1-19.

Gao, Xiangpeng, and Hongwei Wu. 2014. 'Aerodynamic properties of biochar particles: Effect of grinding and implications', *Environmental Science & Technology Letters*, 1: 60-64.

Gee, G. W., and J. W. Bauder. 1986. Ed A. Klute (ed.), *Particle-size analysis* (American Society of Agronomy and Soil Science Society of America: Madison, Wisconsin, USA).

German, Laura A. 2003. 'Historical contingencies in the coevolution of environment and livelihood: contributions to the debate on Amazonian Black Earth', *Geoderma*, 111: 307-31.

Glaser, B., L. Haumaier, G. Guggenberger, and W. Zech. 1998. 'Black carbon in soils: the use of benzenecarboxylic acids as specific markers', *Organic Geochemistry*, 29: 811-19.

Glaser, Bruno, Eugene Balashov, Ludwig Haumaier, Georg Guggenberger, and Wolfgang Zech. 2000. 'Black carbon in density fractions of anthropogenic soils of the Brazilian Amazon region', *Organic Geochemistry*, 31: 669-78.

Glaser, Bruno, Ludwig Haumaier, Georg Guggenberger, and Wolfgang Zech. 2001. 'The ’Terra Preta’ phenomenon: a model for sustainable agriculture in the humid tropics', *Naturwissenschaften*, 88: 37-41.

Glaser, Bruno, Johannes Lehmann, and Wolfgang Zech. 2002. 'Ameliorating physical and chemical properties of highly weathered soils in the tropics with charcoal – a review', *Biology and Fertility of Soils*, 35: 219-30.

Goldberg, Edward. 1985. *Black carbon in the environment* (Wiley and Sons: New York, NY).

Gu, B., J. Schmitt, Z. Chen, L. Liang, and J. F. McCarthy. 1994. 'Adsorption and desorption of natural organic matter on iron oxide: mechanisms and models', *Environ Sci Technol*, 28: 38-46.

Hagare, P., R. Thiruvenkatachari, and H. H. Ngo. 2001. 'A Feasibility Study of Using Hematite to Remove Dissolved Organic Carbon in Water Treatment', *Separation Science and Technology*, 36: 2547-59.

Haider, Ghulam, Diedrich Steffens, Christoph Müller, and Claudia I Kammann. 2016. 'Standard Extraction Methods May Underestimate Nitrate Stocks Captured by Field-Aged Biochar', *Journal of Environmental Quality*.

Hansen, Hans Chr. B., Christian B. Koch, Hanne Nancke-Krogh, Ole K. Borggaard, and Jan SÃ¸rensen. 1996. 'Abiotic Nitrate Reduction to Ammonium: Key Role of Green Rust', *Environmental Science & Technology*, 30: 2053-56.

Highwood, Eleanor J., and Robert P. Kinnersley. 2006. 'When smoke gets in our eyes: The multiple impacts of atmospheric black carbon on climate, air quality and health', *Environment International*, 32: 560-66.

Hockaday, W. C., A. M. Grannas, S. Kim, and P. G. Hatcher. 2006. 'Direct molecular evidence for the degradation and mobility of black carbon in soils from ultrahigh-resolution mass spectral analysis of dissolved organic matter from a fire-impacted forest soil', *Organic Geochemistry*, 37: 501-10.

Hockaday, William C., Amanda M. Grannas, Sunghwan Kim, and Patrick G. Hatcher. 2007. 'The transformation and mobility of charcoal in a fire-impacted watershed', *Geochimica et Cosmochimica Acta*, 71: 3432-45.

Hodges, Steven C. 1995. "Soil Fertility Basics." In, edited by North Carolina State University, 75.

Huang, Yong H., and Tian C. Zhang. 2004. 'Effects of low pH on nitrate reduction by iron powder', *Water Research*, 38: 2631-42.
Huisman, D. J., F. Braadbaart, I. M. van Wijk, and B. J. H. van Os. 2012. 'Ashes to ashes, charcoal to dust: micromorphological evidence for ash-induced disintegration of charcoal in Early Neolithic (LBK) soil features in Elsloo (The Netherlands)', *Journal of Archaeological Science*, 39: 994-1004.
Hunter, John. 1863. 'LI. On the absorption of gases by charcoal', *Philosophical Magazine Series 4*, 25: 364-68.
Iida, Tatsuya, Yoshimasa Amano, Motoi Machida, and Fumio Imazeki. 2013. 'Effect of Surface Property of Activated Carbon on Adsorption of Nitrate Ion', *CHEMICAL ^|^ PHARMACEUTICAL BULLETIN*, 61: 1173-77.
Illes, E., and E. Tombacz. 2006. 'The effect of humic acid adsorption on pH-dependent surface charging and aggregation of magnetite nanoparticles', *J Colloid Interface Sci*, 295: 115-23.
Illés, Erzsébet, and Etelka Tombácz. 2003. 'The role of variable surface charge and surface complexation in the adsorption of humic acid on magnetite', *Colloids and Surfaces A: Physicochemical and Engineering Aspects*, 230: 99-109.
Jacobs, Jennifer M, Binayak P Mohanty, En-Ching Hsu, and Douglas Miller. 2004. 'SMEX02: Field scale variability, time stability and similarity of soil moisture', *Remote Sensing of Environment*, 92: 436-46.
Jaffé, Rudolf, Yan Ding, Jutta Niggemann, Anssi V. Vähätalo, Aron Stubbins, Robert G. M. Spencer, John Campbell, and Thorsten Dittmar. 2013. 'Global Charcoal Mobilization from Soils via Dissolution and Riverine Transport to the Oceans', *Science*, 340: 345.
Jang, Je-Hun, Brian A. Dempsey, and William D. Burgos. 2007. 'Solubility of Hematite Revisited: Effects of Hydration', *Environmental Science & Technology*, 41: 7303-08.
Jansen, R. J. J., and H. van Bekkum. 1994. 'Amination and ammoxidation of activated carbons', *Carbon*, 32: 1507-16.
Jeffery, S., F. G. A. Verheijen, M. van der Velde, and A. C. Bastos. 2011. 'A quantitative review of the effects of biochar application to soils on crop productivity using meta-analysis', *Agriculture, Ecosystems & Environment*, 144: 175-87.
Jones, D. L., and A. C. Edwards. 1998. 'Influence of sorption on the biological utilization of two simple carbon substrates', *Soil Biology and Biochemistry*, 30: 1895-902.
Joseph, S, ER Graber, C Chia, P Munroe, S Donne, T Thomas, S Nielsen, C Marjo, H Rutlidge, and GX Pan. 2013. 'Shifting paradigms: development of high-efficiency biochar fertilizers based on nano-structures and soluble components', *Carbon Management*, 4: 323-43.
Kaiser, K., and G. Guggenberger. 2007. 'Sorptive stabilization of organic matter by microporous goethite: sorption into small pores vs. surface complexation', *European Journal of Soil Science*, 58: 45-59.
Kaiser, Klaus, and Georg Guggenberger. 2000. 'The role of DOM sorption to mineral surfaces in the preservation of organic matter in soils', *Organic Geochemistry*, 31: 711-25.

Kaiser, Klaus, and Wolfgang Zech. 2000. 'Dissolved organic matter sorption by mineral constituents of subsoil clay fractions', *Journal of Plant Nutrition and Soil Science*, 163: 531-35.

Kämpf, N., and U. Schwertmann. 1983. 'Goethite and hematite in a climosequence in southern Brazil and their application in classification of kaolinitic soils', *Geoderma*, 29: 27-39.

Kämpf, Nestor, William I Woods, Wim Sombroek, Dirse C Kern, and Tony JF Cunha. 2003. 'Classification of Amazonian Dark Earths and other ancient anthropic soils.' in, *Amazonian Dark Earths* (Springer).

Kastner, James R., Joby Miller, and K. C. Das. 2009. 'Pyrolysis conditions and ozone oxidation effects on ammonia adsorption in biomass generated chars', *Journal of Hazardous Materials*, 164: 1420-27.

Keil, Richard G., Daniel B. Montluçon, Fredrick G. Prahl, and John I. Hedges. 1994. *Nature*, 370: 549-52.

Kern, Dirse Clara, Gilmation D'aquino, Tarcisio Ewerton Rodrigues, Francisco Juvenal Lima Frazao, Wim Sombroek, Thomas P Myers, and Eduardo Góes Neves. 2003. 'Distribution of Amazonian dark earths in the Brazilian Amazon.' in, *Amazonian Dark Earths* (Springer).

Ketrot, D., A. Suddhiprakarn, I. Kheoruenromne, and B. Singh. 2013. 'Interactive effects of iron oxides and organic matter on charge properties of red soils in Thailand', *Soil Research*, 51: 222.

Khodadad, Christina L. M., Andrew R. Zimmerman, Stefan J. Green, Sivakumar Uthandi, and Jamie S. Foster. 2011. 'Taxa-specific changes in soil microbial community composition induced by pyrogenic carbon amendments', *Soil Biology and Biochemistry*, 43: 385-92.

Kuzyakov, Yakov, Irina Bogomolova, and Bruno Glaser. 2014. 'Biochar stability in soil: Decomposition during eight years and transformation as assessed by compound-specific 14C analysis', *Soil Biology and Biochemistry*, 70: 229-36.

Laird, David, Pierce Fleming, Baiqun Wang, Robert Horton, and Douglas Karlen. 2010. 'Biochar impact on nutrient leaching from a Midwestern agricultural soil', *Geoderma*, 158: 436-42.

Lalonde, K., A. Mucci, A. Ouellet, and Y. Gelinas. 2012. 'Preservation of organic matter in sediments promoted by iron', *Nature*, 483: 198-200.

Lattao, Charisma, Xiaoyan Cao, Jingdong Mao, Klaus Schmidt-Rohr, and Joseph J. Pignatello. 2014. 'Influence of Molecular Structure and Adsorbent Properties on Sorption of Organic Compounds to a Temperature Series of Wood Chars', *Environmental Science & Technology*, 48: 4790-98.

Le Borgne, E. 1955. 'Abnormal magnetic susceptibility of the top soil', *Annales de géophysique*, 11: 399-419.

LeCroy, Chase, Caroline A Masiello, Jennifer A Rudgers, William C Hockaday, and Jonathan J Silberg. 2013. 'Nitrogen, biochar, and mycorrhizae: alteration of the symbiosis and oxidation of the char surface', *Soil Biology and Biochemistry*, 58: 248-54.

Lehmann, Johannes. 2007. 'A handful of carbon', *Nature*, 447: 143-44.

Lehmann, Johannes, Matthias C. Rillig, Janice Thies, Caroline A. Masiello, William C. Hockaday, and David Crowley. 2011. 'Biochar effects on soil biota – A review', *Soil Biology and Biochemistry*, 43: 1812-36.

Liang, B., J. Lehmann, D. Solomon, J. Kinyangi, J. Grossman, B. O'Neill, J. O. Skjemstad, J. Thies, F. J. LuizÃ£o, J. Petersen, and E. G. Neves. 2006. 'Black Carbon Increases Cation Exchange Capacity in Soils', *Soil Science Society of America Journal*, 70: 1719-30.

Lima, H. N., C. E. R. Schaefer, J. W. V. Mello, R. J. Gilkes, and J. C. Ker. 2002. 'Pedogenesis and pre-Colombian land use of "Terra Preta Anthrosols" ("Indian black earth") of Western Amazonia', *Geoderma*, 110: 1.

Lin, Xiurong, Kurt A Spokas, Rodney T Venterea, Renduo Zhang, John M Baker, and Gary W Feyereisen. 2014. 'Assessing microbial contributions to N2O impacts following biochar additions', *Agronomy*, 4: 478-96.

Lutgens, Frederick K., and Edward J. Tarbuck. 1999. *Essentials of Geology* (Prentice Hall).

Macedo, J, and RB Bryant. 1989. 'Preferential microbial reduction of hematite over goethite in a Brazilian Oxisol', *Soil Science Society of America Journal*, 53: 1114-18.

Madari, Beáta E, Wim G Sombroek, and William I Woods. 2004. 'Research on Anthropogenic Dark Earth Soils. Could It Be a Solution for Sustainable Agricultural Development in the Amazon?' in, *Amazonian Dark Earths: Explorations in space and time* (Springer).

Major, Julie, Johannes Lehmann, Marco Rondon, and Christine Goodale. 2010. 'Fate of soil-applied black carbon: downward migration, leaching and soil respiration', *Global Change Biology*, 16: 1366-79.

Malanima, Paolo. 2006. 'Energy crisis and growth 1650 - 1850: the European deviation in a comparative perspective', *Journal of Global History*, 1: 101-21.

Masiello, C. A., O. A. Chadwick, J. Southon, M. S. Torn, and J. W. Harden. 2004. 'Weathering controls on mechanisms of carbon storage in grassland soils', *Global Biogeochemical Cycles*, 18: GB4023.

Mattos, Jaqueline Rezende (ed.)^(eds.). 2006. *Sistema brasileiro de classificação de solos* (EMBRAPA: Rio de Janeiro, RJ).

Mizuta, Kei, Toshitatsu Matsumoto, Yasuo Hatate, Keiichi Nishihara, and Tomoki Nakanishi. 2004. 'Removal of nitrate-nitrogen from drinking water using bamboo powder charcoal', *Bioresource Technology*, 95: 255-57.

Mukherjee, A., A. R. Zimmerman, and W. Harris. 2011. 'Surface chemistry variations among a series of laboratory-produced biochars', *Geoderma*, 163: 247-55.

Mullins, C. E. 1977. 'Magnetic Susceptibility of the Soil and it's Significance in Soil Science - A Review', *Journal of Soil Science*, 28: 223-46.

Naisse, Christophe, Cyril Girardin, Romain Lefevre, Alessandro Pozzi, Robert Maas, Arne Stark, and Cornelia Rumpel. 2014. 'Effect of physical weathering on the carbon sequestration potential of biochars and hydrochars in soil', *GCB Bioenergy*: in press.

Namasivayam, C., and D. Sangeetha. 2005. 'Removal and recovery of nitrate from water by ZnCl2 activated carbon from coconut coir pith, an agricultural solid waste', *Indian Journal of Chemical Technology*, 12: 513-21.

Nelson, D. W., and L. E. Sommers. 1996. D. L. Sparks (ed.), *Total carbon, organic carbon, and organic matter* (Soil Science Society of America).

Nelson, David C., Gavin R. Flematti, Emilio L. Ghisalberti, Kingsley W. Dixon, and Steven M. Smith. 2012. 'Regulation of Seed Germination and Seedling Growth by Chemical Signals from Burning Vegetation', *Annual Review of Plant Biology*, 63: 107-30.

Neves, Eduardo G., James B. Petersen, Robert N. Bartone, and Carlos Augusto Da Silva. 2003. 'Historical and Socio-cultural Origins of Amazonian Dark Earth.' in Johannes Lehmann, Dirse C. Kern, Brund Glaser and William I. Wodos (eds.), *Amazonian Dark Earths: Origin Properties Management* (Springer Netherlands: Dordrecht).

Ngueleu, Stéphane K., Peter Grathwohl, and Olaf A. Cirpka. 2013. 'Effect of natural particles on the transport of lindane in saturated porous media: Laboratory experiments and model-based analysis', *Journal of Contaminant Hydrology*, 149: 13-26.

Nichols, Gary J., Jenny A. Cripps, Margaret E. Collinson, and Andrew C. Scott. 2000. 'Experiments in waterlogging and sedimentology of charcoal: results and implications', *Palaeogeography, Palaeoclimatology, Palaeoecology*, 164: 43-56.

Novak, Jeffrey M., Warren J. Busscher, David L. Laird, Mohamed Ahmedna, Don W. Watts, and Mohamed A. S. Niandou. 2009. 'Impact of Biochar Amendment on Fertility of a Southeastern Coastal Plain Soil', *Soil Science*, 174: 105-12.

Novak, Jeffrey M., Warren J. Busscher, Donald W. Watts, James E. Amonette, James A. Ippolito, Isabel M. Lima, Julia Gaskin, K. C. Das, Christoph Steiner, Mohamed Ahmedna, Djaafar Rehrah, and Harry Schomberg. 2012. 'Biochars Impact on Soil-Moisture Storage in an Ultisol and Two Aridisols', *Soil Science*, 177: 310-20.

Novak, JeffreyM, KeriB Cantrell, DonaldW Watts, WarrenJ Busscher, and MarkG Johnson. 2014. 'Designing relevant biochars as soil amendments using lignocellulosic-based and manure-based feedstocks', *Journal of Soils and Sediments*: 1-14.

Otto, J. B., W. K. Blank, and D. A. Dahl. 1988. 'A nitrate precipitation technique for preparing strontium for isotopic analysis', *Chemical Geology: Isotope Geoscience section*, 72: 173-79.

Parr, S. W., and D. R. Mitchell. 1930. 'The Slacking of Coal and Its Proper Interpretation', *Industrial & Engineering Chemistry*, 22: 1211-12.

Puri, Balwant Rai, K Murari, and DD Singh. 1961. 'The sorption of water vapor by charcoal as influenced by surface oxygen complexes', *The Journal of Physical Chemistry*, 65: 37-39.

Puri, Balwant, DD Singh, J Nath, and Lech Sharma. 1958. 'Chemisorption of oxygen on activated charcoal and sorption of acids and bases', *Industrial & Engineering Chemistry*, 50: 1071-74.

Qin, Sijun, Kuibao Jiao, Deguo Lyu, Lu Shi, and Lingzhi Liu. 2015. 'Effects of maize residue and cellulose-decomposing bacteria inocula on soil microbial community,

functional diversity, organic fractions, and growth of Malus hupehensis Rehd', *Archives of Agronomy and Soil Science*, 61: 173-84.
Ransom, B., R. H. Bennett, R. Baerwald, and K. Shea. 1997. 'TEM study of in situ organic matter on continental margins: occurrence and the "monolayer" hypothesis', *Marine Geology*, 138: 1-9.
Reilly, James F, Alex J Horne, and Craig D Miller. 1999. 'Nitrate removal from a drinking water supply with large free-surface constructed wetlands prior to groundwater recharge', *Ecological Engineering*, 14: 33-47.
Riedel, Thomas, Dominik Zak, Harald Biester, and Thorsten Dittmar. 2013. 'Iron traps terrestrially derived dissolved organic matter at redox interfaces', *Proceedings of the National Academy of Sciences*: 10101-05.
Robertson, W. D., G. I. Ford, and P. S. Lombardo. 2005. 'Wood-Based Filter for Nitrate Removal In Septic Systems', *Transactions of the American Society of Agricultural and Biological Engineers*, 48: 121-28.
Rumpel, C., M. Alexis, A. Chabbi, V. Chaplot, D. P. Rasse, C. Valentin, and A. Mariotti. 2006. 'Black carbon contribution to soil organic matter composition in tropical sloping land under slash and burn agriculture', *Geoderma*, 130: 35-46.
Safiur Rahman, M., Marc Whalen, and Graham A. Gagnon. 2013. 'Adsorption of dissolved organic matter (DOM) onto the synthetic iron pipe corrosion scales (goethite and magnetite): Effect of pH', *Chemical Engineering Journal*, 234: 149-57.
Schaefer, C. E. G. R., J. D. Fabris, and J. C. Ker. 2008. 'Minerals in the clay fraction of Brazilian Latosols (Oxisols): a review', *Clay Minerals*, 43: 137-54.
Schaefer, Carlos E. R. 2001. 'The B horizon microstructure of Brazilian Latosols as long term biotic constructs.', *Australian Journal of Soil Research*, 39: 909.
Schmidt, Michael W. I., Margaret S. Torn, Samuel Abiven, Thorsten Dittmar, Georg Guggenberger, Ivan A. Janssens, Markus Kleber, Ingrid Kogel-Knabner, Johannes Lehmann, David A. C. Manning, Paolo Nannipieri, Daniel P. Rasse, Steve Weiner, and Susan E. Trumbore. 2011. 'Persistence of soil organic matter as an ecosystem property', *Nature*, 478: 49-56.
Schwertmann, U. 1971. 'Transformation of hematite to goethite in soils', *Nature*, 232: 624-5.
———. 1985. 'The Effect of Pedogenic Environments on Iron Oxide Minerals.' in B. A. Stewart (ed.), *Advances in Soil Science* (Springer-Verlag: New York).
Seredych, Mykola, Albert V. Tamashausky, and Teresa J. Bandosz. 2010. 'Graphite Oxides Obtained from Porous Graphite: The Role of Surface Chemistry and Texture in Ammonia Retention at Ambient Conditions', *Advanced Functional Materials*, 20: 1670-79.
Shaw, J. N., C. C. Truman, and D. W. Reeves. 2002. 'Mineralogy of eroded sediments derived from highly weathered Ultisols of central Alabama', *Soil and Tillage Research*, 68: 59-69.
Shepherd, Thomas J, Carlos Ayora, Dioni I Cendon, Simon R Chenery, and Alain Moissette. 1998. 'Quantitative solute analysis of single fluid inclusions in halite by LA-ICP-MS and cryo-SEM-EDS; complementary microbeam techniques', *European Journal of Mineralogy*, 10: 1097-108.

Sigua, G. C., J. M. Novak, D. W. Watts, K. B. Cantrell, P. D. Shumaker, A. A. Szögi, and M. G. Johnson. 2014. 'Carbon mineralization in two ultisols amended with different sources and particle sizes of pyrolyzed biochar', *Chemosphere*: 313-21.

Silva, Francisco Weliton Rocha, Hedinaldo Narciso Lima, Wenceslau Geraldes Teixeira, Marcelo Batista Motta, and Rodrigo Macedo Santana. 2011. 'Caracterizacao quimica e mineralogia de solos antropicos (terras pretas de indio) na amazonia central', *Revista Brasileira de Diencia do Solo*, 35: 9.

Singh, Balwant, Bhupinder Pal Singh, and Annette L Cowie. 2010. 'Characterisation and evaluation of biochars for their application as a soil amendment', *Soil Research*, 48: 516-25.

Smith, KA, T Ball, F Conen, KE Dobbie, J Massheder, and A Rey. 2003. 'Exchange of greenhouse gases between soil and atmosphere: interactions of soil physical factors and biological processes', *European Journal of Soil Science*, 54: 779-91.

Spokas, K. A., W. C. Koskinen, J. M. Baker, and D. C. Reicosky. 2009. 'Impacts of woodchip biochar additions on greenhouse gas production and sorption/degradation of two herbicides in a Minnesota soil', *Chemosphere*, 77: 574-81.

Spokas, Kurt A. 2010. 'Review of the stability of biochar in soils: predictability of O: C molar ratios', *Carbon Management*, 1: 289-303.

Spokas, Kurt A. 2013. 'Impact of biochar field aging on laboratory greenhouse gas production potentials', *GCB Bioenergy*, 5: 165-76.

Spokas, Kurt A., Jeffrey M. Novak, Catherine E. Stewart, Keri B. Cantrell, Minori Uchimiya, Martin G. DuSaire, and Kyoung S. Ro. 2011. 'Qualitative analysis of volatile organic compounds on biochar', *Chemosphere*, 85: 869-82.

Spokas, Kurt A., and Donald C. Reicosky. 2009. 'Impact of sixteen different biochars on soil greenhouse gas production', *Annals of Environmental Science*, 3: 14.

Spokas, KurtA., JeffM. Novak, and RodneyT. Venterea. 2012. 'Biochar's role as an alternative N-fertilizer: ammonia capture', *Plant and Soil*, 350: 35-42.

Su, Chunming, and Robert W. Puls. 2007. 'Removal of added nitrate in the single, binary, and ternary systems of cotton burr compost, zerovalent iron, and sediment: Implications for groundwater nitrate remediation using permeable reactive barriers', *Chemosphere*, 67: 1653-62.

Taghizadeh-Toosi, Arezoo, Tim J. Clough, Robert R. Sherlock, and Leo M. Condron. 2011. 'Biochar adsorbed ammonia is bioavailable', *Plant and Soil*, 350: 57-69.

Théry-Parisot, Isabelle, Lucie Chabal, and Julia Chrzavzez. 2010. 'Anthracology and taphonomy, from wood gathering to charcoal analysis. A review of the taphonomic processes modifying charcoal assemblages, in archaeological contexts', *Palaeogeography, Palaeoclimatology, Palaeoecology*, 291: 142-53.

Tsukagoshi, S., H. Shinoyama, K. Noda, and F. Ikegami. 2010. 'The Effect Of Charcoal Amendment On The Lettuce Growth And NO3-N Discharge From The Soil Medium', *Acta Horticulturae*, 852.

Vinke, P., M. van der Eijk, M. Verbree, A. F. Voskamp, and H. van Bekkum. 1994. 'Modification of the surfaces of a gasactivated carbon and a chemically activated carbon with nitric acid, hypochlorite, and ammonia', *Carbon*, 32: 675-86.

Wang, C., M. T. Walter, and J. Y. Parlange. 2013. 'Modeling simple experiments of biochar erosion from soil', *Journal of Hydrology*, 499: 140-45.
Wang, D., W. Zhang, X. Hao, and D. Zhou. 2013. 'Transport of biochar particles in saturated granular media: effects of pyrolysis temperature and particle size', *Environmental Science & Technology*, 47: 821-8.
Warnock, Daniel D, Johannes Lehmann, Thomas W Kuyper, and Matthias C Rillig. 2007. 'Mycorrhizal responses to biochar in soil–concepts and mechanisms', *Plant and soil*, 300: 9-20.
White, Art F., and Susan L. Brantley. 2003. 'The effect of time on the weathering of silicate minerals: why do weathering rates differ in the laboratory and field?', *Chemical Geology*, 202: 479-506.
Woods, William I. 2003. 'Development of Anthrosol Research.' in Johannes Lehmann, Dirse C. Kern, Brund Glaser and William I. Wodos (eds.), *Amazonian Dark Earths: Origin Properties Management* (Springer Netherlands: Dordrecht).
Wu, Hongwei, Kongvui Yip, Zhaoying Kong, Chun-Zhu Li, Dawei Liu, Yun Yu, and Xiangpeng Gao. 2011. 'Removal and recycling of inherent inorganic nutrient species in mallee biomass and derived biochars by water leaching', *Industrial & Engineering Chemistry Research*, 50: 12143-51.
Yanai, Yosuke, Koki Toyota, and Masanori Okazaki. 2007. 'Effects of charcoal addition on N2O emissions from soil resulting from rewetting air-dried soil in short-term laboratory experiments', *Soil Science and Plant Nutrition*, 53: 181-88.
Yao, Qin, Junjie Liu, Zhenhua Yu, Yansheng Li, Jian Jin, Xiaobing Liu, and Guanghua Wang. 2017. 'Three years of biochar amendment alters soil physiochemical properties and fungal community composition in a black soil of northeast China', *Soil Biology and Biochemistry*, 110: 56-67.
Yao, Ying, Bin Gao, Ming Zhang, Mandu Inyang, and Andrew R. Zimmerman. 2012. 'Effect of biochar amendment on sorption and leaching of nitrate, ammonium, and phosphate in a sandy soil', *Chemosphere*, 89: 1467-71.
Yargicoglu, Erin N, Bala Yamini Sadasivam, Krishna R Reddy, and Kurt Spokas. 2015. 'Physical and chemical characterization of waste wood derived biochars', *Waste Management*, 36: 256-68.
Yuan, G., and L. M. Lavkulich. 1997. 'Sorption behavior of copper, zinc, and cadmium in response to simulated changes in soil properties', *Communications in Soil Science and Plant Analysis*, 28: 571-87.
Zanella, Odivan, Isabel Tessaro, and Liliana Féris. 2015. 'Nitrate sorption on activated carbon modified with CaCl2: Equilibrium, isotherms and kinetics', *CI CEQ*, 21: 23-33.
Zhao, Jian, Zhenyu Wang, Qing Zhao, and Baoshan Xing. 2013. 'Adsorption of phenanthrene on multilayer graphene as affected by surfactant and exfoliation', *Environmental Science & Technology*, 48: 331-39.
Zimmerman, Andrew R., Bin Gao, and Mi-Youn Ahn. 2011. 'Positive and negative carbon mineralization priming effects among a variety of biochar-amended soils', *Soil Biology and Biochemistry*, 43: 1169-79.